

## **Distribution Agreement**

In presenting this thesis or dissertation as a partial fulfillment of the requirements for an advanced degree from Emory University, I hereby grant to Emory University and its agents the non-exclusive license to archive, make accessible, and display my thesis or dissertation in whole or in part in all forms of media, now or hereafter known, including display on the world wide web. I understand that I may select some access restrictions as part of the online submission of this thesis or dissertation. I retain all ownership rights to the copyright of the thesis or dissertation. I also retain the right to use in future works (such as articles or books) all or part of this thesis or dissertation.

Signature:

---

Cara E. Shields

---

Date

BMI1 is a novel, preclinical target in fusion-positive  
rhabdomyosarcoma

By

Cara E. Shields  
Doctor of Philosophy

Graduate Division of Biological and Biomedical Sciences  
Cancer Biology

---

Karmella A. Haynes, Ph.D.  
Advisor

---

Robert W. Schnepf, M.D., Ph.D.  
Advisor

---

Carlos S. Moreno, Ph.D.  
Committee Member

---

Christopher C. Porter, M.D.  
Committee Member

---

Wei Zhou, Ph.D.  
Committee Member

Accepted:

---

Lisa A. Tedesco, Ph.D.

Dean of the James T. Laney School of Graduate Studies

---

Date

BMI1 is a novel, preclinical target in fusion-positive  
rhabdomyosarcoma

By

Cara E. Shields

B.S., University of Tampa, 2016

Advisor: Karmella A. Haynes, Ph.D.

Advisor: Robert W. Schnepf, M.D., Ph.D.

An abstract of

A dissertation submitted to the Faculty of the James T. Laney School of Graduate Studies of  
Emory University

in partial fulfillment of the requirements for the degree of

Doctor of Philosophy

In

Graduate Division of Biological and Biomedical Sciences  
Cancer Biology

2021

## Abstract

BMI1 is a novel, preclinical target in fusion-positive rhabdomyosarcoma  
By Cara E. Shields

Rhabdomyosarcoma (RMS) is a rare, understudied pediatric cancer. There are two main types of RMS: fusion-negative rhabdomyosarcoma (FN-RMS) and fusion-positive rhabdomyosarcoma (FP-RMS). FP-RMS harbors the PAX3-FOXO1 or PAX7-FOXO1 fusion proteins, which is associated with global epigenetic dysregulation. To restore dysfunctional epigenetic signaling in FP-RMS, we investigated B lymphoma Mo-MLV insertion region 1 (BMI1), a druggable chromatin protein member of Polycomb Repressive Complex 1 as a potential target. We discovered that FP-RMS expresses high levels of BMI1 and that inhibition of BMI1 by chemical or genetic methods leads to a dramatic decrease in FP-RMS proliferation and an increase in cell death. We utilized PTC-028, a small molecule inhibitor of BMI1, to study the effects of BMI1 inhibition in FP-RMS. We found that PTC-028 treatment leads to downregulation of DNA replication and halted cell progression to S phase. To understand how BMI1 regulated oncogenic signaling, we next examined Hippo signaling due to its importance in cancer and previous data linking BMI1 to a YAP, a protein involved in the Hippo pathway. Our data show that BMI1 suppresses Hippo pathway activation through repression of LATS1/2 phosphorylation, therefore keeping growth and proliferation genes “on” in FP-RMS. In addition to this, we explored the differences between FP-RMS cell line responses to BMI1 inhibition. We noted similar and contrasting responses in the downstream transcription of Hippo YAP/TAZ/TEAD targets, revealing intertumor heterogeneity in FP-RMS and possibly different mechanisms of LATS1/2 phosphorylation. We then explored other effects of BMI1 inhibition and discovered that PTC-028 treatment results in a downregulation of metabolic pathways and DNA replication, and an increase in p53 signaling. Overall, we find that BMI1 inhibition is an effective therapy in FP-RMS and should be considered a potential translatable target.

BMI1 is a novel, preclinical target in fusion-positive  
rhabdomyosarcoma

By

Cara E. Shields

B.S., University of Tampa, 2016

Advisor: Karmella A. Haynes, Ph.D.

Advisor: Robert W. Schnepf, M.D., Ph.D.

A dissertation submitted to the Faculty of the James T. Laney School of Graduate Studies of  
Emory University

in partial fulfillment of the requirements for the degree of

Doctor of Philosophy

In

Graduate Division of Biological and Biomedical Sciences  
Cancer Biology

2021

## Acknowledgments

I joined the Emory Cancer Biology program in August 2016 at 19-years-old, with the goal of acquiring my doctorate by 25. It was difficult to leave my partner, family, friends in Tampa and initially live alone in Atlanta (though it's only an 8-hour drive to Tampa on I-75S, 6 hours if you speed like Atlanta drivers); however, my graduate school journey has shaped me into the scientist I am today. Every individual has unique challenges to overcome in graduate school, both personal and academic. My journey has had many road bumps, large and small, with the most notable being two of my advisors leaving Emory in succession. I am greatly appreciative of the time I did have to learn from them. Overall, my experiences have taught me resilience and adaptability, both of which are necessary for research and life. I could not have done it without the support of many people in my life.

First and foremost, I would like to thank my advisors. To Bob: I am so glad that I joined your lab and got to learn from you. Your drive and passion for translational research inspired me many times, and you helped me build "grit," as you often called it. You always supported me and encouraged me to think outside the box. While you had to leave, I will always miss the Schnepf lab, and you were a terrific PI and Topgolfer. I am genuinely grateful for everything, and I am sure we will continue to keep in contact! To Karmella: I cannot thank you enough for inviting me to join the Haynes lab. Finishing my degree has been difficult, especially during the pandemic, but your mentorship and support have helped me cross the finish line. I am excited to begin my postdoctoral studies under your mentorship.

I would like to express my most profound appreciation to my dissertation committee: Carlos, Chris, Wei, and previously Dolores. Your continual feedback on my project over the past couple of years has been invaluable. I appreciate your guidance, investment in my work, and my growth as a scientist. Thank you for everything.

To my previous labmates: Doris, Priya, and Ben... Adeiye, Julie and Selma... You have all helped to make my lab experience be the best it can be. I miss the Doris and Priya show and lunches with the Schnepf lab. We all supported each other through failed experiments, struggling to write papers, think of new ideas and life in general. I miss you guys all time, and I'm so grateful to you all. To my current labmates: Natecia, Isioma, Kierra, and Harrison. We haven't gotten to know each other as much due to the pandemic and having shifts/virtual meetings, but talking to you all and getting advice on experiments and writing has always been helpful, so thank you!

More personally, I would like to extend my gratitude to my partner, family, and friends. To Meghan, my life partner: We have been together since 2011 and are coming up on our 10<sup>th</sup> anniversary. We have grown together over so many years, and I couldn't imagine life without you. Every day you have been there for me through my Ph.D., through struggling with experiments, sharing gross details about mouse work, bringing me food during late nights at the lab; you've supported me through all the highs and lows and continuously encouraged me to keep going. I think you should receive an honorary Ph.D. for going through everything with me. You have brought me so much joy, and I am so

grateful for the life we built together (including our cats Spartacus and Callie), and I cannot wait to start the next chapter.

To my family: Mom, I know you hated me leaving Tampa because you would miss me, but you have always supported me and my dreams. You always helped me no matter what I wanted to do, when I was a kid and wanted to be an archaeologist, a veterinarian, a physician... even when I almost started undergrad as an English major. I miss you all the time, especially since we still haven't seen each other since Christmas 2019. Thank you for always listening and offering advice, and we will see each other soon. To my stepfather, Tom: I appreciate your constant support in my life. Thank you for being there for me and always listening. To my father, Scott: Thank you for supporting my graduate career, your guidance, and life advice – I am deeply grateful. To the rest of my family: my uncles (Mike and Jim), siblings (Noah, Adam, Sean, Debbie), cousins (Jenny, Rachid). I haven't seen you all in what feels like forever, though we will see each other soon, and thank you for being there for me throughout my Ph.D.

To my dear friends: Alana, Bryan, Tanika, Candace, Amy, Cassidy, Haley, Kate, Davis. We may not all live near one another, but we still treat each other like family and talk often. We have lived, laughed, and loved together for years, and we often joke about starting a commune. Thank you for your support and friendship. To my friends from high school that I've known for so long: Aaron, Adam, Manny, Nicholas. We've supported each other through our high school, undergraduate, and graduate careers. I miss hanging out with you all in person, but all the times we've spent up late playing games together and laughing have been some of the best. To my friends from undergrad: Irena, Mindy, Paulo. Wow, we have gone through a lot. I am proud of each of you for achieving the goals you set for yourselves, and I know you feel the same for me. We have cheered each other on through it all, and I know you will all continue to do great things. Thank you for always encouraging me throughout undergraduate and graduate school.

Thank you again to everyone. While the past year has been challenging for us all, we have helped each other stay sane, and you have all made me happier than you know over the past five years. The completion of this dissertation would not be possible without you all.

# Table of Contents

1. Introduction .....	1
1.1 Overview of cancer .....	2
1.1.1 History of cancer .....	2
1.1.2 Hallmarks of cancer.....	3
1.1.3 Adult and pediatric cancer .....	4
1.1.4 Pediatric soft-tissue sarcomas.....	5
1.2 Rhabdomyosarcoma .....	6
1.2.1 Background.....	6
1.2.2 Fusion-negative and fusion-positive rhabdomyosarcoma .....	7
1.3 Epigenetic therapies in cancer.....	8
1.3.1 What is epigenetics? .....	8
1.3.2 Overview of epigenetic machinery .....	10
1.3.3 Current epigenetic therapies.....	12
1.3.4 Efficacy of epigenetic therapies in rhabdomyosarcoma .....	13
1.4 Polycomb group complexes .....	15
1.4.1 Polycomb groups .....	15
1.4.2 Alternative Polycomb roles .....	17
1.5 BMI1.....	18
1.5.1 BMI1 function and expression.....	18
1.5.2 BMI1 is recruited to DNA breaks and regulates repair.....	19
1.5.3 BMI1 promotes the epithelial to mesenchymal transition.....	20
1.5.4 BMI1 inhibition as a novel therapeutic.....	21
1.6 Scope of this dissertation.....	22
2. Epigenetic regulator BMI1 promotes alveolar rhabdomyosarcoma proliferation and constitutes a novel therapeutic target.....	28
Abstract .....	31
2.1 Introduction.....	32
2.2 Materials & Methods .....	35
2.2.1 In silico data.....	35
2.2.2 Cell culture.....	35
2.2.3 Plasmids, lentiviral preparation, and transduction .....	35
2.2.4 siRNA transfection .....	36
2.2.5 Real-Time PCR and western blots.....	37
2.2.6 Cell growth assays .....	37
2.2.7 Flow cytometry .....	38
2.2.8 <i>In vivo</i> xenograft model .....	38
2.2.9 Immunohistochemistry .....	39
2.2.10 Statistical analyses.....	40
2.3 Results.....	41
2.3.1 BMI1 is highly expressed in rhabdomyosarcoma .....	41
2.3.2 Genetic knockdown of BMI1 leads to reduced cellular proliferation in ARMS cells ...	42
2.3.3 Pharmacologic inhibition of BMI1 decreases cell proliferation <i>in vitro</i> .....	42
2.3.4 Targeting BMI1 decreases cell cycle progression and increases apoptosis in ARMS ..	44
2.3.5 Single agent PTC-028 treatment causes tumor growth delay <i>in vivo</i> .....	45
2.3.6 BMI1 negatively influences Hippo signaling.....	45
2.4 Discussion .....	49



2.5 Conclusions .....	52
3. Differential epigenetic effects of BMI1 inhibitor PTC-028 on two fusion-positive rhabdomyosarcoma cell line models .....	73
Abstract .....	75
3.1 Introduction.....	76
3.2 Materials & Methods.....	78
3.2.1 Cell culture .....	78
3.2.2 RNA-seq study design .....	78
3.2.3 Data analyses and graph production.....	79
3.3 Results.....	80
3.3.1 BMI1 inhibition influences global gene expression in FP-RMS .....	80
3.3.2 Gene ontology and pathway analyses reveal downregulation of DNA replication and activation of cellular differentiation during BMI1 inhibition.....	81
3.3.3 TEAD-regulated gene expression in Rh30 is more sensitive to BMI1 and Hippo pathway inhibition.....	83
3.3.4 BMI1 inhibition increases the expression of distinct LATS1/2 kinases in Rh28 and Rh30 .....	84
3.4 Discussion .....	86
4. Discussion and future directions.....	102
4.1 Summary of findings in Chapters 2 and 3.....	103
4.2 DNA damage repair.....	106
4.3 Intersection of BMI1 with metabolic pathways .....	108
4.4 Invasion and metastasis.....	109
4.5 Further modeling of PRC1 and BMI1 in FP-RMS .....	110
4.6 Combining BMI1 inhibition with other translatable targets .....	112
4.7 Final conclusions and thoughts.....	114
References .....	117

## List of Figures

Figure 1.1 Hallmarks of cancer. ....	23
Figure 1.2 Mutation rate in pediatric cancers versus adult cancers. ....	24
Figure 1.3 Epithelial to mesenchymal transition.....	25
Figure 1.4 Eukaryotic chromatin organization. ....	26
Figure 1.5 Polycomb repressive complexes promote heterochromatin formation and prevent efficient gene transcription. ....	27
Figure 2.1 BMI1 is highly expressed in rhabdomyosarcoma .....	55
Figure 2.2 Genetic knockdown of BMI1 leads to reduced cellular proliferation in ARMS cells ...	57
Figure 2.3 Pharmacologic inhibition of BMI1 decreases cell proliferation <i>in vitro</i> .....	59
Figure 2.4 Targeting BMI1 decreases cell cycle progression and increases apoptosis in ARMS ..	61
Figure 2.5 Single agent PTC-028 treatment causes tumor growth delay <i>in vivo</i> .....	63
Figure 2.6 BMI1 negatively influences Hippo signaling .....	64
Figure 3.1 BMI1 inhibition influences global gene expression in FP-RMS .....	90
Figure 3.2 Gene ontology analyses reveal pathways and biological activities affected by BMI1 inhibition .....	92
Figure 3.3 Gene expression in Rh30 is more sensitive to BMI1 and Hippo pathway inhibition .	94
Figure 3.4 BMI1 inhibition differentially affects expression of LATS1/2 kinases in Rh28 and Rh30.....	97
Figure 4.1 Hippo pathway schematic.....	115
Figure 4.2 Canonical and non-canonical PRC1 complexes.. ....	116
Supplementary Figure S 2.1, related to Figure 2.1. <i>BMI1</i> is highly expressed in rhabdomyosarcoma .....	66
Supplementary Figure S 2.2, related to Figure 2.3. Pharmacologic inhibition of BMI1 decreases cell proliferation <i>in vitro</i> .....	67
Supplementary Figure S 2.3, related to Figure 2.4. Targeting BMI1 decreases cell cycle progression and increases apoptosis in FP-RMS .....	69
Supplementary Figure S 2.4, related to Figure 2.6. BMI1 negatively influences Hippo signaling	71
Supplementary Figure S 3.1 Principal component analyses plot of RNA-seq samples.....	100
Supplementary Figure S 3.2 Western blot of YAP/TAZ targets in Rh28 and Rh30 .....	101
Supplementary Table 2.1 .....	72
Supplementary Table 3.1 Top differentially expressed genes (DEGs) in PTC-028 treated Rh28 and Rh30 cell lines.....	98
Supplementary Table 3.2 TEAD-motif IDs .....	99

# 1. Introduction

## **1.1 Overview of cancer**

Cancer remains one of the most prevalent and challenging diseases in the world. Broadly defined, cancer refers to neoplasms – new growths. Typically, this results from dysregulated cell proliferation and invasion into other tissues. Not all neoplasms are aggressive, and some remain benign. When they are malignant, they pose grave health risks. Cancer is a significant public health issue that afflicted nearly 1.8 million Americans in 2019, with almost 600,000 fatalities (Centers for Disease Control and Prevention). It is challenging to treat due to many factors, including metastases to inaccessible sites in the body, heterogeneity within tumors and across tumor types, drug resistance, and more. Emerging molecular technologies allow us to separate cancers into subtypes with the hope of targeting each subtype specifically and effectively.<sup>1</sup>

Now, in our modern world, we can identify many cancers early on with screening. Compared to the past, subsets of patients are beginning to have more favorable outcomes than past data.<sup>2</sup> Every year, cancer incidence and mortality rates decrease due to earlier detection and more effective therapies. However, some cancers remain as difficult to treat now as before.

### **1.1.1 History of cancer**

Cancer is a timeless affliction. Termed the *Emperor of All Maladies* (Mukherjee, S. 2011), cancer has affected humans throughout history. The word “cancer” originates from the ancient Greek word *karkinos* or *karkinoma* to describe non-healing wounds first seen by Hippocrates in 5<sup>th</sup> century B.C.<sup>3</sup> This was not the first recording of cancer, as early hominid fossils dating back 1.6 million years ago have been found to have osteosarcoma,

or bone cancer.<sup>4</sup> Metazoans, in general, have the predisposition to be affected by malignancy, and similar cancers have been identified even in dinosaur fossils.<sup>4</sup> The capacity for malignancy is primordial, embedded in our most base cellular developmental pathways originating from our ancient ancestors.

### **1.1.2 Hallmarks of cancer**

While developmental pathways act in concert to shape the development of unique organisms, when they are dysregulated, it can lead to various afflictions, including cancer. Classically, cancer was thought to be caused by carcinogenic somatic mutations in oncogenes or tumor suppressors.<sup>5,6</sup> While these can contribute to the initiation of neoplastic disorders, notably the colorectal adenoma-carcinoma sequence<sup>7</sup>, we now understand that cancer can be a collection of several mechanisms and hallmarks. Defined by Hanahan and Weinberg in 2000<sup>8</sup>, then updated in 2011<sup>9</sup>, the hallmarks of cancer (Figure 1.1) remain a group of seminal principles to comprehend this complex disease. There are ten hallmarks, as follows: 1. continuous proliferative signaling, 2. evading growth suppressors, 3. avoiding immune destruction, 4. replicative immortality, 5. inflammation, 6. invasion/metastasis, 7. angiogenesis, 8. genome instability, 9. resisting apoptosis, and 10. deregulation of cell metabolism. Not all malignant cells will have each of these hallmarks, and these hallmarks can also be sequential steps in tumorigenesis. Many apply to the primary tumor itself, while others apply to metastatic lesions.

Solid tumors are heterogeneous mixtures of cells, including sub-clonal populations of cancer cells themselves and various components present in the microenvironment such as stromal cells, endothelial cells, blood vessels, infiltrating immune cells, and the

extracellular matrix.<sup>10-12</sup> These cells communicate with each other through many mechanisms. It has been shown that these exchanges have a significant impact on many steps of carcinogenesis, particularly the epithelial to mesenchymal transition (EMT).<sup>12,13</sup> EMT is considered the first step of invasion and metastasis, as immotile epithelial cells transition to invasive mesenchymal cells that disseminate from the primary tumor.<sup>14-17</sup> These mesenchymal-like tumor cells proliferate more rapidly when associated with inflammatory and endothelial cells in the microenvironment and stimulate angiogenesis.<sup>14</sup> Other cells in the microenvironment, such as cancer-associated fibroblasts, have been found to promote cancer cell migration through the alignment of fibronectin.<sup>18</sup>

### **1.1.3 Adult and pediatric cancer**

The majority of cancer research is chiefly focused on adult carcinomas, particularly tumors arising from the breast, lung, prostate, colon, and other sites.<sup>19</sup> This is in contrast to pediatric cancers, which are comparatively rarer and mainly comprised of hematological malignancies, solid brain tumors, and extra-cranial solid tumors, including neuroblastomas or sarcomas.<sup>19</sup> However, it is essential to note that cancer is still the second most common cause of death in children and adolescents.<sup>19</sup> By definition, pediatric cancer can take away a developing life. There is a significant increase in the relative risk of secondary malignant neoplasms due to aggressive multiagent chemotherapy and ionizing radiation. The 30-year cumulative incidence of cancer in pediatric cancer survivors is 20.5%, six times higher than the relative risk in the general population.<sup>20</sup> There is also an increase in 5-year pediatric cancer survivor mortality rates compared to the general population, and over half of those deaths can be attributed to

recurrent disease.<sup>21</sup> The majority of pediatric cancers remain understudied compared to adult cancers due to the comparative rarity and thought process that research done on adult cancers should also apply to pediatric cancers. While this is partially true, there are discrete overarching differences between pediatric and adult malignancies which must be also be considered.

To date, the critical difference lies in the genome. In adults, the genomic alteration rate is about 2 mutations in coding regions per Megabase (Mb). In comparison, in pediatric cancers, the mutation rate is only around 0.14 mutations in coding regions per Mb (Figure 1.2).<sup>22</sup> Thus, the somatic mutation rate is **14 times lower in pediatric cancer**.<sup>22</sup> This presents a difficult challenge, as there is a lack of targetable mutations in the pediatric cancer coding genome. However, other targetable options may be gene amplification or deletions, germline mutations, or mutations in non-coding regions. Data suggests that up to 50% of pediatric cancers have targetable genetic events.<sup>22</sup> There are additional mechanisms that alter the expression of key genes, such as through epigenetic regulation. This thesis will be focusing on epigenetic vulnerabilities that could influence multiple downstream oncogenic targets.

#### **1.1.4 Pediatric soft-tissue sarcomas**

Sarcomas are a unique and diverse group of cancers. Soft-tissue sarcomas specifically refer to sarcomas of the muscle, fat, ligaments, tendons, and other soft tissues.<sup>23</sup> They differ from carcinomas in origin, as carcinomas emerge from the ectodermal layer and soft-tissue sarcomas from the mesodermal layer.<sup>23</sup> These rare mesenchymal tumors are found in a range of patients across all ages, from children to the elderly. However, several

soft-tissue sarcomas disproportionately affect children and adolescents.<sup>24,25</sup> After neuroblastoma, soft-tissue sarcomas are the second-most frequent extra-cranial tumor in pediatric patients.<sup>26</sup> In 2020, approximately 13,000 cases of soft-tissue sarcomas were diagnosed, and there were an estimated 5,000 deaths; both are increases compared to previous years.<sup>27</sup> Patient survival outcomes have improved in recent years, though survival outcomes for patients with metastatic disease remain dismal.<sup>28</sup> The most common type of soft-tissue sarcomas are rhabdomyosarcomas, which are the focus of this dissertation.<sup>24,25</sup>

## **1.2 Rhabdomyosarcoma**

### **1.2.1 Background**

Rhabdomyosarcoma (RMS) is an aggressive soft-tissue sarcoma that resembles skeletal muscle precursor cells.<sup>24</sup> It is a rare disease but still one of the most common pediatric solid tumors, affecting ~350 children per year in the US.<sup>25</sup> Unfortunately, there are currently no targeted therapies for RMS. The current standard of care involves surgery, multiagent chemotherapies (vincristine, actinomycin-D, cyclophosphamide, among other agents), and radiation.<sup>29</sup> The 5-year survival rate for RMS is over 60%.<sup>24,25,30</sup> However, there are significant side effects from aggressive clinical treatment later in life, along with cancer recurrence or relapse. Late effects of utilizing alkylating agents or anthracycline chemotherapy for this cancer can include infertility in both sexes, cardiomyopathy, and increased risk of cardiac dysfunction.<sup>31</sup> Depending on the location and dose, radiation treatment can lead to joint dysfunction, growth deficiencies, atrophy, fibrosis, and peripheral nerve damage.<sup>31</sup> Additionally, the survival rate for patients with



metastatic disease is less than 20%.<sup>25,30</sup> There are currently no targeted therapies for RMS, underscoring the urgent need to identify potential translatable targets.

### **1.2.2 Fusion-negative and fusion-positive rhabdomyosarcoma**

There are two main subtypes of RMS, alveolar RMS (ARMS) and embryonal RMS (ERMS). These were initially characterized based on histological observations and are now primarily described by their molecular features, with alveolar being termed fusion-positive RMS (FP-RMS) and embryonal as fusion-negative RMS (FN-RMS).<sup>24</sup> This nomenclature denotes the presence or absence of the PAX-FOXO1 fusion protein, which represents a translocation of either the PAX3 or PAX7 DNA binding domain to the transactivation domain of FOXO1 (t(2;13) (q35;q14) and t(1;13) (p36;q14), respectively).<sup>32,33</sup>

In FN-RMS, there are genetic alterations within RAS-PI3K signaling pathways. Around one-third of patients who have FN-RMS have activating mutations in *NRAS*, *KRAS*, or *HRAS*. Additionally, over half of FN-RMS patients harbor a mutation impacting RAS/MAPK or PI3K/mTOR pathways.<sup>34,35</sup> High levels of Akt and MAPK phosphorylation are observed in patient tumor samples, indicating activation of these pathways. Approximately 80% of FN-RMS tumor samples show PI3K activation.<sup>36</sup> Receptor tyrosine kinases (RTKs) can signal using these pathways, which can be mutated in FN-RMS. RTKs such as ephrin receptors are upregulated, and FN-RMS cell lines with decreased levels of ephrin receptors are more likely to differentiate and are less invasive.<sup>37</sup>

Next, in FP-RMS, PAX-FOXO1 essentially acts as a novel transcription factor, resulting in global dysregulation of transcription. Around 60% of patients with ARMS express PAX3-FOXO1, while 20% express PAX7-FOXO1, and the remaining patients are FN.<sup>24</sup> This subset of FN-ARMS behaves more like ERMS, hence the trend toward focusing on fusion status rather than histological presentation. To date, efforts to inhibit PAX-FOXO1 directly have not been clinically fruitful. Transcription factors and fusion proteins remain challenging targets. This is due to several reasons, such as the increased stability of the PAX3-FOXO1 fusion protein compared to PAX3 alone, and a lack of hydrophobic pockets for small molecule inhibitors to bind to. Experiments in which the expression of PAX3-FOXO1 is knocked down by RNA interference indicate significant inhibition of cell growth and an increase in apoptosis levels.<sup>38-40</sup> However, it has been found that PAX3-FOXO1 may be necessary for initiation and maintenance of FP-RMS cells, but not recurrence.<sup>41</sup> This indicates that even if PAX3-FOXO1 did have a perfect *in vivo* drug, multiple approaches might still be necessary to target these tumors.

### **1.3 Epigenetic therapies in cancer**

#### **1.3.1 What is epigenetics?**

The term epigenetics refers to changes in gene expression which are heritable and not caused by alterations in DNA itself.<sup>42</sup> It describes events in chromatin and DNA regulation that lead to changes in gene expression.<sup>42,43</sup> These changes are reversible and referred to as plasticity, which is necessary for cells to move from an undifferentiated to differentiated state during development.<sup>43</sup> The plasticity of cells is often exploited in malignant contexts, especially with relation to cell stemness and the epithelial to

mesenchymal transition (EMT). EMT is a cell motility program required for many stages in embryonic development and can play a vital role in cancer cell invasion (Figure 1.3).<sup>15,44</sup> Epigenetic mechanisms that control EMT and others are partially controlled by chromatin structure.

The nucleosome is the building block of chromatin organization and structure.<sup>45</sup> 147 base pairs of DNA wrap around a histone octamer core, with two histones each of H2A, H2B, H3 and H4.<sup>45,46</sup> This method of DNA condensation/organization is necessary during mitosis, and control of gene expression (Figure 1.4). Epigenetic complexes influence the accessibility of the DNA and thus the ability for the corresponding genes to be transcribed. It is generally accepted that heterochromatin is condensed and contains mainly repressed genes, while euchromatin is looser and so the genes are more easily activated (Figure 1.5).<sup>47-49</sup> The histone proteins have N-terminal tails, which protrude from the nucleosome and can contact nearby nucleosomes.<sup>50</sup> These tails impact physical and chemical interactions around the nucleosome and lead to overall chromatin structure changes.<sup>50</sup> Due to the loose structure of the tail, they are easily modified by epigenetic complexes that can influence gene expression.<sup>42,51</sup> Most commonly, histone tails can be methylated or acetylated, though 16 types of modifications can occur at 60 reported residues.<sup>48</sup>

These modifications are called histone marks, and while they are complex and varied, they can be broadly categorized as “active” or “repressive” marks. For instance, trimethylation of lysine 27 on histone H3 (H3K27me3) near promoters at the transcription start sites are linked to repression of expression of that gene, while acetylation of H3K27 is associated with enhanced transcription.<sup>52</sup> The enzyme

responsible for trimethylating H3K27 is Enhancer of Zeste homolog 2 (EZH2), a member of the Polycomb repressive complex 2 (PRC2). Overexpression of components of histone-modifying complexes, such as EZH2, are correlated with widespread gene silencing in solid tumors, increased tumor aggression, and worse overall patient outcomes.<sup>52,53</sup> These complexes are essential in cancer initiation and progression; therefore, epigenetic therapies are being explored (Figure 1.5).<sup>54</sup>

### **1.3.2 Overview of epigenetic machinery**

Generally, the epigenetic machinery of human cells can be separated into two groups: DNA modifications and histone modifications. DNA methylation was one of the first identified epigenetic mechanisms of regulation.<sup>55</sup> The addition of a methyl group to cytosine (5'-methylcytosine or 5mC) is catalyzed by DNA methyltransferases (DNMTs).<sup>56,57</sup> The majority of DNA methylation occurs on cytosines which precede guanine, also known as CpG sites.<sup>58</sup> In normal cells, DNA methylation is predominantly present in repetitive genomic regions. CpG islands (regions that are enriched in CpGs ranging from 300-3,000 bp) are largely unmethylated and are found close to the transcription start sites (TSSs) of genes.<sup>56,58</sup> In cancer cells, the genome is hypomethylated compared to their normal tissue counterparts. Loss of methylation at pericentric heterochromatin and hypermethylation of CpG islands near tumor suppressors are associated with many cancers, such as colorectal cancer, breast cancer, and prostate cancer.<sup>57,59,60</sup> DNA methylation and histone modifications go hand in hand in epigenetic regulation of developmental programs.<sup>61</sup>

There are two central conserved systems of histone regulation: the Polycomb groups (PcG) and Trithorax groups (TrxG), which have opposing roles in gene expression.<sup>42,62</sup> Traditionally, Polycomb groups repress groups of developmental genes, while Trithorax groups function as activators.<sup>62</sup> They were initially discovered in *Drosophila* as maintaining *Hox* gene expression.<sup>63</sup> Various PcG and TrxG complexes are cell-type and developmental-stage specific, allowing them to perform multiple functions. Since then, they were discovered to contribute to cellular proliferation, stem-cell renewal, and senescence, all of which are often dysregulated in cancer.<sup>64-66</sup> There are multiple PcG and TrxG complexes that are cell-type and developmental-stage specific, allowing them to perform a variety of functions.

Other regulators of histone structure are called histone acetyltransferases (HATs) and histone deacetylases (HDACs), both of which contribute to gene expression and development.<sup>67,68</sup> There are 18 HDACs in humans separated into four classes that have diverse functions and can be cell-type specific. HDACs function by removing the acetyl groups from lysine residues on histone tails, which typically leads to gene repression. In general, high expression of HDACs in cancer causes worse outcomes in several types of cancer, including breast, lung, and pancreatic cancer.<sup>69</sup> The loss of H3K18Ac or H4K16Ac leads to poor survival in these cancers.<sup>70</sup> Thus, HDAC inhibitors have been instrumental in many cancer studies for translation to the clinic. Inhibitors like SAHA (vorinostat)<sup>71</sup> and belinostat<sup>72</sup> have been approved by the FDA to treat T-cell lymphomas.

### 1.3.3 Current epigenetic therapies

Over the past decade, investigators have increasingly begun to explore drugs targeting aberrant histone modifiers. A few significant targets include HDACs, Bromodomain and extraterminal domain (BET) proteins and EZH2. As mentioned in 1.3.2, several inhibitors of HDACs such as vorinostat and belinostat have been FDA approved for lymphoma, and panobinostat has been approved to treat multiple myeloma.<sup>71-73</sup> Deacetylation of the histones primarily results in heterochromatin formation. This can inhibit transcription of specific genes such as *CDKN1A* and *FOSL1*.<sup>74,75</sup> The broad targeting of HDAC inhibition leads to varied responses across cancer types and cell lines.<sup>67,69</sup> HDAC inhibition can reduce tumor cell proliferation, induce apoptosis, cause differentiation, lead to autophagy, affect the immune response, reduce angiogenesis, and more.<sup>67,69,76</sup> By targeting this single class of epigenetic proteins, many of the hallmarks of cancer are inhibited.

An additional therapy being examined is inhibition of the bromodomains of the BET proteins BRD2, BRD3, and BRD4. These proteins are epigenetic readers that read acetylated lysines and act as scaffolds to recruit transcription elongation complex proteins.<sup>77</sup> Thus, BET proteins are generally associated with active transcription. The most well-known BET inhibitor is JQ1<sup>78</sup>, which has been mentioned in almost 900 peer-reviewed journal articles published in the past decade (PubMed®). JQ1 also inhibits tumor growth and induces apoptosis across many cancer types, from hematological malignancies such as AML and B-ALL to solid tumors, including medulloblastoma and glioblastoma.<sup>79,80</sup> This drug causes global changes in gene expression by preventing the active transcription of many genes involved in cell-cycle progression.<sup>78-80</sup> Unfortunately,

the extremely short half-life of JQ1 (1 hr) makes it an ineffective treatment for moving forward to human trials.<sup>81</sup> Other newer BET inhibitors such as birabresib (OTX-015) are currently in a clinical trial (NCT02259114) in patients with advanced solid tumors (such as castrate-resistant prostate cancer, non-small-cell lung cancer, and NUT midline carcinoma).<sup>82,83</sup> Birabresib has been found to attenuate oncogenic signaling pathways such as MYC and NFκB in mantle cell lymphoma and prevent cell-cycle progression.<sup>84</sup>

Next, EZH2 is the catalytic subunit of PRC2 and contributes to chromatin compaction and gene silencing by H3K27 trimethylation.<sup>52</sup> *EZH2* is aberrantly overexpressed in various malignancies, such as prostate cancer, breast cancer, and ovarian cancer.<sup>54</sup> EZH2 is an essential factor in promoting cancer growth and metastasis in many tumor types.<sup>54,85</sup> Many studies have shown that EZH2 is a targetable epigenetic protein in cancer.<sup>54</sup> The first-generation inhibitor DZNep has been used in several basic studies to investigate the roles of EZH2, but it has significant off-target effects.<sup>86,87</sup> GSK-126 and EPZ-005687 are selective EZH2 inhibitors that can bind to the S-adenosyl-L-methionine pocket of EZH2, leading to diminished H3K27me3 levels and upregulation of the silenced genes.<sup>88,89</sup> An oral EZH2 inhibitor, tazemetostat (EPZ-6438), is currently under evaluation in patients with lymphomas and advanced solid tumors (NCT01897571), and has shown clinical promise in follicular lymphoma.<sup>90</sup>

### **1.3.4 Efficacy of epigenetic therapies in rhabdomyosarcoma**

The potential for epigenetic therapy in RMS is being explored. The fusion protein, PAX3-FOXO1, has been linked to controlling epigenetic regulation through cooperation with BRD4 at super-enhancers, as well as requiring the chromatin remodeling activity of

CHD4.<sup>91,92</sup> Since the genetic landscape of FP-RMS is relatively quiet, some investigators have hypothesized that the epigenome is implicated in development and progression of this disease. Small molecule inhibitors of HDACs, BET proteins, and EZH2 have shown promising results.

HDAC inhibition has been examined in RMS. Treatment with vorinostat or entinostat was found to suppress cell growth *in vitro* and result in apoptosis.<sup>93,94</sup> Entinostat alone or combined with standard of care actinomycin-D delayed tumor progression in an *in vivo* orthotopic xenograft RMS model.<sup>95</sup> More in-depth molecular analyses of HDAC inhibition revealed that HDAC inhibition disrupts FP-RMS core regulatory circuit transcription factors.<sup>96</sup> Core regulatory circuit transcription factors refer to oncogenes such as the MYC family and lineage-specific factors such as *MYOD1* or *MYCN* in FP-RMS.<sup>91,96</sup> The homeostasis of histone acetylation is important for tumor proliferation, and perturbation of this mechanism leads to decreased levels of these oncogenic transcription factors. Additionally, entinostat inhibits PAX3-FOXO1 through an indirect mechanism through the HDAC3–SMARCA4–miR-27a axis.<sup>97</sup> Currently, entinostat is being specifically investigated in a clinical trial for pediatric patients with recurrent or refractory solid tumors, including RMS.<sup>98</sup>

Next, BET inhibition has been found to have similar positive results for the treatment of FP-RMS. Birabresib (OTX-015) was recently reported to exhibit antitumor activity in FP-RMS cells *in vitro*.<sup>91,99</sup> Cell proliferation was reduced, and apoptosis levels increased due to several factors, including the inhibition of AKT activation, inhibition of clonogenic potential, and increased DNA damage.<sup>99</sup> Birabresib also decreased cancer cell



stemness by reducing levels of BRD4 and c-MYC, along with radio-sensitizing FP-RMS cells.<sup>99</sup> Additionally, JQ1 has been investigated as a combination therapy with HDAC inhibitors, and synergistic effects have been demonstrated.<sup>93</sup> JQ1 and quisinostat cooperatively induce apoptosis *in vitro* and in an *in vivo* chicken chorioallantoic membrane (CAM) model of RMS.<sup>93</sup> By treating the tumor cells with JQ1 and quisinostat, BIM and BMF become upregulated, which then leads to pro-apoptotic BAX/BAK activation, caspase-3/7 cleavage, and subsequent cell death.<sup>93</sup>

Another significant epigenetic target, EZH2, has been studied in the context of RMS as well. EZH2 is aberrantly expressed at high levels in RMS in cell lines, patient tumor samples, and PDX models.<sup>100-102</sup> Downregulation of EZH2 by RNAi, DZNep, or MC1945 (a catalytic EZH2 inhibitor) causes apoptosis in RMS both *in vitro* and in subcutaneous RMS cell line xenografts.<sup>101,102</sup> This phenotype is partially due to the depression of the tumor suppressor *FBXO32*, induced by knockdown of EZH2.<sup>102</sup> Tazemetostat is currently in phase II clinical trial for pediatric patients with relapsed/refractory solid tumors.<sup>90</sup> This trial includes patients with RMS. Overall, epigenetic therapies in FP-RMS have shown efficacy and are potentially translatable treatment options.

## **1.4 Polycomb group complexes**

### **1.4.1 Polycomb groups**

An avenue of epigenetic therapy that remains underexplored in FP-RMS are the Polycomb group complexes. Initially discovered in *Drosophila*, these Polycomb

repressive complexes are essential regulators of cell development.<sup>52,53,62,103</sup> As previously mentioned, EZH2 is the catalytic subunit of the Polycomb repressive complex 2 (PRC2), and its inhibition is an effective epigenetic therapy across multiple histotypes, including FP-RMS.<sup>54,102</sup> PRC2 functions by mono-, di-, or tri-methylating histone H3 at K27 (Figure 1.5).<sup>52</sup> The complex has three core subunits: SUZ12, EED, and either the EZH2 or EZH1 histone methyltransferase.<sup>52</sup> Traditionally, it has been accepted that PRC2-mediated H3K27 trimethylation is necessary to recruit Polycomb repressive complex 1 (PRC1) for adequate chromatin compaction.<sup>104</sup> PRC1 recognizes and binds to H3K27me<sub>3</sub>, then mediates monoubiquitination of histone H2A on lysine 119 (H2AK119Ub) through E3 ubiquitin ligation (Figure 1.5).<sup>104</sup> However, recent research has further delved into the relationship between PRC1 and PRC2 and found that knockouts of essential PRC2 proteins had only a minor effect on overall H2AK119Ub levels, suggesting that PRC1 does not entirely rely on H3K27me<sub>3</sub> for recruitment.<sup>105</sup> Overexpression of canonical PRC1 components is additionally correlated with worse outcomes and increased tumor aggression, similar to PRC2.<sup>106-110</sup>

There are several variants of PRC1 in mammals, but the core complex consists of RING1A or RING1B proteins and one of the six PCGF proteins (PCGF1 - PCGF6).<sup>111</sup> Canonical PRC1 complexes contain PCGF2/4 and are specified by the presence of one CBX protein (CBX2, 4, and 6 - 8) that binds H3K27me<sub>3</sub>.<sup>111</sup> There are also variant PRC1 complexes, which can contain any one of the six PCGFs, and incorporate RYBP/YAF2 in place of the CBX proteins, which do not require H3K27me<sub>3</sub>.<sup>111,112</sup> It has been shown that variant complexes are highly active and catalyze the majority of H2AK119Ub marks.<sup>62,113,114</sup> However, canonical PRC1, specifically PCGF4-RING1B, is necessary for

maintaining site-specific monoubiquitination in a precise and limited manner.<sup>115</sup> Abnormal expression of PCGF4, also known as B-lymphoma Moloney murine leukemia virus insertion region 1 (BMI1), is especially known to be oncogenic.<sup>65,106-110,116-123</sup>

#### **1.4.2 Alternative Polycomb roles**

While Polycomb complexes are generally considered to be traditionally repressive, there are additional roles that have been reported in mammalian systems. Polycomb complexes can also act as activators of gene expression. During differentiation of embryonic stem cells, a CBX8-PRC1 complex is required for initiating developmental gene activation.<sup>124</sup> CBX8-PRC1 occupies H3K36me3 active genes, though how this switch occurs remains unknown.<sup>124</sup> Another variant of PRC1, PRC1.5, becomes phosphorylated and reduces the catalytic activity of RING1B.<sup>125</sup> The AUTS2 protein present in the complex then recruits p300, which can acetylate histone tails and contribute to transcriptional activation.<sup>125</sup> PRC1 appears to also have a role in coactivating genes by regulating chromatin interactions. In mice, RING1B functions as a physical molecular bridge between an enhancer and the *Meis2* promoter, contributing to chromatin organization and developmental gene activation.<sup>126</sup> Recently, PRC1 has been found to influence 3D chromatin structure looping in *Drosophila* and mice.<sup>127</sup> In this study, the authors discovered that PRC1 can both repress and activate developmental genes, fine-tune expression, and may be gene-specific.<sup>127</sup> Together, these data indicate that Polycomb groups have a more complex role than simple gene silencing through histone modifications.

## 1.5 BMI1

### 1.5.1 BMI1 function and expression

*Bmi1* was first identified as a Myc-cooperating oncogene in mice and is a target of the Moloney virus insertion, resulting in accelerated B-lymphoid cancers.<sup>128</sup> BMI1 is a necessary component of canonical human PRC1.4<sup>111</sup> and is essential during normal development and hematopoiesis.<sup>129-131</sup> It is not the catalytic subunit, but the loss of BMI1 causes PRC1.4 collapse, resulting in a lack of H2AK119 ubiquitination.<sup>111</sup> Human *BMI1* is on chromosome 10p11.23 and has 10 exons and 9 introns.<sup>132</sup> It is 3.4 kb long and produces a 37 kDa protein consisting of 326 amino acids.<sup>132</sup> The BMI1 protein has three main regions: a helix-turn-helix domain, a conserved N-terminal RING finger, and a C-terminal PEST-like region.<sup>132</sup> The RING domain is required for the protein to localize to DNA, particularly DNA strand breaks.<sup>133</sup>

BMI1 plays an important role in morphogenesis during embryonic development and in hematopoiesis.<sup>134</sup> Deletion of *Bmi1* in mice leads to significant lethality soon after birth. Those mice that do survive have severe abnormalities in their immune systems, skeletal defects, and reduced density of neurons in the cerebellum.<sup>135</sup> Overexpression of BMI1 is known to be oncogenic across various human malignancies. It is involved in cancer cell proliferation, invasion/metastasis, chemosensitivity, and influences overall patient survival. BMI1 is intertwined in many molecular pathways, such as cancer stem cell self-renewal, repairing DNA damage, EMT, and developmental signaling.<sup>65,109,133,134</sup> BMI1 is expressed across human tissues, but most highly in bone marrow, pituitary glands, and testes.<sup>106,108</sup> The most described function of BMI1 is the repression of the *CDKN2A* (*p16-*

*INK4A* and *p14-ARF*) locus.<sup>65</sup> *CDKN2A* regulates retinoblastoma (Rb) and p53; thus, BMI1 is upstream of controlling cell cycle progression.<sup>136</sup> In normal stem cells, such as hematopoietic stem cells, BMI1 is highly expressed.<sup>110</sup> The self-renewal and maintenance of hematopoietic stem cells and neural stem cells are dependent on high BMI1 expression.<sup>106,110</sup> A significant aspect of malignancy is the capacity for self-renewal, and cancer cells can have stem-like properties.<sup>137</sup> Tumors are often heterogenous groups of cells, and some can have multipotent characteristics.<sup>138</sup> In these stem-like populations, aberrant BMI1 expression is reported.<sup>106,109,134,139</sup>

### **1.5.2 BMI1 is recruited to DNA breaks and regulates repair**

Cancerous cells often have unstable genomes prone that are prone to DNA damage.<sup>9</sup> As mentioned in 1.5.1, BMI1 supports the repair of DNA breaks. The induction of a DNA break leads to activation of multiple signaling pathways that lead to local modification of chromatin structure and recruitment of DNA repair complexes.<sup>140,141</sup> Histone H2AX is phosphorylated near sites of DNA breaks by ATM, ATR, and DNA-PK<sup>142</sup> and can spread to encompass a region of chromatin covering several Mb.<sup>143</sup> At sites of DNA damage, H2AK119 is ubiquitinated at both double-strand breaks and UV lesions.<sup>133</sup> Since H2AK119 monoubiquitination is essential to epigenetic regulation during both development and DNA repair, PcG proteins play a role in DNA repair response.<sup>130,133,144-146</sup> RING1B, a component of PRC1, is required for UV damage-induced H2AK119 monoubiquitination.<sup>147</sup> Loss of BMI1 is associated with decreased levels of the DNA damage repair response and checkpoint function. BMI1 is recruited to sites of DNA double-strand breaks for several hours, and data show that BMI1 is required for monoubiquitination of H2AK119 and supports homology-directed repair of DNA

damage.<sup>133</sup> These data indicate that PcG proteins such as RING1B and BMI1 are part of the ubiquitin ligase response involved in double-strand break-associated histone ubiquitination and support a role for BMI1 in DNA damage response.

### **1.5.3 BMI1 promotes the epithelial to mesenchymal transition**

Another hallmark of cancer that BMI1 has been reported to promote is the epithelial to mesenchymal transition (EMT). EMT promotes cancer cell invasion and metastasis. The epithelial cells of a primary solid tumor transition to a more mesenchymal phenotype and disseminate to new organ sites, forming metastatic lesions. High BMI1 expression is positively correlated with metastasis and is a significant predictor of worse patient outcomes in melanoma, breast cancer, and prostate cancer.<sup>107,148-150</sup> The stem-cell-like properties of subpopulations of tumor cells that express high levels of BMI1 may provide plasticity and a proliferative advantage both in the primary tumor and in adapting to metastatic niches.<sup>14,44,151-153</sup> EMT regulators such as TWIST1 have been shown to directly regulate BMI1 expression in head and neck squamous cell carcinoma (HNSCC), and both were found to be critical for tumor initiation.<sup>121</sup> Overexpression of BMI1 was also discovered to induce EMT in this model. Metastatic *in vivo* models of breast cancer additionally demonstrate that BMI1 collaborates with H-RAS to promote invasion and increased brain metastases.<sup>154</sup> Targeting BMI1-high cancer cells in HNSCC sensitizes tumor cells to chemotherapy and eliminates metastases, and prevents tumor relapse.<sup>155,156</sup> Overall, cancers with high levels of BMI1 seem to have greater invasive potential due to the increased stemness and plasticity that high PRC1 activity provides.

#### 1.5.4 BMI1 inhibition as a novel therapeutic approach

Recently, several small molecule inhibitors of BMI1 have been studied in multiple cancers and found to be an effective treatment option. The first-generation inhibitor from PTC Therapeutics, PTC-209, was used in many initial studies of BMI1 inhibition.<sup>119,139,157,158</sup> PTC-209 functions by binding the mRNA of BMI1 within the 5'UTR or 3'UTR and preventing translation.<sup>158</sup> The next generation of BMI1 inhibitor, PTC-028, is orally bioavailable and was efficient at reducing tumor burden across histotypes *in vivo* both as a single agent therapy and combined with standard of care.<sup>116,117,159,160</sup> PTC-028 depletes BMI1 at the protein level through hyperphosphorylation and subsequent degradation.<sup>159</sup> BMI1 inhibition is possibly an indirect effect downstream of microtubule depolymerization.<sup>161</sup> The most recent BMI1 inhibitor, PTC-596, functions similar to PTC-028 but has a much lower IC<sub>50</sub>.<sup>161-165</sup> It has been investigated in various aggressive solid tumors and hematological malignancies.<sup>161-165</sup> PTC-596 was used as a monotherapy in phase I clinical trial (NCT02404480) for advanced solid tumors (colorectal, lung, glioblastoma, and more) in adults.<sup>166</sup> The drug was well-tolerated with mild gastrointestinal side effects.<sup>166,167</sup> Two more clinical trials are recruiting: one for advanced leiomyosarcoma in combination with dacarbazine (NCT03761095) and another for ovarian cancer in combination with neoadjuvant chemotherapy (NCT03206645). Of particular interest is a phase Ib clinical trial (NCT03605550) that is in progress for pediatric patients with diffuse intrinsic pontine glioma (DIPG) and high-grade glioma (HGG), combining PTC-596 with radiation therapy. As FP-RMS is primarily a pediatric cancer, the results from this trial will confirm if this BMI1 inhibition in pediatric patients is safe since BMI1 is an important developmental regulator. PTC-596 has been granted a

fast track designation and orphan drug designation by the FDA, indicating the promise of BMI1 inhibition as a novel, clinically translatable cancer therapeutic.<sup>168</sup>

### **1.6 Scope of this dissertation**

This dissertation seeks to define how BMI1 contributes to tumorigenesis in FP-RMS and investigate the inhibition of BMI1 as a novel therapeutic in this understudied pediatric malignancy. Here, we investigate the hypothesis that BMI1 is a critical factor in FP-RMS cell proliferation and survival and its novel role in influencing Hippo signaling. The long-term goal is to provide preclinical data and mechanisms to argue BMI1 as a tractable therapeutic target in FP-RMS, which may additionally apply to other sarcoma histotypes. Chapter 2 will discuss the genetic knockdown and pharmacologic inhibition of BMI1 and the effects on tumor cell viability *in vitro* and *in vivo*, and how BMI1 influences the Hippo pathway. Chapter 3 will discuss the impacts of BMI1 inhibition on the transcriptome. Chapter 4 will review my findings in relation to the current literature and the future implications of my work.



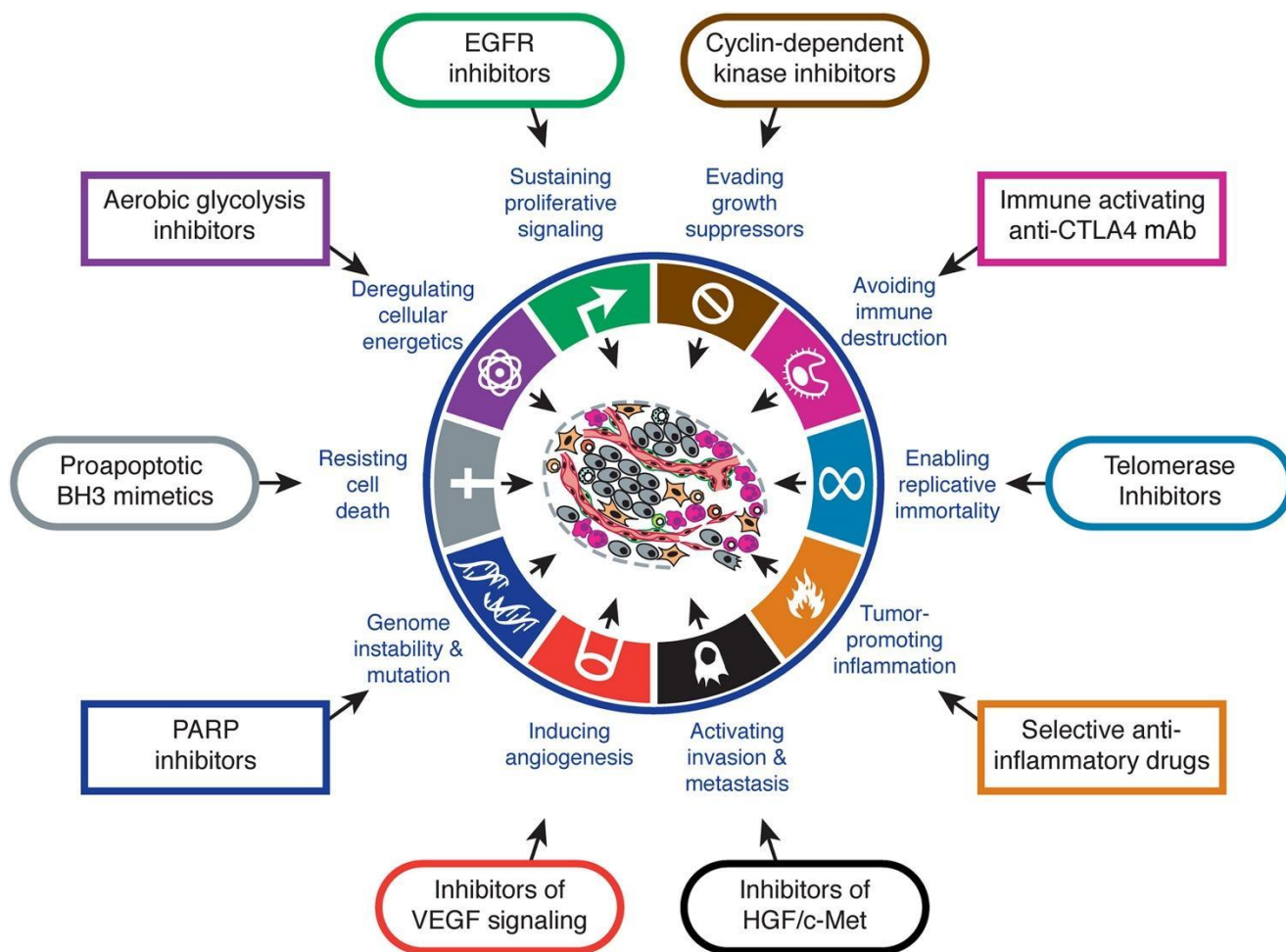


**Figure 1.1 Hallmarks of cancer.** Image adapted from Hanahan and Weinberg.<sup>9</sup> A collection of different facets of cancer progression and potential inhibitors.

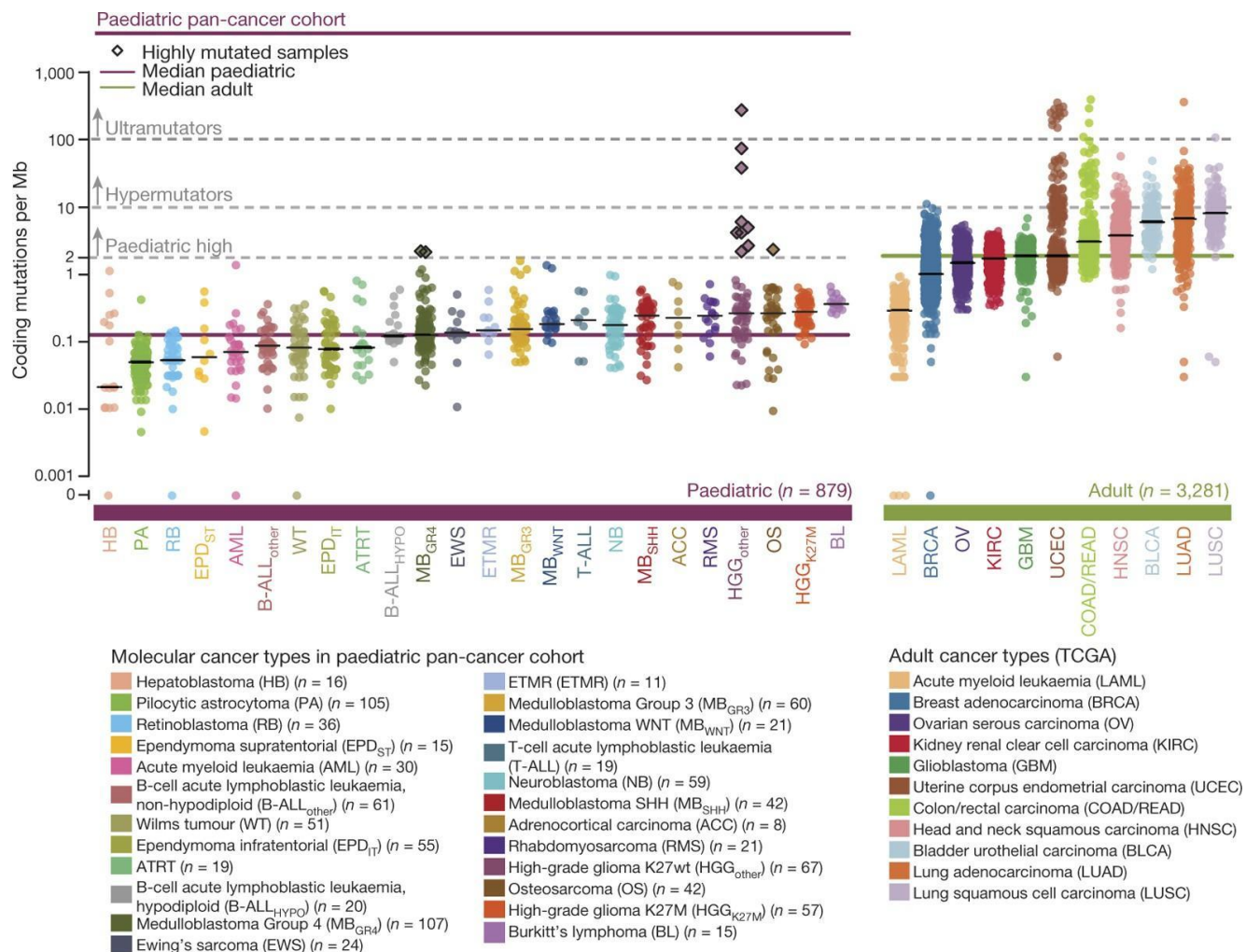


**Figure 1.2 Mutation rate in pediatric cancers versus adult cancers.** Image

adapted from Gröbner *et al.* 2018.<sup>22</sup> Pediatric cancer mutation rates, including RMS, are far lower than adult cancers.

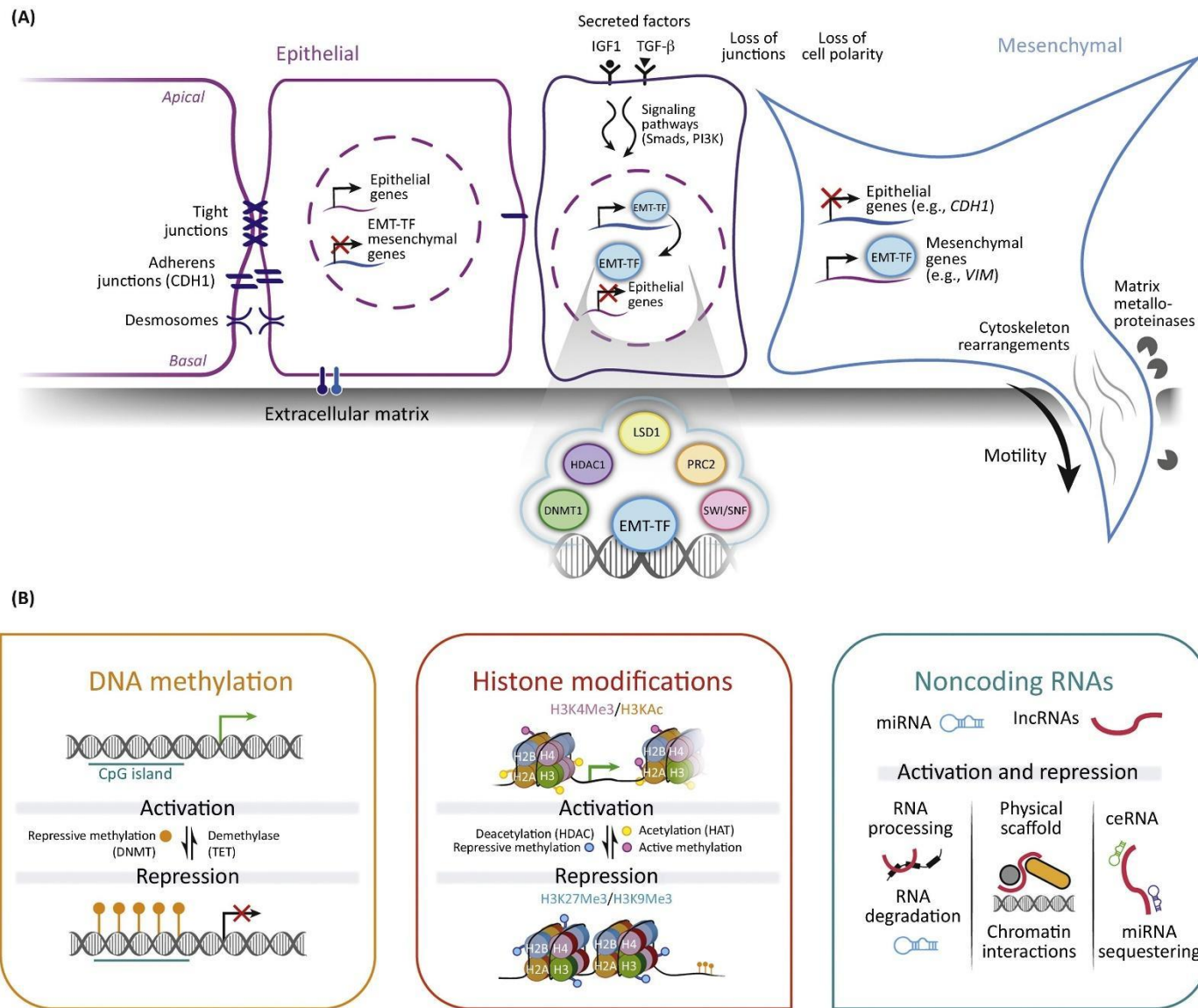


**Figure 1.3 Epithelial to mesenchymal transition.** Image adapted from Skrypek, *et al.*<sup>169</sup> Epigenetic factors such as DNA methylation, histone modifications, and noncoding RNAs contribute to the epithelial to mesenchymal transition.



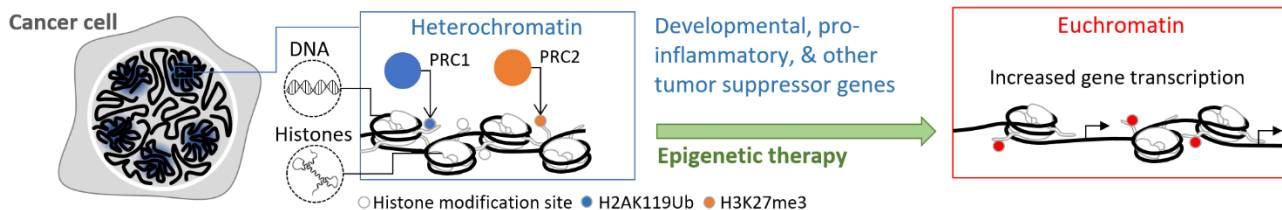


**Figure 1.5 Polycomb repressive complexes promote heterochromatin**

**formation and prevent efficient gene transcription.** Image adapted from Dr.

Karmella Haynes. Polycomb repressive complex 1 (PRC2) monoubiquitinates residue

K119 on histone H2A. Polycomb repressive complex 2 (PRC2) trimethylates residue K27

on histone H3. Both of these histone marks combined lead to heterochromatin

formation and prevent gene transcription. Epigenetic therapy can lead to activation of

tumor suppressor genes through inhibiting PRC1/2 through promoting euchromatin

formation.

**2. Epigenetic regulator BMI1 promotes alveolar rhabdomyosarcoma proliferation and constitutes a novel therapeutic target**

**Epigenetic regulator BMI1 promotes alveolar rhabdomyosarcoma proliferation and constitutes a novel therapeutic target**

Cara E. Shields<sup>1</sup>, Sindhu Potlapalli<sup>1</sup>, Selma M. Cuya-Smith<sup>1</sup>, Sarah K. Chappell<sup>1</sup>, Dongdong Chen<sup>1</sup>, Daniel Martinez<sup>2,3</sup>, Jennifer Pogoriler<sup>3</sup>, Komal S. Rathi<sup>2,4</sup>, Shiv A. Patel<sup>1</sup>, Kristianne M. Oristian<sup>5,6</sup>, Corinne M. Linardic<sup>5,6</sup>, John M. Maris<sup>2,4</sup>, Karmella A. Haynes<sup>7\*</sup>, Robert W. Schnepf<sup>1\*</sup>

<sup>1</sup>Aflac Cancer and Blood Disorders Center, Department of Pediatrics, Division of Pediatric Hematology, Oncology, and Bone Marrow Transplant, Emory University School of Medicine, Atlanta, GA 30322, USA; Winship Cancer Institute, Emory University, Atlanta, GA 30322, USA; Children's Healthcare of Atlanta, Atlanta, GA 30322, USA.

<sup>2</sup>Department of Pediatrics, Perelman School of Medicine, University of Pennsylvania, Philadelphia, PA 19104, USA.

<sup>3</sup>Department of Pathology and Laboratory Medicine, Children's Hospital of Philadelphia, University of Pennsylvania, Philadelphia, PA 19104, USA.

<sup>4</sup>Division of Oncology and Center for Childhood Cancer Research, Children's Hospital of Philadelphia, Philadelphia, PA 19104, USA

<sup>5</sup>Department of Pediatrics, Duke University Medical Center, Durham, NC 27710, USA.

<sup>6</sup>Department of Pharmacology & Cancer Biology, Duke University Medical Center, Durham, NC 27710, USA.

<sup>7</sup>Wallace H. Coulter Department of Biomedical Engineering, Emory University, Atlanta, GA, 30322, USA

\*Corresponding authors: Robert W. Schnepf – robert.schnepf@emory.edu, Karmella A. Haynes – karmella.ann.haynes@emory.edu

**Running Title:** BMI1 promotes rhabdomyosarcoma proliferation

**Keywords:** rhabdomyosarcoma, BMI1, Hippo, epigenetics, pediatric cancer

**Conflicts of interest:** Robert W. Schnepf reports employment at Janssen R&D. There are no other conflicts of interest.

**Figures:** 6 figures, 4 supplementary figures, 1 supplementary table



**Abstract**

Rhabdomyosarcoma (RMS) is an aggressive pediatric soft tissue sarcoma. There are two main subtypes of RMS, alveolar rhabdomyosarcoma (ARMS) and embryonal rhabdomyosarcoma. ARMS typically encompasses fusion-positive rhabdomyosarcoma, which expresses either PAX3-FOXO1 or PAX7-FOXO1 fusion proteins. There are no targeted therapies for ARMS; however, recent studies have begun to illustrate the cooperation between epigenetic proteins and the PAX3-FOXO1 fusion, indicating that epigenetic proteins may serve as targets in ARMS. Here, we investigate the contribution of BMI1, given the established role of this epigenetic regulator in sustaining aggression in cancer.

We determined that *BMI1* is expressed across ARMS tumors, patient-derived xenografts, and cell lines. We depleted BMI1 using RNAi and inhibitors (PTC-209 and PTC-028) and found that this leads to decreased cell growth/increase in apoptosis *in vitro* and delays tumor growth *in vivo*. Our data suggest that BMI1 inhibition activates the Hippo pathway via phosphorylation of LATS1/2 and subsequent reduction in YAP levels and YAP/TAZ target genes. These results identify BMI1 as a potential therapeutic vulnerability in ARMS and warrant further investigation of BMI1 in ARMS and other sarcomas.

## 2.1 Introduction

Rhabdomyosarcoma (RMS) is a tumor of developing skeletal myoblast-like cells that primarily afflicts children.<sup>24</sup> There are two major subtypes of pediatric rhabdomyosarcoma, alveolar and embryonal, which are named based upon their histologic appearance. Approximately 80% of alveolar rhabdomyosarcomas (ARMS) are characterized by either PAX3-FOXO1 or PAX7-FOXO1 fusion proteins and are thus termed fusion-positive; embryonal rhabdomyosarcomas (ERMS) lack these fusions and are termed fusion-negative.<sup>24,32</sup> ARMS is more aggressive and has a worse outcome compared to ERMS. The prognosis is even direr for ARMS patients with metastatic dissemination, who have survival rates of only 30%.<sup>25,171</sup> Currently, the standard of care is multimodal and intensive, consisting of multiagent chemotherapy, radiation, and surgery.<sup>29,172</sup> Given the substantial morbidity and mortality of ARMS, there is a need for new, translatable treatment options.

While the PAX-FOXO1 fusion proteins are pathognomonic for this disease, these proteins remain challenging drug targets.<sup>24,38,40,41</sup> To date, efforts to pharmacologically inhibit PAX-FOXO1 have not yielded robust clinical results.<sup>38</sup> Moreover, a recent study has shown that PAX3-FOXO1 is necessary for the initiation/maintenance of ARMS but may not be required for recurrence, suggesting that the targeting of diverse oncogenic networks may be necessary to optimize the treatment of this cancer.<sup>39,41</sup> The interaction of PAX-FOXO1 fusions with the epigenome has garnered increasing attention.<sup>39,91,173</sup> PAX3-FOXO1-mediated gene regulation requires BRD4 at super-enhancers, revealing a novel epigenetic vulnerability in ARMS.<sup>91</sup> Further, the fusion protein also requires the

chromatin remodeling activity of CHD4 to activate a subset of its target genes.<sup>92</sup> Epigenetic regulation may also act upstream of PAX3-FOXO1. Histone deacetylases control the expression of SMARCA4, a chromatin remodeler, which subsequently allows expression of *miR-27a*, which in turn decreases *PAX3-FOXO1* mRNA stabilization.<sup>97</sup> These studies provide evidence for a significant relationship between the epigenome and the tumorigenicity of ARMS and suggest that druggable epigenetic regulators other than PAX3-FOXO1 remain to be discovered.

Inspired by the studies highlighted above, we searched for druggable epigenetic proteins involved in ARMS that may represent dependencies. The Polycomb group proteins are epigenetic complexes traditionally associated with gene repression by chromatin compaction.<sup>174</sup> These complexes are known regulators of pluripotency, stem cell renewal, and epigenetic memory and have been studied extensively across species and various human diseases.<sup>175</sup> They consist of Polycomb Repressive Complex 1 and 2 (PRC1/2), which control monoubiquitination of H2AK119 and trimethylation of H3K27, respectively.<sup>52,103,130,174</sup> Dysregulation of PRC1/2 protein members are implicated in tumor initiation and progression in many adult cancers but remain relatively understudied in pediatric cancers.<sup>53</sup> High levels of H2AK119Ub and H3K27me3 across the genome in many cancers are associated with worse outcomes<sup>52,53</sup>, possibly due to the repression of tumor suppressor genes such as *CDKN2A*, which has a significant role in controlling the cell cycle.<sup>64</sup> Specifically in ARMS, PRC2 members such as EZH2 have been analyzed and found to promote survival.<sup>102</sup> Thus, we hypothesized that a member of PRC1, B lymphoma Mo-MLV insertion region 1 (BMI1), also known as Polycomb Group Factor 4 (PCGF4), would be a viable epigenetic target in ARMS. BMI1 has no enzymatic

activity itself but is a required component of PRC1 and is a known oncogene in numerous adult cancers, including hematological malignancies, breast cancer, ovarian cancer, and more.<sup>53,106,174,176-178</sup> BMI1 has also been studied in pediatric cancers such as medulloblastoma and Ewing sarcoma, but its possible role in RMS has not yet been identified.<sup>162,179,180</sup> Additionally, BMI1 has been found to promote self-renewal in skeletal muscle and was also one of the components, along with TERT and PAX3-FOXO1, used to transform normal human myoblasts into a cell culture model of ARMS.<sup>181,182</sup> In these studies, we identify BMI1 as a novel therapeutic liability in ARMS.

## **2.2 Materials & Methods**

### **2.2.1 In silico data**

RNA-sequencing data (dbGaP accession # phs001437) of six RMS patient-derived xenograft (PDX) models and cell lines from the Pediatric Preclinical Testing Consortium (PPTC) was processed using the STAR alignment tool and subsequently normalized using the RSEM package based upon the hg38 reference genome and the GENCODE v23 gene annotation. Gene expression values were quantified as Fragments Per Kilobase per Million mapped reads (FPKM).

### **2.2.2 Cell culture**

Rhabdomyosarcoma cell lines (Rh30 and Rh41) were obtained from the Children's Hospital of Philadelphia (courtesy of Dr. Margaret Chou) as well as from the Children's Oncology Group (Rh28 and CW9019). The Emory Genomics Core authenticated cell lines for use, and *Mycoplasma* testing was performed every 3 - 6 months using the *Mycoplasma* test kit (PromoCell, PK-CA91-1024). Cells were cultured in a humidified incubator at 37°C with 5% CO<sub>2</sub>. Rh30 and CW9019 were passaged regularly in DMEM (Corning), and Rh28 and Rh41 were passaged in RPMI 1640 (Corning). Media was supplemented with 10% FBS (Corning) and 1% L-glutamine (Gemini). No antibiotics or antimycotics were added to the media.

### **2.2.3 Plasmids, lentiviral preparation, and transduction**

BMI1 shRNA plasmids were purchased from Sigma (pLKO.1). The catalog numbers are shBMI1-2: TRCN0000020156 and shBMI1-4: TRCN0000218780. YAP-

overexpression plasmids pGAMA-Empty (Addgene plasmid #74755) and pGAMA-YAP (Addgene plasmid #74942) were kind gifts from Jenny Shim in Kelly Goldsmith's lab at Emory University. Generation of infectious lentiviral particles and subsequent cell transduction was performed as previously described<sup>183</sup> with the following key conditions: FuGENE 6 (Promega) was used to transfect select plasmids, with pMD2.G (VSV-G plasmid) and psPAX2 (packaging plasmid), into HEK293T cells. Viral supernatant was collected 2-3 days after transfection, filtered with a 0.45  $\mu\text{m}$  nitrocellulose membrane, supplemented with 8  $\mu\text{g}/\text{mL}$  polybrene (Sigma), and used for transduction of one million cells seeded into 10 cm plates. Fresh media was added 6 hr post-transduction, and the media was replaced the next day again. Two days later, puromycin was added to select transgenic cells.

#### **2.2.4 siRNA transfection**

Cells were plated at 200,000 cells per well in a 6 well plate. The following day, cells were transfected using DharmaFECT 1 (Horizon Discovery) and 25 nM of an siRNA ON-TARGETplus SMARTpool (Horizon Discovery) or ON-TARGETplus Non-targeting Control Pool (Horizon Discovery). Horizon Discovery catalog numbers for each siRNA pool used in this study are ON-TARGETplus Non-targeting Control Pool (D-001810-10-20), BMI1 (L-005230-01-0010), LATS1 (L-004632-00-0010), and LATS2 (L-003865-00-0010). Cells were harvested for analysis 72 hr post-transfection.

### **2.2.5 Real-Time PCR and western blots**

RNA was isolated from cells using the RNeasy Mini Kit (QIAGEN) and Real-Time PCR (RT-PCR) analysis performed as previously described.<sup>183</sup> For western blots, cell samples were lysed in RIPA (Boston Bioproducts) containing cOMplete protease inhibitor cocktail (Roche), and PMSF (Cell Signaling Technology) then sonicated. Protein concentrations were determined using the Bradford assay (Bio-Rad), and samples (20 µg protein) run on SDS PAGE Bis-Tris 4-12% gels (Life Technologies). Lambda protein phosphatase (New England BioLabs) was used per the manufacturer's instructions on select cellular lysates. The gels were transferred to nitrocellulose membranes and membranes blocked in 5% Blotting-Grade Blocker (Bio-Rad) in Tris-Buffered Saline with 1% Tween-20 (Cell Signaling Technology). The blots were incubated with primary antibodies in 5% BSA (Jackson Laboratory) overnight at 4°C. The secondary antibodies used were IRDye 800CW/680RD anti-Rabbit or anti-Mouse (Li-COR Biosciences) at 1:50,000 and 1:5,000, respectively. Whole blots were scanned using the Li-COR Odyssey. The primary antibodies and dilutions are listed in Supplementary Table S2.1. Any quantifications are presented as relative adjusted densities and were performed in ImageJ.

### **2.2.6 Cell growth assays**

CellTiter-Glo (Promega) and Caspase-Glo (Promega) were used to assess the viability of both shRNA/siRNA manipulated and drug-treated cells. On day 0, 2,000 cells/well were plated in a 96 well plate and on day 1 treated with control or drug. To calculate IC<sub>50</sub>s, cells were treated with a 7-log dose range of inhibitor (10<sup>-11</sup>M - 10<sup>-5</sup>M). Cells proliferated for an additional 96 hr before performing CellTiter-Glo or Caspase-Glo

per the manufacturer's instructions. IC<sub>50</sub>s were calculated by log transforming concentrations, fitting to a three-parameter logistic, nonlinear regression curve, and finding the half-maximal concentration.<sup>184</sup>

For crystal violet colony formation assays, we plated 2,000 cells/well in duplicate in 6 well plates. We treated cells with drugged media and allowed cells to proliferate for 10 days before washing/fixing with 3.7% formaldehyde then staining with 0.0025% crystal violet. Plates were dried overnight and were imaged with a Nikon D3400.

### **2.2.7 Flow cytometry**

On day 0, cells were seeded at 1 million cells /10 cm plate, and PTC-028 added on day 1. Cells were harvested after 24 hr for BrdU-APC/7-AAD staining and 72 hr for Annexin V-FITC/PI staining. Staining was performed using Annexin V-FITC/PI (BD Biosciences) or BrdU-APC/7-AAD (BD Biosciences) kits following the manufacturer's instructions. For Annexin V/PI staining, cell media containing dead cells in suspension was also collected. Samples were run within 1 hr on a Cytoflex 96 well plate loader, with 50,000 - 100,000 events collected per sample. Compensation, gating, and analyses were performed in FlowJo.

### **2.2.8 *In vivo* xenograft model**

Heterozygous nude mice (Crl:NU(NCr)-*Foxn1*<sup>nu/+</sup>) between 5 - 6 weeks old (Charles River) were housed in sterile cages at the Health Sciences Research Building Animal Facility at Emory University. Mice acclimated to their new environment for 1 week after being received and were maintained in 12 hr day/night cycles. All experimental



procedures were Emory IACUC approved. 2 million Rh30 cells were mixed 1:1 with Matrigel (Corning) and subcutaneously injected into the right flank of each mouse. As previously described, treatments began when tumors were equal to or greater than 100 mm<sup>3</sup>.<sup>117,159</sup> The mice were tagged and randomly separated into 2 groups: vehicle (n = 10) and PTC-028 (n = 10). Mice received vehicle (0.5% HPMC, 1% Tween-80) or 15 mg/kg PTC-028 twice weekly by oral gavage.<sup>117,159</sup> Weights and tumor sizes were measured three times weekly. Tumor volumes were calculated using an ellipsoid volume formula:  $\pi / 6 \times L \times W \times H$ .<sup>185</sup> In accordance with the IACUC protocol, mice were sacrificed when tumors reached a volume greater than or equal to 1500 mm<sup>3</sup>. Collected tumors were removed post-mortem and snap-frozen in liquid nitrogen for immunoblotting or formalin-fixed and paraffin-embedded for immunohistochemistry.

### **2.2.9 Immunohistochemistry**

A representative tumor array of pediatric solid tumors (duplicate punches) was constructed at The Children's Hospital of Philadelphia. An additional normal pediatric tissue array consisted of duplicate punches of 41 normal pediatric tissues/organs procured from the Children's Hospital of Philadelphia from 2005 – 2012. BMI1 antibody (Cell Signaling Technology) was used to stain formalin-fixed paraffin-embedded tissue slides. Staining was performed on a Bond Rx automated staining system (Leica Biosystems). The Bond Refine polymer staining kit (Leica Biosystems) was used. The standard protocol was followed apart from the primary antibody incubation, which was extended to 1 hr at room temperature, and the post-primary step was excluded<sup>184</sup>. BMI1 antibody was used at a 1:200 dilution, and antigen retrieval was performed with E1 (Leica Biosystems) retrieval solution for 20 min. Slides were rinsed, dehydrated through a series

of ascending concentrations of ethanol and xylene, and then cover slips were added. Stained slides were then digitally scanned at 20x magnification on an Aperio CS-O slide scanner (Leica Biosystems). Tumor microarrays were scored by a pediatric pathologist (JP) for the most prominent intensity of nuclear staining (score 0-3 with 1 representing weak/equivocal, 2 moderate, and 3 strong positive staining) as well as for percentage of tumor nuclei staining.<sup>186</sup> An overall score was obtained by multiplying intensity by the percentage of tumor cells staining. Both cores for each of the two cores per tumor were averaged for the final score.

#### **2.2.10 Statistical analyses**

Data analyses were performed in GraphPad Prism 8. Statistical significance was determined using an unpaired student two-tailed t-test for two groups. Groups of three or more were analyzed using an ANOVA. All assays were performed in duplicate unless otherwise stated and presented using mean and standard deviation. Survival curves were generated in Prism 8 using the Kaplan-Meier method.<sup>187</sup>

## 2.3 Results

### 2.3.1 BMI1 is highly expressed in rhabdomyosarcoma

To investigate BMI1 as a potential therapeutic vulnerability in ARMS, we sought to define its expression pattern in sarcomas, broadly considered. We first examined OncoPrint and determined the expression of *BMI1* in both adult and pediatric sarcomas.<sup>188</sup> We noted that *BMI1* is robustly expressed in pediatric sarcomas, such as Ewing sarcoma and osteosarcoma, as well as in adult subtypes, including leiomyosarcoma and chondrosarcoma (Supp. Fig. S2.1A - B).<sup>179,188,189</sup>

We then focused on RMS. We began by interrogating available datasets and first examining human exon array data from ARMS and ERMS patient tumor samples.<sup>190</sup> We observed that *BMI1* expression levels are expressed across both subtypes (Fig. 2.1A). To focus on ARMS specifically, we analyzed *BMI1* levels from RNA-seq ARMS patient-derived xenograft (PDX) from the Pediatric Preclinical Testing Consortium (PPTC).<sup>191</sup> We found that *BMI1* mRNA levels are expressed in ARMS. (Fig. 2.1B). Furthermore, we probed the OncoPrint database and found *BMI1* to be expressed in both ARMS and ERMS (Supp. Fig. S2.1C).<sup>34</sup> Using immunohistochemistry, we stained a tumor microarray bearing ARMS patient samples and confirmed that BMI1 is expressed at the protein level (Fig. 2.1C), with normal pediatric cerebellum shown as a negative control.

Finally, we surveyed the expression of BMI1 across the ARMS cell lines Rh28, Rh30, Rh41, and CW9019 and found that BMI1 is expressed across all models (Fig. 1D). Notably, Rh28, Rh30, and Rh41 have the PAX3-FOXO1 fusion, while CW9019 harbors the PAX7-FOXO1 fusion.<sup>192</sup>

### **2.3.2 Genetic knockdown of BMI1 leads to reduced cellular proliferation in ARMS cells**

Our analyses demonstrate that BMI1 is highly expressed in both fusion-positive and negative rhabdomyosarcoma. Given the clinical aggression of ARMS, in subsequent investigations, we focused exclusively on this subtype. We chose two ARMS cell line models, Rh28 and Rh30, for genetic knockdown studies, as these models have been well-studied and are readily transduced and transfected. First, we depleted BMI1 using two independent shRNAs directed against BMI1 and confirmed effective knockdown of BMI1 by western blot (Fig. 2.2A - B). We observed that BMI1 knockdown significantly reduces cell proliferation by CellTiter-Glo, an assay that quantitates ATP to determine the number of viable cells present (Fig. 2.2A - B).<sup>193</sup> To further validate these findings, we utilized pooled siRNAs (comprised of 4 different siRNAs directed against BMI1) to deplete BMI1 transiently and again demonstrated significantly decreased proliferation (Fig. 2.2C - D). Knockdown of *BMI1* was confirmed by RT-PCR (Fig. 2.2C - D). Thus, with both transient and longer-term depletion of BMI1, we observed decreased proliferation.

### **2.3.3 Pharmacologic inhibition of BMI1 decreases cell proliferation *in vitro***

We assessed the effects of pharmacologic inhibition of BMI1 on ARMS. To do so, we initially employed PTC-209, an inhibitor that reduces BMI1 protein levels and lowers PRC1 activity in cancer cells, with minimal effects in non-cancerous cell line models<sup>139</sup>. In several aggressive cancer models, such as colorectal cancer and biliary tract cancer, PTC-209 has been found to impair cell growth by promoting cell cycle arrest and causing cell death.<sup>119,139</sup> Guided by previous studies, we treated 4 ARMS cell lines with PTC-209 across a 7-log dose range ( $10^{-11}$  M -  $10^{-5}$  M). Treatment with PTC-209 significantly

decreases cell proliferation (Fig. 2.3A - D) in all 4 cell lines, with IC<sub>50</sub>s ranging from 483 nM to 872 nM (Fig. 2.3K). Protein levels of BMI1 were also reduced with PTC-209 treatment (Supp. Fig S2.2A).

Next, we assessed the impact of a second-generation BMI1 inhibitor, PTC-028, on ARMS proliferation. PTC-028 inhibits BMI1 by a different method than PTC-209, resulting in hyperphosphorylation of BMI1 and disrupting its function.<sup>159</sup> It is also orally bioavailable, allowing for preliminary investigation of BMI1 disruption in the *in vivo* setting; for these reasons, in subsequent studies, we employed PTC-028. Treatment with PTC-028 similarly decreases cell proliferation (Fig. 2.3F - J) in all 4 cell lines, yielding decreased BMI1 protein levels (Supp. Fig. S2.2A). To test if this was due to hyperphosphorylation of the BMI1 protein as previously reported<sup>159</sup>, we treated Rh30 cells with PTC-028 at 100 nM and 1  $\mu$ M, then collected lysates after 12 hr (Supp. Fig. S2.2B). Some lysates were treated with a Lambda ( $\lambda$ ) protein phosphatase to remove phosphorylation bands and confirm BMI1 protein loss. We indeed found that BMI1 is being hyperphosphorylated after PTC-028 addition at both 100 nM and 1  $\mu$ M doses, and the BMI1 protein level decreases slightly at 1  $\mu$ M treatment (Supp. Fig. S2.2B). Next, as expected, IC<sub>50</sub>s were lower for PTC-028 than for PTC-209, consistent with the greater potency of PTC-028 (Fig. 2.3K). Additionally, brightfield microscopy and colony formation assays showed that viability is significantly diminished with 50 nM and 100 nM doses of PTC-028 in Rh30 and CW9019 (Supp. Fig. S2.2C - D). Thus, our data indicate that two BMI1 inhibitors significantly decrease proliferation in ARMS cell line models, mimicking the effects we observed with genetic disruption of BMI1.

### 2.3.4 Targeting BMI1 decreases cell cycle progression and increases apoptosis in ARMS

We next aimed to define the mechanisms by which BMI1 promotes cell proliferation. Previous investigations have demonstrated that BMI1 influences cell cycle progression in part through repression of the *CDKN2A* (*p16-INK4a*) locus<sup>108</sup>, although this regulation is not observed in all contexts. BMI1 also possesses functions independent of *CDKN2A* repression, including regulating genes involved in differentiation and cell contact inhibition in Ewing sarcoma and androgen receptor expression in prostate cancer.<sup>179,194</sup>

To investigate the influence of BMI1 on cell cycle progression, we treated Rh30 with PTC-028 at doses below and near the IC<sub>50</sub> of Rh30 and then performed BrdU/7-AAD staining. We observed a ~10% increase in the sub-G1 population ( $p = 0.0358$ ) and a 50% decrease in the percentage of cells in S phase ( $p = 0.0426$ ) when the cells were treated with 50 nM of PTC-028 for 24 hr (Fig. 2.4A - 4B). Given the increase in the sub-G1 population, we speculated that BMI1 additionally increases apoptosis *in vitro*. Therefore, we performed Annexin V/PI staining after 72 hr of PTC-028 treatment and observed a dose-dependent increase (20-50% across cell lines,  $p < 0.05$ ) in the percentage of apoptotic cells (Fig. 2.4C - 4D). To further verify the apoptotic phenotype, we probed for cleaved PARP and noted an increase in PARP cleavage with PTC-028 addition (Fig. 4E). Additionally, we performed Caspase-Glo analyses of shBMI1/siBMI1 Rh28 and Rh30 cell lines to complement these data. We discovered an increase (shBMI1: 2-4 fold across cell lines,  $p < 0.05$ , siBMI1: 3-5 fold,  $p < 0.05$ ) in caspase 3/7 activity (Supp. Fig. S2.3A - B). We delved down further and analyzed apoptosis in siBMI1 transfected Rh28 and Rh30

cells by Annexin V/PI staining and again noted an increase (2.8-5 fold,  $p < 0.05$ ) in the apoptotic fractions (Supp. Fig. S2.3C). Together, these data confirm that pharmacologically targeting BMI1 impairs progression to S phase and results in apoptosis.

### **2.3.5 Single agent PTC-028 treatment causes tumor growth delay *in vivo***

To provide the initial foundation for targeting BMI1 in ARMS, we employed PTC-028, which is orally bioavailable.<sup>117,159</sup> Nude mice bearing Rh30 xenografts were treated with vehicle or PTC-028 (15 mg/kg by oral gavage) daily, a dosing scheme guided by previous studies.<sup>117,159</sup> As shown in Fig. 2.5A, treatment with PTC-028 delays tumor growth compared to vehicle (Fig. 2.5A,  $p = 0.0005$ ). The treatment was well-tolerated, with no significant change in weights (Fig. 2.5B) and no signs of pain or distress in the mice observed. The median survival of the vehicle group was 19 days, while the median survival of the PTC-028 treated group was 39 days (Fig. 2.5C,  $p = 0.0002$ ). The tumors were harvested and analyzed for BMI1 protein levels. By western blot, we noted that tumors in PTC-028 treated mice had an approximately 30% reduction in BMI1 levels compared to control. (Fig. 2.5D). Interestingly, however, in contrast to the *in vitro* setting, we noted no increase in cleaved PARP (Fig. 2.5E). Collectively, these results suggest that single-agent treatment with PTC-028 delays, though does not abrogate, the growth of an ARMS xenograft.

### **2.3.6 BMI1 negatively influences Hippo signaling**

Given our findings demonstrating the positive influence of BMI1 on cell cycle progression, we first asked whether BMI1 inhibits *CDKN2A* expression in ARMS.<sup>65</sup> A

canonical target of BMI1 is *CDKN2A*, and repression of *CDKN2A* controls cell cycle progression to S phase.<sup>65,108</sup> We found that BMI1 inhibition by PTC-028 treatment leads to a slight upregulation in *CDKN2A* protein levels in Rh30 (Supp. Fig. S2.4A).

We then undertook a candidate-based approach to identify additional novel BMI1-influenced signaling networks in ARMS. We focused on Hippo signaling for the following reasons: 1. BMI1 has been reported to interact with the Yes-Associated Protein (YAP) in Ewing sarcoma, though whether this occurs in RMS is unclear<sup>179</sup>, 2. PAX3-FOXO1 has been found to suppress the Hippo pathway in ARMS<sup>195</sup>, and 3. Loss of Hippo signaling by Mst knockout was shown to accelerate ARMS tumorigenesis.<sup>196</sup>

We initially explored the effects of BMI1 inhibition on canonical Hippo signaling. Normally, YAP/TAZ binds TEAD, and YAP/TAZ/TEAD complexes influence groups of genes implicated in cell cycle progression and growth.<sup>197</sup> MST1 phosphorylates and activates LATS1/2, which in turn phosphorylates YAP/TAZ, leading to YAP/TAZ degradation and exclusion from the nucleus, with subsequent reduction in the amount of YAP/TAZ/TEAD complexes capable of transcriptional activation.<sup>197</sup> Upon treatment with PTC-028, we observed that LATS1/2 phosphorylation increases and YAP levels decrease (Fig. 2.6A), indicating that the Hippo pathway is activated when BMI1 is inhibited. However, there is no change in total LATS1/2 levels or MST1 phosphorylation (Supp. Fig. S2.4B - C), suggesting a possible alternative mechanism for the increase in LATS1/2 phosphorylation. We depleted BMI1 using siRNAs and similarly observed an increase in LATS1/2 phosphorylation and a decrease in YAP protein expression (Fig. 2.6B). BMI1 inhibition appears to promote Hippo pathway activation through LATS1 phosphorylation.



We then looked further downstream at several canonical YAP/TAZ targets. We chose several canonical YAP/TAZ targets, AXL, CYR61 (CCN1), and CTGF (CCN2), which are involved in processes such as cellular proliferation, cell cycle progression and cell migration/invasion.<sup>197-200</sup> We found that levels of all these proteins decrease with PTC-028 addition (Fig. 2.6C). Our current model (Fig. 2.6D) summarizes these data, which suggest that BMI1 promotes tumor cell growth by inhibiting LATS1/2 phosphorylation and allowing YAP/TAZ/TEAD to transcribe canonical target genes (such as AXL, CYR61, and CTGF). When BMI1 is lost, either by genetic knockdown or PTC-028 treatment, Hippo is activated, LATS1/2 remain phosphorylated, and YAP is subsequently degraded (Fig. 2.6D).

Next, we sought to demonstrate that BMI1 promotes cell proliferation by inhibiting Hippo signaling; we took two approaches to rescue the phenotype of BMI1 inhibition. First, in Rh28 and Rh30, we knocked down LATS1, LATS2, or both LATS1/2 by siRNA transfection (Fig. 2.6E) and showed that YAP levels increase when LATS1 or both LATS1/2 are knocked down. Then we treated cells transfected with siCtl, siLATS1, siLATS2, and siLATS1/2 with PTC-028 at a 7-log range of doses ( $10^{-11}$  M -  $10^{-5}$  M) to recalculate IC<sub>50</sub>s (Fig. 2.6F). We found that knockdown of LATS1, LATS2, and LATS1/2 increased PTC-028 IC<sub>50</sub>s approximately 2-4 fold compared to control (Fig. 6G). In our second approach, we overexpressed YAP directly by transducing Rh28 and Rh30 cells with lentiviral particles containing pGAMA-Empty (empty vector) or pGAMA-YAP (YAP tagged with mCherry). We confirmed overexpression by western blot (Fig. 2.6H). We treated Rh28/Rh30 pGAMA-empty and pGAMA-YAP cell lines with a 7-log range of doses

( $10^{-11}$  M -  $10^{-5}$  M) and calculated IC<sub>50</sub>s (Fig. 2.6I-J). The IC<sub>50</sub>s were approximately 2-3 fold higher in YAP-overexpressing cells (Fig. 2.6J), suggesting a link between BMI1 and LATS1/2-YAP signaling within the Hippo pathway. Collectively, these data demonstrate that BMI1 influences cell proliferation by negatively regulating Hippo signaling. The effects of BMI1 inhibition can be partly reversed by inhibiting LATS1/2 and the upregulation of YAP.

## 2.4 Discussion

Our understanding of, and hence optimal treatment for ARMS, remains inadequate. Motivated by a growing understanding that PAX3-FOXO1 fusion proteins interact with diverse epigenetic complexes, including BRD4<sup>91,173</sup> and CHD4<sup>92</sup>, we hypothesized that BMI1 would contribute to ARMS aggression and that inhibiting this protein could potentially confer therapeutic benefit. Notably, while studies suggest that BMI1 inhibition is a downstream effect of PTC-028<sup>162</sup>, our studies show that genetic depletion of BMI1 using multiple independent siRNAs/shRNAs diminishes proliferation (Fig. 2.2). Moreover, we find that pharmacologic disruption using PTC-209, which inhibits effective translation of *BMI1* mRNA<sup>139</sup>, decreases ARMS cellular viability significantly (Fig. 2.3). We provide evidence that BMI1 inhibition diminishes cell cycle progression and increases apoptosis (Fig. 2.4).

In the *in vivo* setting, we show that single-agent treatment significantly decreases, though does not abrogate, ARMS growth (Fig. 2.5). Notably, while PTC-028 displays better *in vivo* characteristics than PTC-209, PTC-028 is still an early generation inhibitor. PTC-596 is the clinical analog of PTC-028 that has recently entered clinical trials for patients with advanced solid malignancies.<sup>166</sup> A1016 is an additional BMI1 inhibitor related to PTC-596 and has shown similar positive results in glioblastoma.<sup>162</sup> Future investigations will investigate the impact of these newer generation inhibitors on ARMS. Recently, investigators showed that the combination of PTC-596 and standard chemotherapy (gemcitabine and nab-paclitaxel) resulted in regressions in multiple aggressive pancreatic cancer models and, importantly, was well-tolerated.<sup>163</sup> Based on such studies, we speculate that combining BMI1 inhibition with standard-of-care

chemotherapeutic regimens in RMS may both be well-tolerated and result in greater inhibition of tumor growth. However, further studies are needed to investigate this hypothesis.

While the current study delineates the impact of BMI1 on cell cycle progression and evasion of apoptosis, BMI1 has been implicated in multiple hallmarks of cancer, including DNA repair and self-renewal, among others.<sup>108</sup> In melanoma, *BMI1* expression was correlated with an invasive signature and promoted multiple aspects of melanoma metastasis, including anoikis, invasion, migration, and chemoresistance.<sup>107</sup> Might BMI1 contribute to metastatic dissemination in ARMS, and could disruption of its function impede metastatic dissemination? Finally, while our studies focused on ARMS, we find that *BMI1* is broadly expressed in multiple pediatric and adult sarcomas (Fig. 2.1), raising the possibility that BMI1 may shape the initiation, maintenance, and progression of diverse sarcoma histotypes. To facilitate such studies, it would be of substantial interest to investigate the impact of BMI1 overexpression and deletion on various genetically engineered sarcoma mouse models (GEMMs).

In addition to proposing a role for BMI1 in ARMS, our studies also reveal the influence of BMI1 on Hippo signaling and raise further mechanistic questions. For example, we find that inhibition of BMI1 results in increased levels of LATS1/2 phosphorylation at Thr1079/Thr1041, which is associated with LATS1/2 activation.<sup>201</sup> However, inhibiting BMI1 does not appear to influence either the expression or phosphorylation of MST1, which lies upstream of LATS1 (Fig. S4A). It is possible that

BMI1 epigenetically represses an unidentified kinase of LATS1/2, or perhaps BMI1 engages with LATS1/2 through protein-protein interactions (Fig. 2.6D). This would be especially novel, considering the canonical role of BMI1 almost exclusively acting through epigenetic mechanisms. More investigation will be necessary to define the upstream mechanism of action by which BMI1 influences Hippo signaling. Looking downstream, we find that YAP protein levels decrease upon BMI1 inhibition, and several downstream canonical YAP/TAZ targets (AXL, CYR61, and CTGF) all decrease at the protein level (Fig. 2.6C). This is consistent with our hypothesis that BMI1 suppresses Hippo pathway activation.<sup>108</sup> We additionally rescued the effects of BMI1 inhibition by PTC-028 by knocking down LATS1, LATS2, and LATS1/2, confirming that YAP levels increase and negate the anti-proliferative effects of BMI1 inhibition (Fig. 2.6E-G). We performed a complementary experiment wherein we overexpressed YAP directly and found similar results (Fig. 2.6H-J), further confirming the significance of Hippo signaling in ARMS through BMI1. Interestingly, there is evidence for the deregulation of the Hippo pathway and subsequent activation of YAP/TAZ in undifferentiated pleomorphic sarcomas.<sup>202</sup> It is intriguing to posit a broad role for BMI1 involvement in the Hippo pathway across sarcomas and to speculate that BMI1 inhibition may provide a method of activating the Hippo pathway in these malignancies.

In conjunction with further dissection of BMI1-Hippo signaling, it will be essential to define the entire repertoire of genes influenced by BMI1 using both RNA-seq and ChIP-seq approaches and to see how BMI1-influenced genes converge and diverge from other malignancies by analyzing target gene expression states.<sup>118,162,194</sup> Furthermore, it will be

of substantial interest to determine if BMI1 acts through its canonical role as a member of the PRC1 complex, or by associating with other complexes to control gene expression in ARMS. There are six canonical PRC1 complexes (and even more non-canonical), each with a different PCGF (BMI1 is PCGF4). It would be interesting to determine if the inhibition of other PRC1 complexes would have similar effects to targeting BMI1.<sup>111</sup> Perhaps combining inhibitors of different PRC1 complexes could have a synergistic effect, as it is possible that PRC1 groups could compensate for another if one or more is lost. Moreover, what effects does BMI1 inhibition have on global chromatin changes? Additional ChIP-seq experiments investigating where BMI1/PRC1 localizes in ARMS, then further exploring the impact of BMI1 inhibition on repressive histone marks such as H2AK119Ub and H3K27me3, along with active marks like H3K27ac, will help clarify the molecular mechanisms by which BMI1 influences the malignant phenotype.

## **2.5 Conclusions**

Our studies propose a novel role for BMI1 signaling in ARMS, connect BMI1 to the Hippo pathway, and raise additional questions regarding BMI1 function and signaling. They provide a strong foundation for investigating the utility of BMI1 inhibition in ARMS and should spur further investigations of BMI1 and other PRC1/2 proteins as potential dependencies in RMS and other sarcomas.

**Author contributions**

Conception and design: C.E. Shields, K.M Oristian, C.M. Linardic, K.A. Haynes, R.W.

Schnepp

Development of methodology: C.E. Shields, R.W. Schnepp

Acquisition of data: C.E. Shields, S. Potlapalli, S.M. Cuya-Smith, S.K. Chappell, D. Chen, D. Martinez, J. Pogoriler, S. Patel, R.W. Schnepp

Analysis and interpretation of data (biostatistics, statistical analysis, interpretation of clinical data and genomic datasets): C.E. Shields, K.S. Rathi, R.W. Schnepp

Writing, review, and/or revision of the manuscript: C.E. Shields, K.A. Haynes, R.W.

Schnepp

Administrative, technical, or material support: K.M Oristian, C.M. Linardic, J.M. Maris, K.A. Haynes, R.W. Schnepp

Study supervision: K.A. Haynes, R.W. Schnepp

**Acknowledgments**

This work was supported in part by NIH Grant Ko8-7Ko8CA194162-02 (R.W.S), NIH Grant R35 CA220500 (J.M.M.), the Sarcoma Foundation of America (R.W.S), CURE Childhood Cancer (R.W.S), Austen's Army (R.W.S), NIH Grant U54-CA231630 (C.M.L), NIH Grant F31-CA254301 (K.M.O), the Aflac Cancer and Blood Disorders Center Trust (R.W.S and K.A.H.), and the William Woods, M.D., Aflac Clinical Investigator Chair (R.W.S.).

Additionally, this study was supported in part by the Emory Flow Cytometry Core (EFCC), one of the Emory Integrated Core Facilities (EICF), and is subsidized by the Emory University School of Medicine. Additional support was provided by the National Center

for Georgia Clinical & Translational Science Alliance of the National Institutes of Health under Award Number UL1TR002378. The content is solely the responsibility of the authors and does not necessarily represent the official views of the National Institutes of Health.

**Conflicts of Interest**

Robert W. Schnepf reports employment at Janssen R&D. There are no other conflicts of interest.



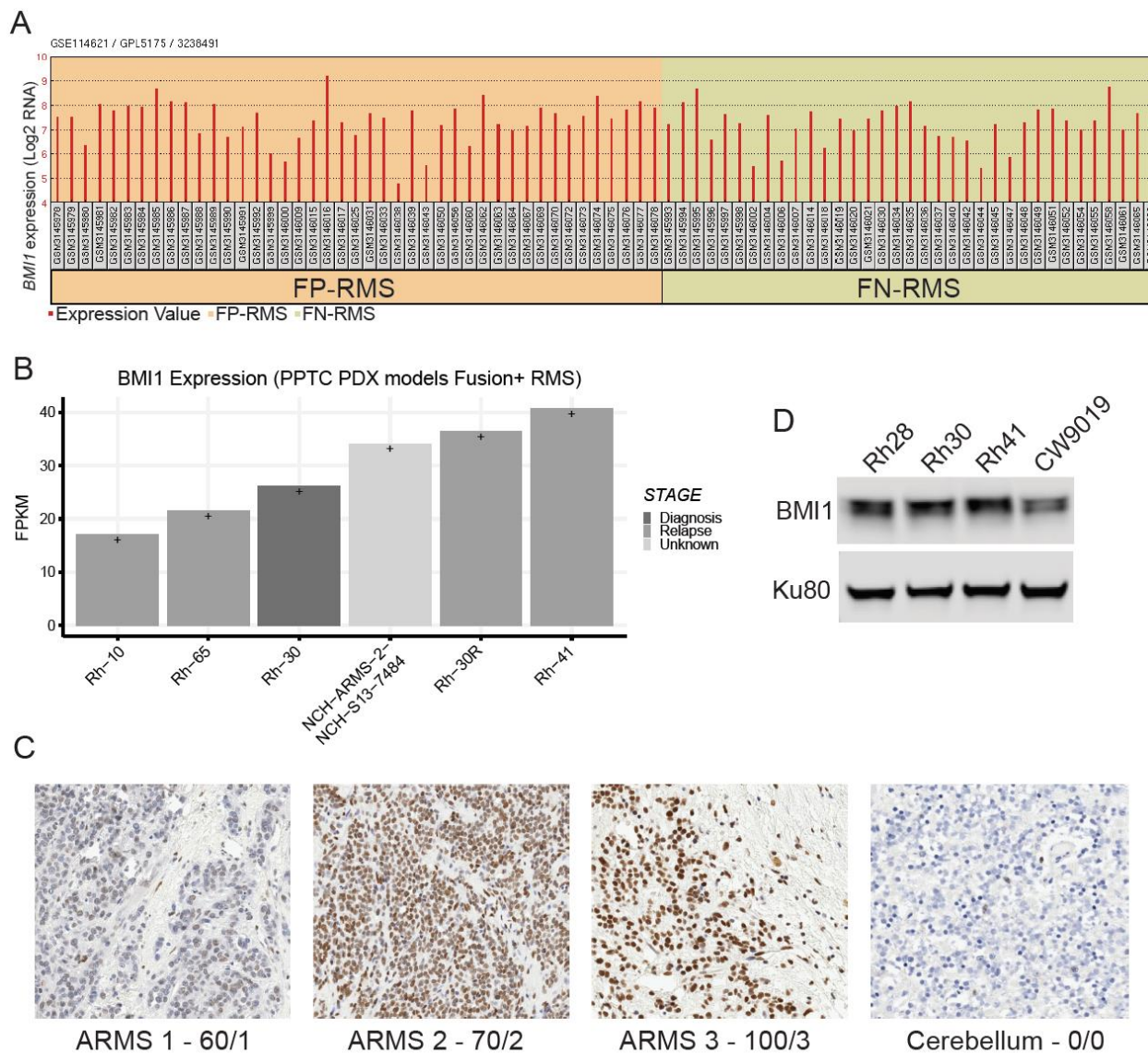


**Figure 2.1 BMI1 is highly expressed in rhabdomyosarcoma**

(A) Barplot of *BMI1* gene expression (Log<sub>2</sub> RNA signal intensity) from human exome array data across fusion-positive RMS and fusion-negative RMS patient tumor samples (GSE114621)<sup>190</sup>. (B) Boxplot of *BMI1* gene expression values from RNA-sequencing data of ARMS PDX and cell line models (n = 6). Y-axis represents fragments per kilobase of exon per million reads (FPKM) values. (C) Tumor microarray with three representative

ARMS tumors from patients and a negative control normal pediatric cerebellum. BMI1 is brown (DAB). The nuclear counterstain for BMI1-negative cells is purple (hematoxylin). The first number refers to the percentage of tumor cell nuclei expressing BMI1, while the second number is the strength of the staining, which ranges from 0 (negative) to 3 (strong staining).<sup>186</sup> (D) Western blot of ARMS cell lines Rh28, Rh30, Rh41 and CW9019 showing BMI1 protein expression with a Ku80 loading control.

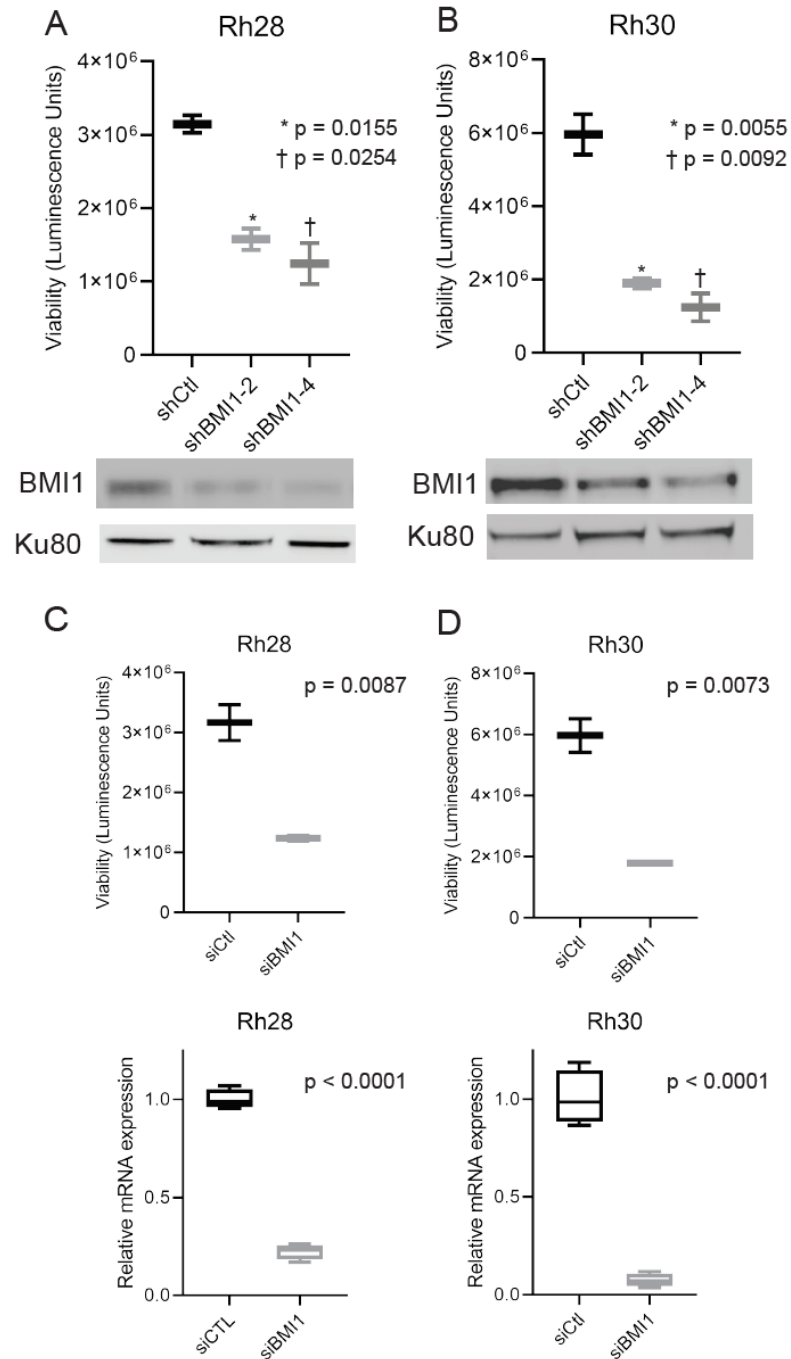


**Figure 2.2 Genetic knockdown of BMI1 leads to reduced cellular proliferation in ARMS cells**

(A) Rh28 (A) and Rh30 (B) cell lines were infected with control lentiviruses or lentiviruses expressing two independent shRNAs directed against BMI1. Cell proliferation in control and BMI1-depleted cell lines as assessed by Cell-TiterGlo. Western blotting of BMI1 and Ku80 in corresponding cell lines. (C-D) Rh28 (C) and Rh30 (D) cells were transfected with control siRNAs or pooled siRNAs directed against BMI1. Cell proliferation was assessed by Cell-TiterGlo, with corresponding siCtl and siBMI1 RT-PCR data depicted below. Standard deviation bars shown. Results are representative of at least three independent experiments. P-values are shown in the figure.

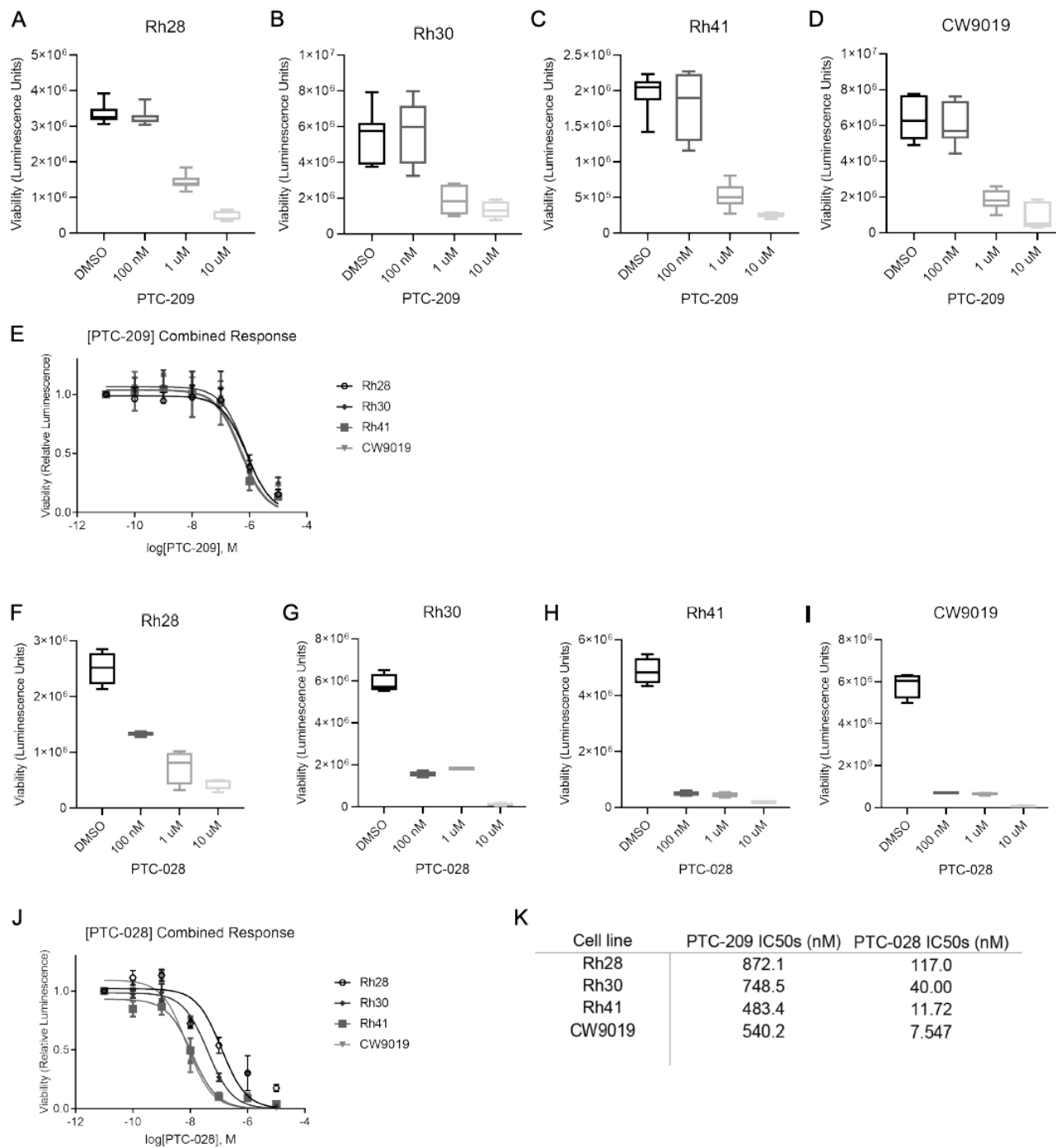


**Figure 2.3 Pharmacologic inhibition of BMI1 decreases cell proliferation *in vitro***

(A-D) Cell lines Rh28 (A), Rh30 (B), Rh41 (C), and CW9019 (D) were treated with a 7-log dose range of PTC-209. Graphs display cell viability measured with CellTiter-Glo with varying concentrations of PTC-209. E. Dose-response curve of PTC-209 ranging from  $10^{-11}$  M –  $10^{-5}$  M. (F-I) Cell lines Rh28 (F), Rh30 (G), Rh41 (H), and CW9019 (I) were treated with a 7-log dose range of PTC-028. Graphs display cell viability measured with CellTiter-Glo at varying concentrations of PTC-028. (J) Dose-response curve of PTC-028 ranging from  $10^{-11}$  M –  $10^{-5}$  M. (K) Table summarizing IC<sub>50</sub> values of PTC-209 and PTC-028. Standard deviation bars depicted. Results are representative of at least three independent experiments.

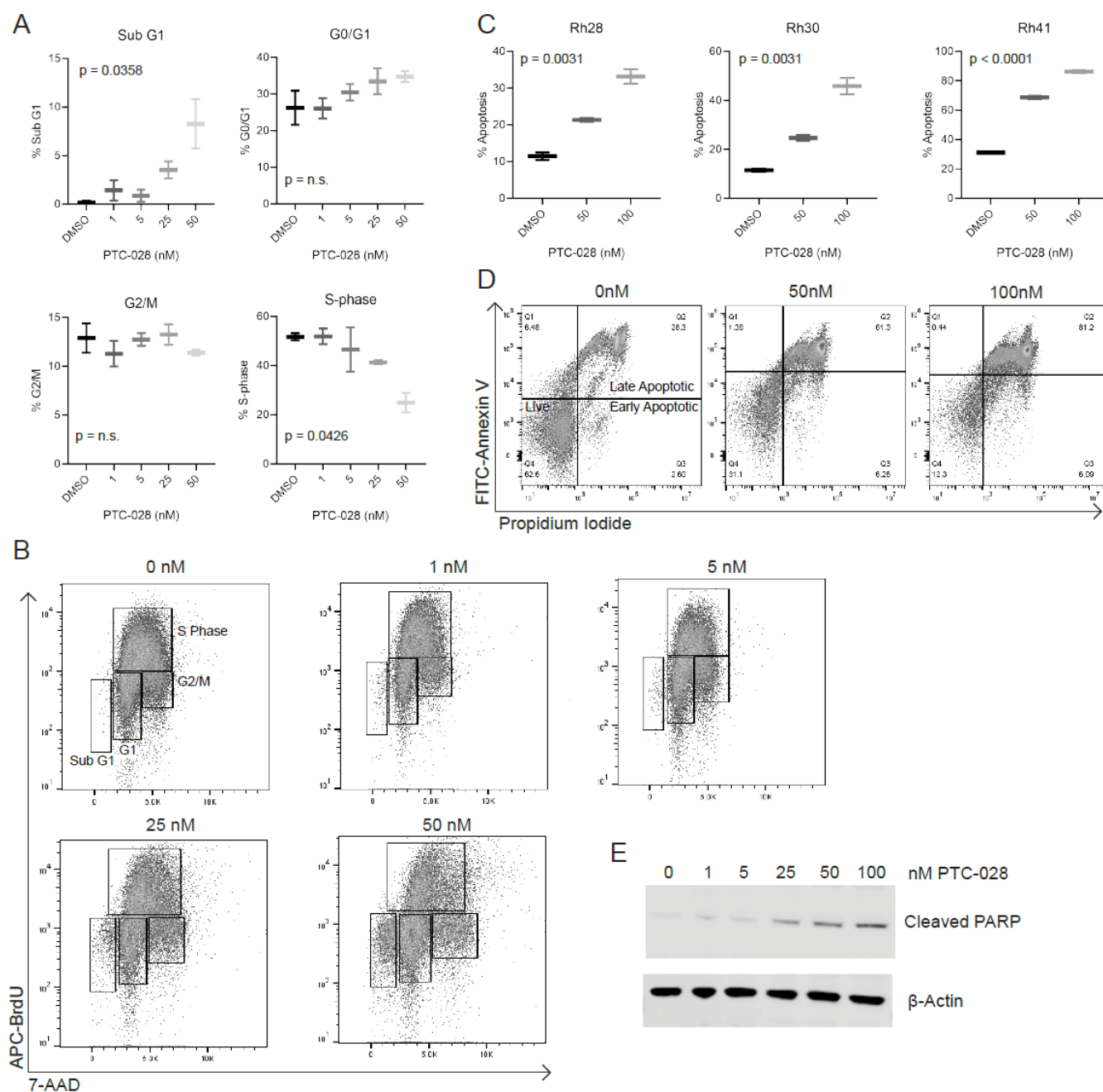


**Figure 2.4 Targeting BMI1 decreases cell cycle progression and increases apoptosis in ARMS**

(A) Graphs depict cell cycle distribution in the Rh30 cell line treated with PTC-028 (0 - 50 nM for 24 hr). (B) Representative cell cycle distribution from Rh30. BrdU is depicted

on the y-axis with 7-AAD on the x-axis. (C) Flow cytometry analysis of Annexin V/PI staining in Rh28, Rh30, and Rh41, with PTC-028 treatment ranging from 0 - 100 nM for 72 hr. (D) Representative example of flow cytometry data illustrating apoptosis with Annexin V (y-axis) and propidium iodide (x-axis). (E) Rh30 was treated with PTC-028 for 72 hr, with western blot depicting cleaved PARP and actin. Standard deviation bars depicted. Results are representative of at least three independent experiments. P-values are shown in the figure.



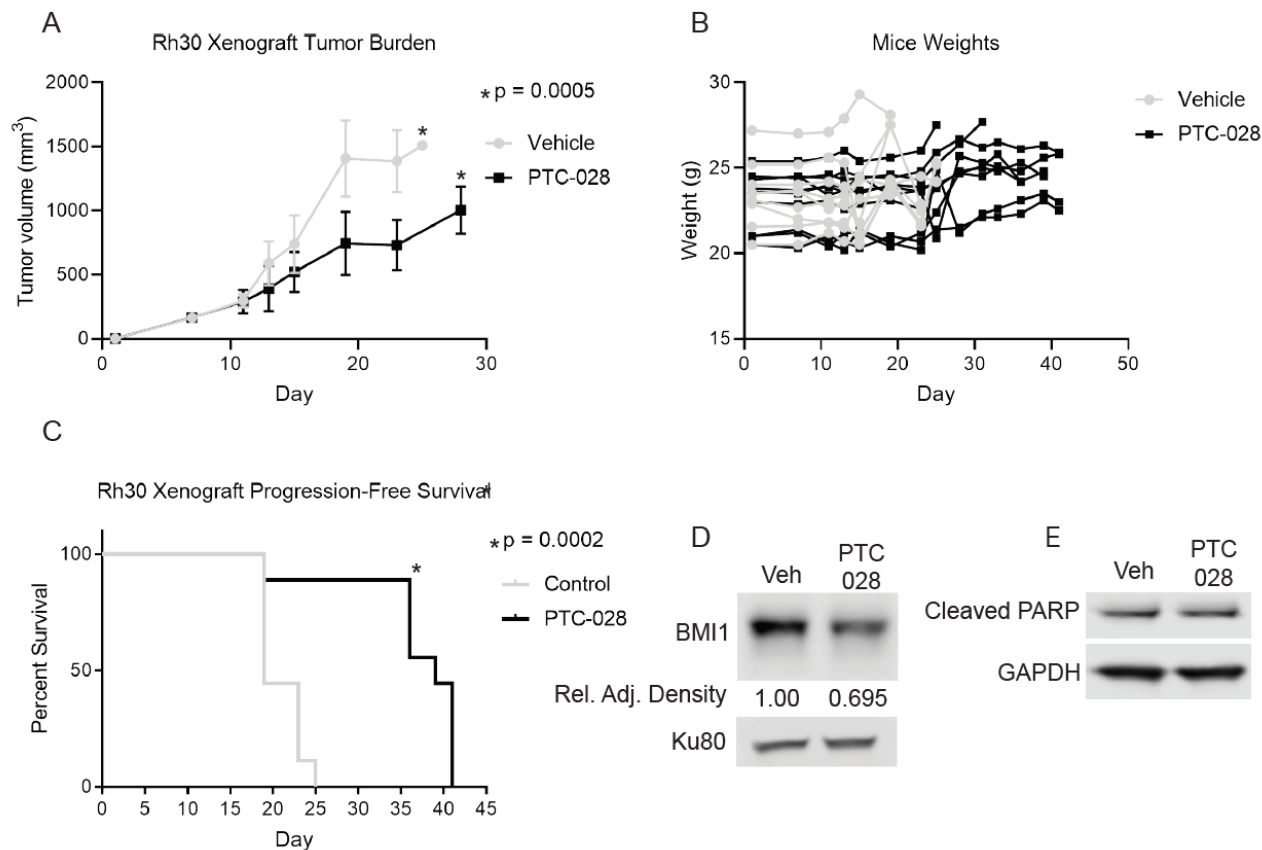


**Figure 2.5 Single agent PTC-028 treatment causes tumor growth delay *in vivo***

Rh30 xenografts were treated with vehicle or PTC-028 (15 mg/kg 2x/weekly). (A) Response of tumor volumes to vehicle and PTC-028. (B) Weight change from baseline on study arms. (C) Kaplan-Meier analyses for Rh30 xenografts. (D) Representative western blot of BMI1 and Ku80 in control and PTC-028 treated tumors. (E) Western blot of cleaved PARP levels with GAPDH as a loading control. Standard deviation bars are included. P-values are shown in the figure.

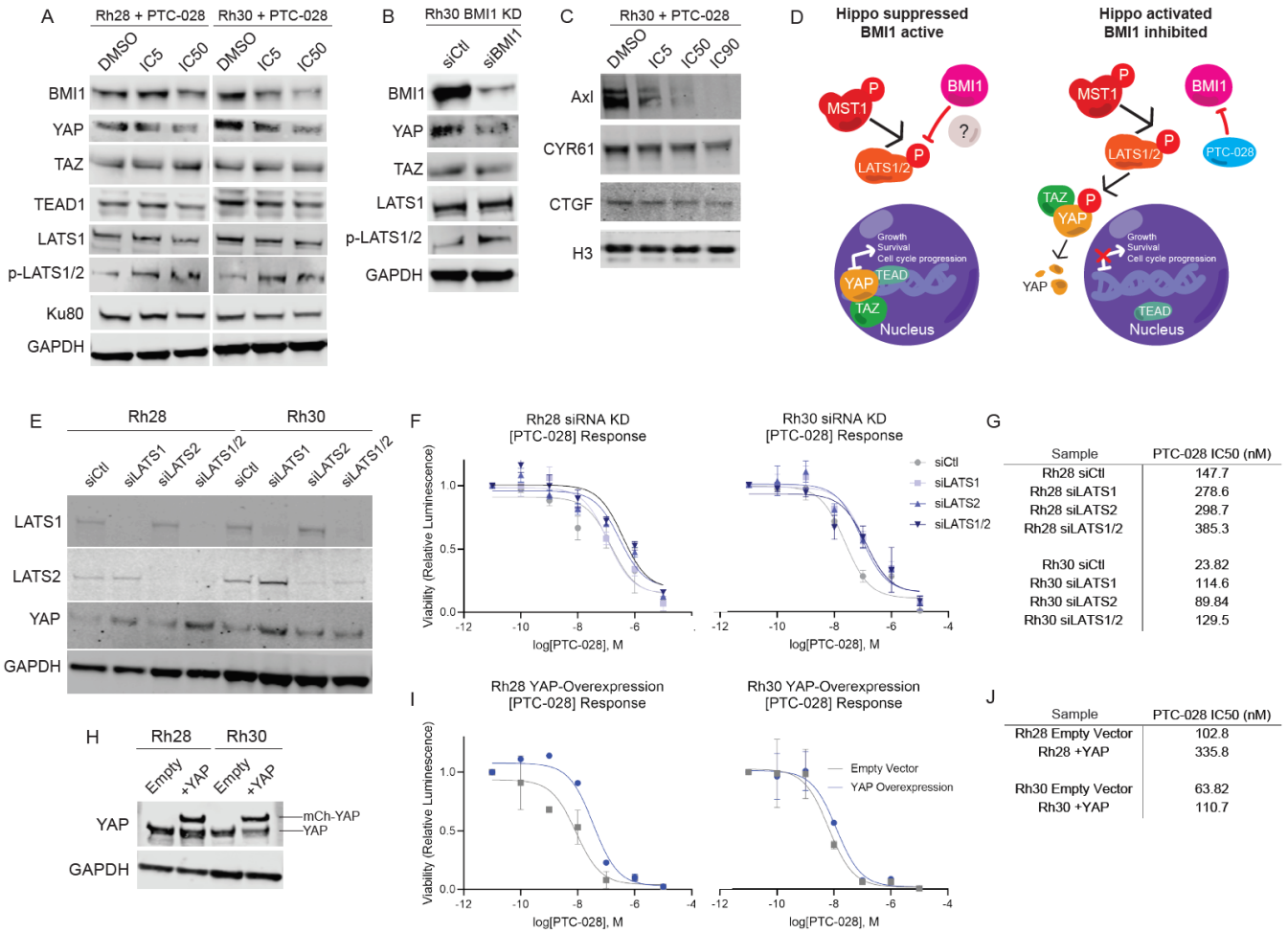
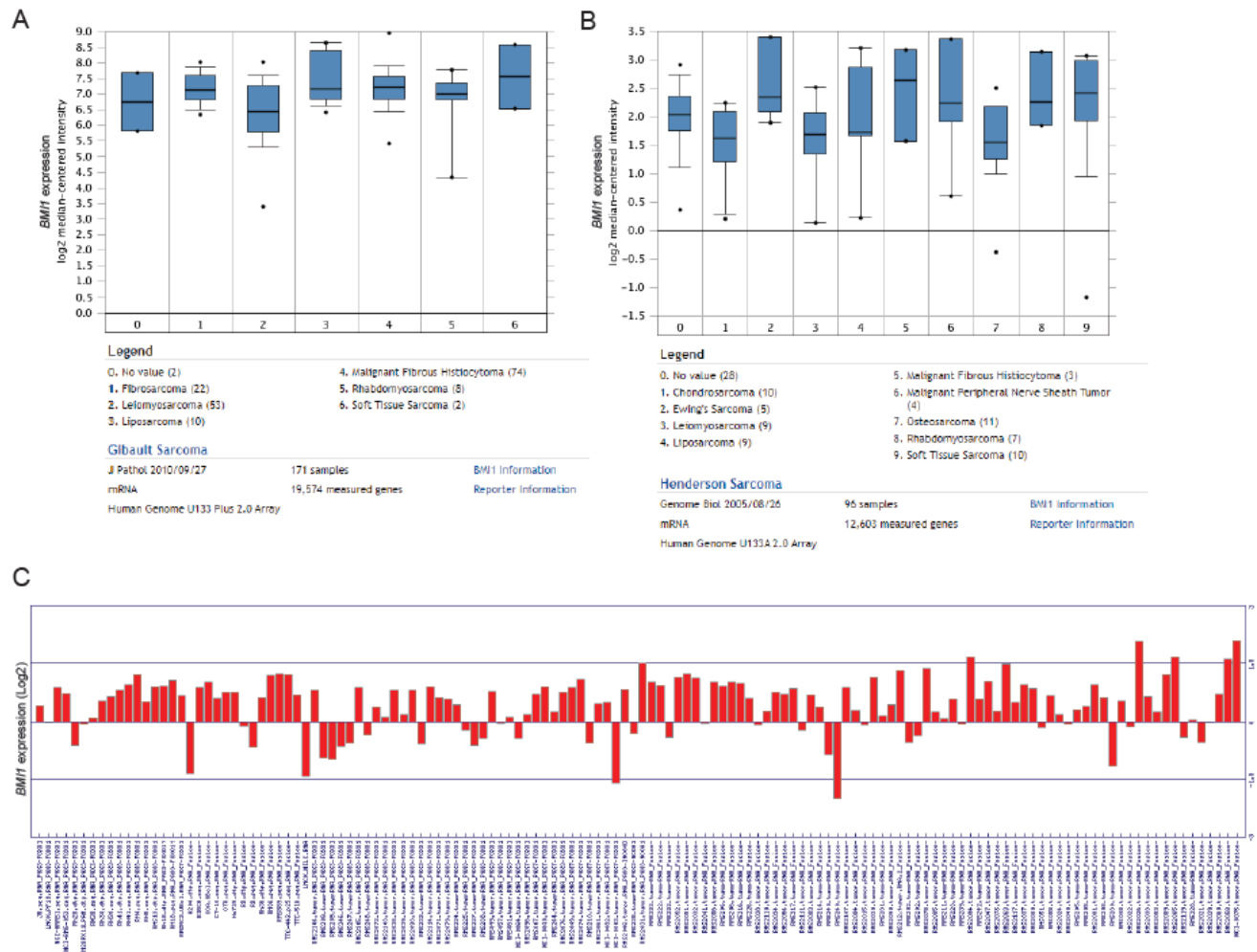


**Figure 2.6 BMI1 negatively influences Hippo signaling**

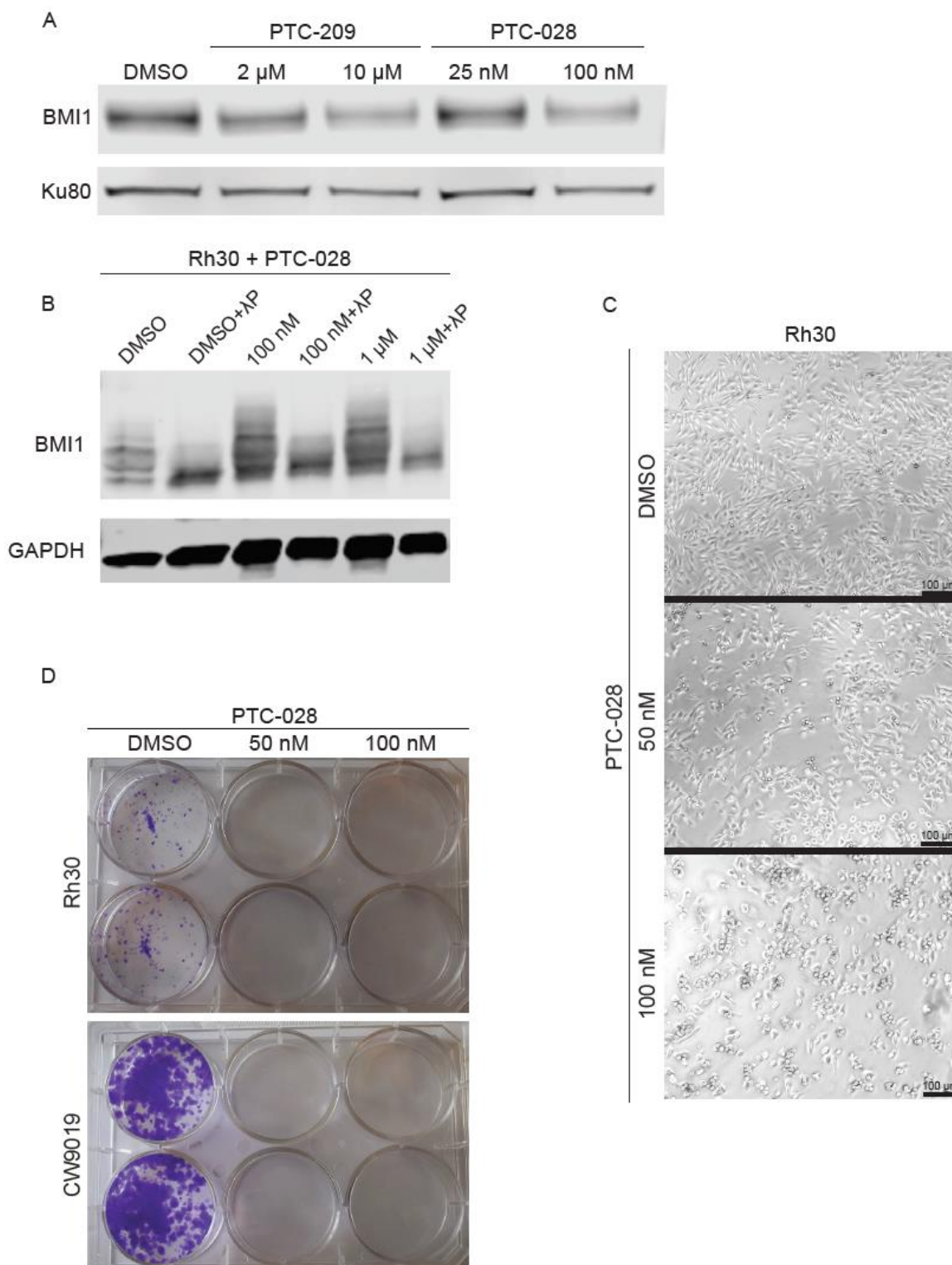
(A) Rh28 and Rh30 cells were treated with PTC-028 at respective IC<sub>5</sub> or IC<sub>50</sub> concentrations for 72 hr, with DMSO as a control. Western blot of BMI1 and Hippo pathway members YAP, TAZ, TEAD1, LATS1, p-LATS1/2, and Ku80/GAPDH as loading controls. (B) Rh30 cells were transfected with an siRNA pool against BMI1, and western blot analyses were performed after 72 hr. Western blot of BMI1 and Hippo pathway members YAP, TAZ, LATS1, p-LATS1/2, and GAPDH as loading controls. (C) Rh30 cells were treated with PTC-028 at respective IC<sub>5</sub>, IC<sub>50</sub>, or IC<sub>90</sub> doses, with DMSO as a control. Western blot of AXL, CYR61, and CTGF with histone H<sub>3</sub> as a loading control. (D)

Model of BMI1 involvement in the Hippo pathway. In ARMS, BMI1 inhibits Hippo signaling, decreasing LATS1/2 phosphorylation, allowing YAP/TAZ/TEAD to transcribe genes related to growth, survival, and cell cycle progression. When BMI1 is inhibited pharmacologically or genetically, LATS1/2 are phosphorylated, leading to YAP degradation and diminishing the transcription of YAP/TAZ/TEAD target genes. (E) Rh28 and Rh30 cells were transiently transfected with pooled siRNAs against LATS1, LATS2, or both, with a non-targeting pool as a control (siCtl). Western blot shows protein levels of LATS1, LATS2, YAP, with GAPDH as a loading control. (F) Dose-response curve of PTC-028 ranging from  $10^{-11}$  M -  $10^{-5}$  M, using transiently transfected siCtl, siLATS1, siLATS2, siLATS1/2 cells from (E). (G) Table summary of PTC-028 IC<sub>50</sub>s from (F). (H) Western blot representing stably lentivirus-transduced cell lines Rh28/Rh30 pGAMA-Empty (Empty) and Rh28/Rh30 pGAMA-YAP. pGAMA-YAP contains mCherry-tagged YAP (mCh-YAP), which runs at a higher molecular weight ( $\approx$  85 kDa) than endogenous YAP ( $\approx$  65 kDa). GAPDH as a loading control. (I) Dose-response curve of PTC-028 ranging from  $10^{-11}$  M -  $10^{-5}$  M, using stable cell lines Rh28-Empty, Rh28+YAP, Rh30-Empty, and Rh30+YAP from (H). (J) Table summary of PTC-028 IC<sub>50</sub>s from (I). Results are representative of at least three independent experiments.



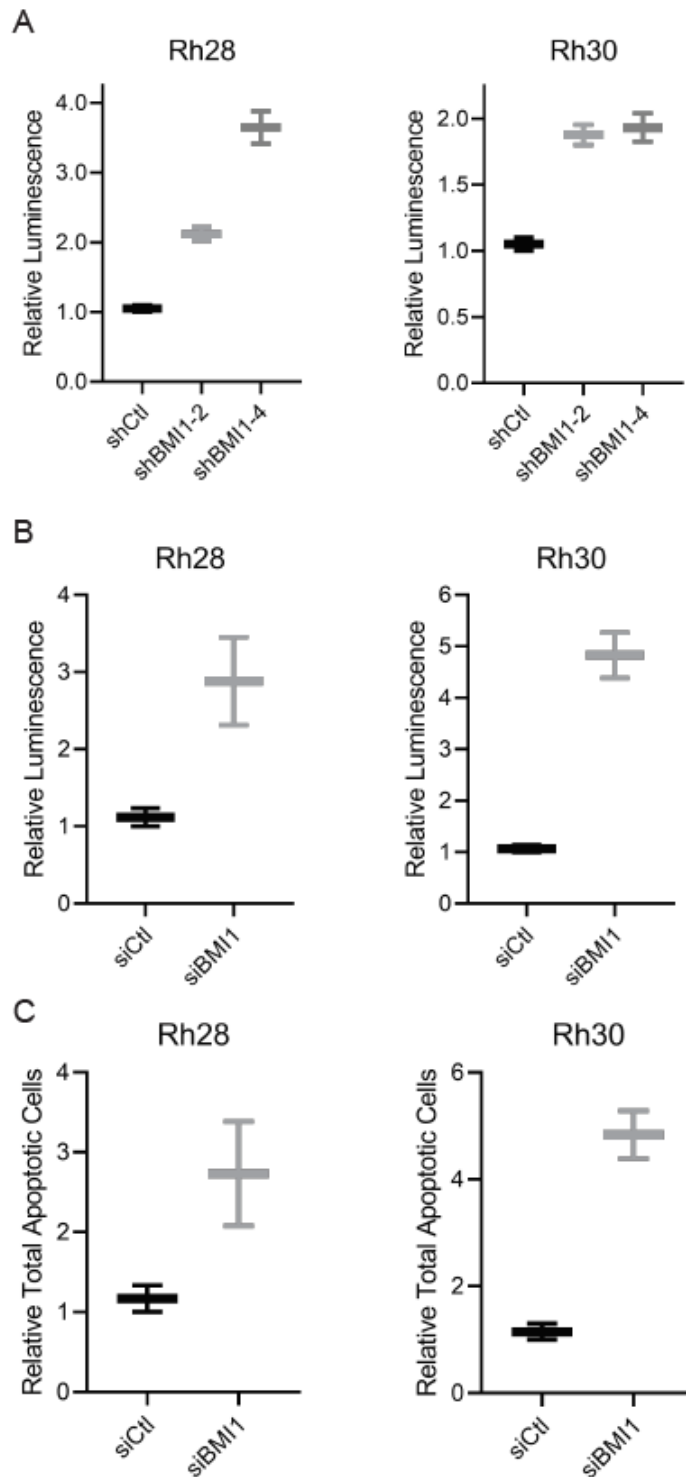
## Supplementary Figure S 2.1, related to Figure 2.1. *BMI1* is highly expressed in rhabdomyosarcoma

(A-B) *BMI1* mRNA expression from Gibault (A) and Henderson Sarcoma (B). Human exome array data from the Oncomine database.<sup>36</sup> Y-axis is Log<sub>2</sub> median-centered intensity. (C) Data from the OncoGenomics database.<sup>40</sup> *BMI1* expression on the y-axis (Log<sub>2</sub>) from RNA-seq from FP-RMS and FN-RMS PDX models.



**Supplementary Figure S 2.2, related to Figure 2.3. Pharmacologic inhibition of BMI1 decreases cell proliferation *in vitro***

(A) Rh30 cells were treated with a range of PTC-209 and PTC-028 doses and harvested after 72 hr. Western blots were performed, and BMI1 levels were analyzed. Ku80 serves as a loading control. (B) Rh30 cells were treated with DMSO, 100 nM PTC-028, or 1  $\mu$ M PTC-028 and harvested after 12 hours. Western blots were performed, and BMI1 levels were analyzed. Samples treated with lambda phosphatase indicated by + $\lambda$ P. GAPDH as a loading control. (B) Brightfield microscopy images (scale bar = 100  $\mu$ m) of Rh30 cells treated with DMSO, 50 nM PTC-028, or 100 nM PTC-028 after 72 hr. (C) Images of crystal violet stained Rh30 or CW9019 cells treated with either DMSO or PTC-028 after 10 days of colony formation.



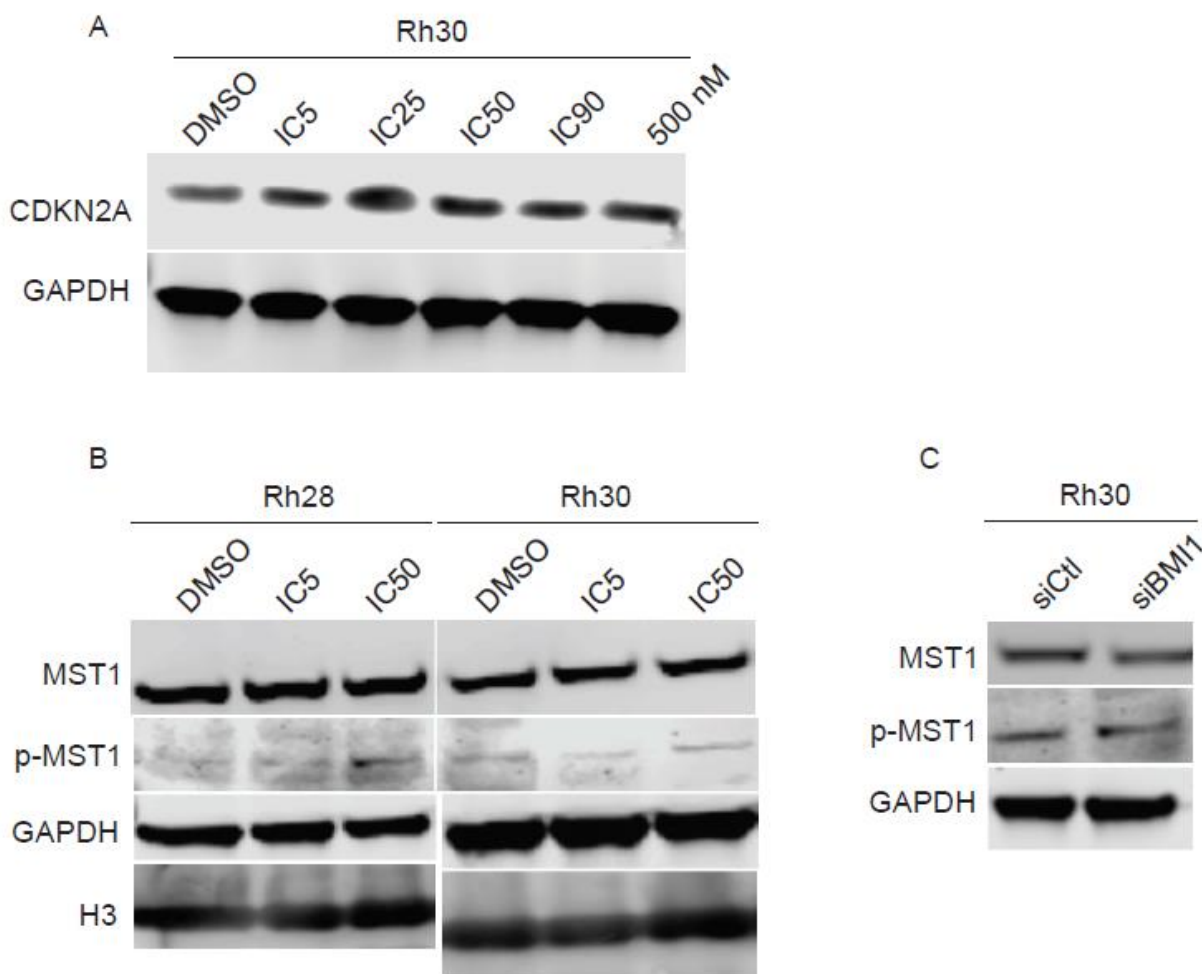
**Supplementary Figure S 2.3, related to Figure 2.4. Targeting BMI1 decreases cell cycle progression and increases apoptosis in FP-RMS**

(A) Rh28 and Rh30 cells were transduced with two separate BMI1 (2 and 4) shRNAs compared to a nontargeting shRNA shCtl. Relative Caspase-Glo data measured in relative luminescence (y-axis) compared to shCtl. Western blotting as depicted in Figure 2.4A-B.

(B) Rh28 and Rh30 cells were transfected transiently with an siRNA pool against BMI1. After 72 hr, the Caspase-Glo assay was performed and measured in relative luminescence (y-axis). RT-PCR as depicted in Figure 2.4C-D.

(C) Annexin-V/PI staining was performed on siRNA transfected cells after 72 hr, and total apoptotic cells were calculated. Standard deviation bars depicted. Experiments were performed in duplicate.





**Supplementary Figure S 2.4, related to Figure 2.6. BMI1 negatively influences Hippo signaling**

(A). Western blot of CDKN2A levels across a range of PTC-028 doses in Rh30 cells. Cells were harvested after 72 hr. GAPDH as a loading control. (B). Western blot of MST1 and p-MST1 levels across a range of PTC-028 doses in Rh28 and Rh30 cells. GAPDH and H3 as loading controls. (C) Western blot of siRNA transfected cells of MST1 and p-MST1 levels in Rh30 cells. Western blotting of BMI1 as depicted in Figure 2.6C. GAPDH as a loading control.

**Supplementary Table 2.1**

List of antibodies, sources, and dilutions used in all western blot assays.

<b>Antibody</b>	<b>Company</b>	<b>Dilution</b>
BMI1	Cell Signaling Technology	1:1000
Ku80	Cell Signaling Technology	1:5000
Cleaved PARP	Cell Signaling Technology	1:1000
$\beta$ -Actin	Cell Signaling Technology	1:1000
GAPDH	Cell Signaling Technology	1:5000
MST1	Cell Signaling Technology	1:1000
p-MST1/2 (Thr183)/(Thr180)	Cell Signaling Technology	1:500
LATS1	Cell Signaling Technology	1:1000
p-LATS1/2 (Thr1079)/(Thr1041)	Cell Signaling Technology	1:500
YAP/TAZ	Cell Signaling Technology	1:500
AXL	Cell Signaling Technology	1:500
CYR61	Cell Signaling Technology	1:500
CTGF	Cell Signaling Technology	1:500
CDKN2A (p16-INK4A)	Proteintech	1:1000
Histone H3	Abcam	1:1000

**3. Differential epigenetic effects of BMI1  
inhibitor PTC-028 on two fusion-positive  
rhabdomyosarcoma cell line models**

## **Differential epigenetic effects of BMI1 inhibitor PTC-028 on two fusion-positive rhabdomyosarcoma cell line models**

Cara E. Shields<sup>1,2</sup>, Robert W. Schnepf<sup>1</sup>, Karmella A. Haynes<sup>2</sup>

<sup>1</sup>Aflac Cancer and Blood Disorders Center, Department of Pediatrics, Division of Pediatric Hematology, Oncology, and Bone Marrow Transplant, Emory University School of Medicine, Atlanta, GA 30322, USA; Winship Cancer Institute, Emory University, Atlanta, GA 30322, USA; Children's Healthcare of Atlanta, Atlanta, GA 30322, USA.

<sup>2</sup>Wallace H. Coulter Department of Biomedical Engineering, Emory University, Atlanta, GA, 30322, USA

**Running Title: RNA-seq of PTC-028 treated rhabdomyosarcoma**

**Keywords: rhabdomyosarcoma, PTC-028, BMI1, RNA-seq**

**Figures: 4 figures, 2 supplementary figures, 2 supplementary tables**

**Abstract**

**Purpose:** This study aims to identify novel targets in the rare pediatric cancer, fusion-positive rhabdomyosarcoma (FP-RMS), and examine differences/similarities in FP-RMS tumor responses to BMI1 (B lymphoma Mo-MLV insert region 1 homolog) inhibition.

**Methods:** FP-RMS cell lines Rh28 and Rh30 were treated with DMSO (vehicle) or PTC-028, a BMI1 inhibitor, and RNA was collected after 24 or 48 hr in triplicate. RNA-seq was performed, and gene expression data were analyzed through Gene Ontology (GO) and KEGG (Kyoto Encyclopedia of Genes and Genomes) pathway analyses. Data from OncoPPI and the STRING database were also utilized in this study.

**Results:** Both Rh28 and Rh30 had some overlapping pathways affected by PTC-028, notably downregulation of cell cycle progression, the DNA damage response, and cholesterol biosynthesis. Rh30+PTC-028 had more genes containing TEAD-motifs downregulated compared to Rh28+PTC-028. Rh28 and Rh30 also had differing changes in expression in kinases of LATS1/2, EPHA2, and PDGFRA.

**Conclusion:** Overall, these results bring new insights into pathways influenced by BMI1 expression and contrasting inter-tumoral drug responses in FP-RMS.

### 3.1 Introduction

Rhabdomyosarcoma (RMS) is the most common pediatric soft-tissue sarcoma.<sup>24,25</sup> There are two main histological subtypes: alveolar rhabdomyosarcoma (ARMS) and embryonal rhabdomyosarcoma (ERMS).<sup>24</sup> Typically, ARMS encompasses fusion-positive RMS (FP-RMS), which express the fusion proteins PAX3/7-FOXO1, while ERMS is fusion-negative (FN-RMS).<sup>24</sup> Patients with FP-RMS have worse outcomes than patients with FN-RMS; those with FP-RMS have a ~60% 5-year survival rate and an even lower survival rate if there is metastatic dissemination.<sup>24,25</sup> There are currently no available targeted therapies for patients with FP-RMS; therefore, novel therapeutic opportunities need to be investigated.

In the United States, the first line of treatment for FP-RMS is a multi-modal approach that includes surgery, a combination of chemotherapies vincristine, actinomycin-D, and cyclophosphamide (VAC), and radiation.<sup>24,29,203</sup> These aggressive chemotherapies disrupt microtubule formation and prevent protein synthesis by disrupting transcriptional elongation and DNA and RNA alkylation. There is a significant knowledge gap as to why some patients with FP-RMS respond to treatment and others do not, why primary FP-RMS tumors metastasize to specific sites (lungs, bone marrow, bone, lymph nodes), and why FP-RMS tumor recurrence/relapse is so frequent.<sup>24,26,29,203-205</sup> Tumor heterogeneity at the cellular and gene expression level may give rise to inconsistent responses to treatment, tumor progression, and recurrence.<sup>138,206</sup> Thus, it is imperative to understand the cellular and gene regulatory events that occur in response to anti-cancer agents.

Epigenetic therapy is an emerging treatment approach that aims to restore gene expression to healthy, non-cancer levels and inhibit cancer cell behavior. For instance, 5-azacytidine, which inhibits DNA methyltransferase, is one of the first successful, FDA-approved epigenetic therapies in myelodysplastic syndromes (MDS) and significantly improves patient outcomes.<sup>207-209</sup> Another druggable chromatin protein is known as BMI1 (B lymphoma Mo-MLV insertion region 1 homolog), a Polycomb Repressive Complex 1 (PRC1) member, is overexpressed several types of cancer<sup>65,106,108,110,139,148,189</sup> and can be blocked with small molecule inhibitors such as PTC-028. Previously, we have shown that FP-RMS cell lines are sensitive to inhibition of BMI1.<sup>210</sup> We observed that FP-RMS cells treated with PTC-028 undergo activation of the tumor-suppressive Hippo pathway and apoptosis. Hippo pathway proteins LATS1/2 showed increased phosphorylation in PTC-208-treated cells, suggesting a role for BMI1 at the post-translational level. However, BMI1 and its complex PRC1 are best known for regulating the transcription of genes in the nucleus. Therefore, in this study, we used a global expression analysis to explore how BMI1 inhibition by PTC-028 affects the transcription levels of genes in FP-RMS cells.

## **3.2 Materials & Methods**

### **3.2.1 Cell culture**

The Rh28 cell line was obtained from the Children's Oncology Group, and the Rh30 cell line was obtained from the Children's Hospital of Philadelphia (Dr. Margaret Chou). Cell line authentication (STR profiling) was performed by the Emory Integrated Genomics Core. Mycoplasma testing was performed regularly using a Mycoplasma test kit (PromoCell, PK-CA91-1024). Cells were cultured in a humidified incubator at 37°C with 5% CO<sub>2</sub>. Rh30 was passaged every 2 days in DMEM (Corning, Bedford, MA, USA), and Rh28 was passaged every 2-3 days in RPMI 1640 (Corning). All media was supplemented with 10% FBS (Corning) and 1% (2 mM) l-glutamine (Gemini, West Sacramento, CA, USA). No antibiotics or antimycotics were added to the media.

### **3.2.2 RNA-seq study design**

Cells were treated with PTC-028 at their respective IC<sub>50</sub>s (Rh28 = 117 nM Rh30 = 40 nM)<sup>210</sup> for 24 or 48 hrs, or with DMSO (24 hrs) as a control. Three biological replicates were collected for each condition. RNA was extracted using guanidinium-phenol (TRIzol) and the RNAeasy mini kit (Qiagen, Hilden, Germany). mRNA libraries were prepared by Novogene Co., Ltd (Beijing, China) and sequenced on a NovaSeq (PE150, 50-60 million reads per sample).

Downstream analysis was performed by Novogene using a combination of programs including STAR, HTseq, Cufflink, and wrapped scripts. The reference genome (hg38) and gene model annotation files were downloaded from the genome website browser UCSC directly. Indexes of the reference genome were built using STAR, and



paired-end clean reads were aligned to the reference genome using STAR (v2.5). STAR used Maximal Mappable Prefix (MMP), which generates a precise mapping result for junction reads. HTSeq v0.6.1 was utilized to count the reads mapped to each gene, and FPKM (Fragments Per Kilobase of transcript per Million mapped reads) of each gene was calculated.<sup>211</sup> Alignments were parsed using Tophat, and differential expressions were determined via DESeq2/edgeR. GO, and KEGG enrichments were determined by ClusterProfiler. Novogene processed RNAseq data (FPKM) were clustered using the hierarchical clustering distance method with the function of heatmap, SOM (Self-organization mapping), and kmeans using silhouette coefficient to adapt the optimal classification with default parameter in R (hclust). Differential expression analysis between DMSO versus PTC-028 (24 or 48 hrs) treated cells (three biological replicates per condition) was performed using the DESeq2 R package (2\_1.6.3). The resulting P-values were adjusted using Benjamini and Hochberg's approach for controlling the False Discovery Rate (FDR). Genes with an adjusted P-value <0.05 found by DESeq2 were assigned as differentially expressed.

### **3.2.3 Data analyses and graph production**

Data analyses were performed in R, Graphpad Prism 9, and Microsoft Excel. Heatmaps were produced in R and Graphpad Prism 9. Volcano plots and boxplots were produced in Graphpad Prism 9. GO/KEGG bar charts were produced in R. Protein interaction networks were created in Cytoscape 3.8.2.

### 3.3 Results

#### 3.3.1 BMI1 inhibition influences global gene expression in FP-RMS

We have previously identified BMI1 as a therapeutic vulnerability in FP-RMS. Importantly, we illuminated a mechanism whereby BMI1 negatively regulates phosphorylation of LATS1/2 and YAP, thus suppressing Hippo pathway activation. In BMI1-inhibited, Hippo-activated cells, YAP becomes phosphorylated and is degraded, and YAP becomes unavailable to interact with Transcriptional enhanced associate domain (TEAD). As a result, TEAD target genes, which promote cancer growth, survival, and cell cycle progression, lose expression. Previously we observed reduced protein levels for a few key TEAD targets (AXL, CTGF, and CYR61).<sup>210</sup> To investigate the broader impact of BMI1-inhibition on gene regulation, we profiled the entire transcriptome in PTC-028-treated FP-RMS cells.

We performed RNA-seq on two FP-RMS cell lines, Rh28 and Rh30, which harbor the same PAX3-FOXO1 fusion proteins. We treated Rh28 and Rh30 samples in triplicate with PTC-028 at their respective IC<sub>50</sub>s for 24 or 48 hrs or with DMSO for 24 hrs as a control. Hierarchical clustering of the differentially expressed genes (DEGs) within the samples showed less variability of replicates within treatment groups than between groups, as expected (Fig. 3.1A). Principal component analysis (PCA) (Supplementary Figure S3.1) showed that one sample (Rh30 48 hrs, R30\_48) did not cluster with the other two replicates, so this outlier sample was removed from further analyses. The striking difference in the overall expression profiles of control-treated Rh28 and Rh30 suggest differences in basal gene expression states. Differential expression analysis showed that very few genes were up- or down-regulated ( $\geq 1.5$  fold change, adjusted p-

value ( $p_{adj} < 0.05$ ) in the Rh30+PTC-028 24 hrs group (down = 7, up = 10) compared to the Rh28+PTC-028 24 hrs group (down = 103, up = 100). Then, in the 48 hrs groups, fewer genes were downregulated in both cell lines (100 - 300) versus upregulated (600 - 700). This suggests that treatment time may influence the total number of affected genes, and more genes are being upregulated upon PTC-028 treatment than downregulated. Overall, the results show that while the two FP-RMS cell lines have different basal gene expression profiles, both are sensitive to epigenetic perturbation with the BMI1 inhibitor PTC-028.

### **3.3.2 Gene ontology and pathway analyses reveal downregulation of DNA replication and activation of cellular differentiation during BMI1 inhibition**

To understand the biological significance of the gene transcription changes we observed with RNA-seq, we analyzed gene ontology (GO) enrichment terms<sup>12,213</sup> of the differentially expressed genes (top DEGs in Supplementary Table 1). First, we examined downregulated genes because we expect BMI1 inhibition to reduce the expression of TEAD targets involved in cell growth, survival, and cell cycle.<sup>210</sup> The top five enriched GO terms in PTC-028-treated Rh28 are related to DNA replication (GO: 0006260) (Fig. 3.2A). KEGG pathway enrichment identified ribosomal components (hsa03010) and DNA replication (hsa03030) as the most significantly affected pathways. In Rh30, the top five enriched GO terms involve RNA processing (GO: 0006396) (Fig. 3.2A), which is consistent with the enriched KEGG pathways that involve the spliceosome (hsa03040) and RNA transport (hsa03013).

Next, we investigated the upregulated genes to determine how the activation of biological activities might contribute to the cells' sensitivity to BMI1. Up-regulated genes in Rh28 and Rh30 were enriched for GO biological processes related to muscle differentiation (GO:0042692) and contraction (GO:0006936), respectively, which suggests the induction of pathways that promote differentiation rather than plasticity and proliferation (Fig. 3.2B). KEGG pathway enrichment showed upregulation of p53 signaling (hsa04115) in Rh28, suggesting the reactivation of the tumor-suppressive p53 pathway. We found no significantly enriched KEGG pathways in Rh30.

To identify commonly affected biological processes in PTC-028-treated Rh28 and Rh30, we identified shared up- or down-regulated genes (Fig. 3.2C). Only 2 common genes were downregulated in both Rh28 and Rh30: *MVD* and *LOC102724250*. *MVD* encodes mevalonate diphosphate decarboxylase, while *LOC102724250* encodes Neuroblastoma Breakpoint Family Member 1 (NBPF1). The downregulation of *MVD* indicates that BMI1 influences the early stages of cholesterol biosynthesis in FP-RMS. The upregulated group showed 66 co-upregulated genes in Rh28 and Rh30, so we performed GO analyses using PANTHERdb.<sup>214</sup> The upregulated group shows that actin-myosin filament sliding (45-fold enrichment) and skeletal muscle contraction (44-fold enrichment) are enriched upon PTC-028 treatment. These results agree with the previous indication that muscle differentiation/muscle contraction was upregulated in Rh28 and Rh30 (Fig. 3.2A). Our gene ontology and pathway analyses suggest that BMI1 inhibition might disrupt overall plasticity in both FP-RMS cell lines while also affecting distinct pathways in a context-dependent manner, i.e., DNA replication in Rh28 and RNA processing in Rh30.

### **3.3.3 TEAD-regulated gene expression in Rh30 is more sensitive to BMI1 and Hippo pathway inhibition**

Although Rh28 and Rh30 were selected to represent the same disease<sup>192</sup>, they possess phenotype and karyotype differences that might correspond with differences in gene regulation that could influence how each cell line responds to BMI1 inhibition. For instance, Rh28 is near-tetraploid<sup>215</sup>, and Rh30 is near-triploid.<sup>216</sup> In our previous study, we found that BMI1 inhibition led to activation of the Hippo pathway, a tumor-suppressive pathway involved in tissue regeneration, self-renewal, and organ development, which is often dysregulated in cancer.<sup>200,217,218</sup> When the Hippo pathway is active, YAP/TAZ remains in the cytoplasm and cannot enter the nucleus and bind TEADs.<sup>197,219,220</sup> When deactivated, YAP/TAZ enter the nucleus, and YAP/TAZ/TEAD complexes bind to and activate the promoters of several genes related to cell growth, proliferation, and cell cycle progression.<sup>197,219,220</sup> To further understand how the Hippo pathway is affected by BMI1 inhibition, we examined the downstream targets of the Hippo pathway.

To test the hypothesis that TEAD target genes lose expression during BMI1 inhibition, we searched for TEAD binding motifs within the promoters of all differentially expressed genes (DEGs) in PTC-028 treated Rh28 and Rh30 cells. We identified TEAD1, TEAD3, and TEAD4 binding sites in 7.8 - 9.8% of all DEGs ( $|\log_2(\text{fold change})| > 0$ ,  $\text{padj} < 0.05$ , 262 of 3,336 in Rh28 and 2,678 in Rh30) using the Transcription Factor Target Gene Database<sup>221</sup> (see Supplementary Table 2 for TEAD motif ID codes), which combines 2,331 DNA motifs with empirical data such DNase I footprints and ChIP-seq data from 8.4 million loci collected from 41 cell lines/tissues. TEAD motif-containing genes (TMGs)

in Rh30 are downregulated (71%) upon PTC-028 treatment, which supports our hypothesis (Fig. 3.3A). However, most (63%) of the genes in Rh28 appear to become upregulated, as well as several (29%) of TEAD targets in Rh30 (Fig. 3.3A). Differences in basal expression levels of the TMGs might underlie their responses to BMI1 inhibition. We observed that the upregulated gene groups show lower median levels when expression is compared between untreated Rh28 and Rh30 cells (Fig. 3.3B). To determine whether differential gene responses affect protein product levels, we performed western blots on the products of canonical YAP/TAZ/TEAD targets for which reliable antibodies were available. Consistent with the mRNA transcript levels (Fig. 3.3C), AXL, CYR61, and CTGF protein levels were reduced in Rh30 and were increased or did not change in Rh28 (Supplementary Figure S3.2).<sup>197,200,210</sup> These results show that BMI1 inhibition can decrease or increase the expression of YAP/TAZ/TEAD target genes and that most of the genes are affected in a cell line-specific manner.

### **3.3.4 BMI1 inhibition increases the expression of distinct LATS1/2 kinases in Rh28 and Rh30**

Next, we set out to explore how direct regulation of genes by BMI1, a Polycomb chromatin protein, might affect the function of the Hippo pathway during pharmacological BMI1 inhibition. Our previous data showed that LATS1/2 phosphorylation increases upon BMI1 inhibition by PTC-028 treatment, thus activating Hippo signaling. Since BMI1 has no known kinase activity, we surmised that BMI1, through its role in PRC1, epigenetically suppresses a gene that encodes a kinase that phosphorylates LATS1/2. We set out to test the hypothesis that BMI1-inhibited cells show increased expression of a gene that encodes a LATS1/2 kinase.

To identify putative kinases of LATS1/2, we downloaded information from the OncoPPI database<sup>222</sup>, which uses data from time-resolved fluorescence resonance energy transfer (TR-FRET) experiments and curated published experimental data from STRING.<sup>223</sup> LATS2 was used as the primary hub since OncoPPI had data for LATS2 and not LATS1. The interaction network linked 11 kinases to LATS2. These kinases might also phosphorylate LATS1 because the kinase and activation loops of LATS1 and LATS2 have very similar sequences (85% similarity).<sup>197,224</sup> Integration of the interaction network with our RNA-seq data (in Cytoscape) (Figs. 3.4A, 3.4B) identified EPHA2 (Ephrin type-A receptor 2) ( $\log_2(\text{fold change}) = 1.5$ ) and PDGFRA (Platelet-derived growth factor receptor alpha) ( $\log_2(\text{fold change}) = 1.3$ ) as upregulated kinases that interact with LATS1/2 in Rh28 and Rh30, respectively. Evidence from TR-FRET experiments agrees with the hypothesis that EPHA2 and PDGFRA could bind and phosphorylate LATS1/2.<sup>222</sup> These results support the idea that epigenetic upregulation of kinases may lead to increased phosphorylation of LATS1/2 and activation of the Hippo pathway.

### 3.4 Discussion

Discerning differential tumor responses to drug treatment remains a challenge in oncology. Our study examined the effects of a small molecule inhibitor of BMI1, PTC-028, on two FP-RMS cell lines: Rh28 and Rh30. Our previous work showed that BMI1 inhibition through genetic knockdown or PTC-028 treatment leads to cell cycle arrest and apoptosis in FP-RMS cell lines. However, by further dissecting how PTC-028 influences oncogenic signaling, we reveal both similar and contrasting treatment responses in Rh28 and Rh30 at the level of gene transcription.

Both Rh28 and Rh30 harbor the PAX3-FOXO1 fusion and were derived from metastatic tissue from patients with FP-RMS by the lab of Dr. Edwin Douglass at St. Jude's Children's Research Hospital (Memphis, TN).<sup>192</sup> Rh28 was obtained from an axillary node metastasis, and Rh30 from bone marrow metastasis. Both patients were previously untreated, young (16/17-years-old), and race information is unavailable. Rh28 cells are near-tetraploid<sup>215</sup>, and Rh30 cells are near-triploid.<sup>216</sup> There are genetic differences between these two cell lines, such as Rh30 having an amplification of the *CDK4* locus<sup>225</sup> and a heterozygous *TP53* mutation.<sup>216</sup> These features could contribute to differences in basal expression levels and the different cellular pathways affected in PTC-028 treated cells.

Our RNA-seq study reveals that genes affected by BMI1 inhibition belong to pathways associated with muscle differentiation, DNA replication, and RNA processing. We found that hundreds of genes are affected by BMI1 inhibition by PTC-028 (Fig. 3.1). First, we analyzed upregulated genes, as PRC1 is mainly repressive; thus, BMI1 inhibition



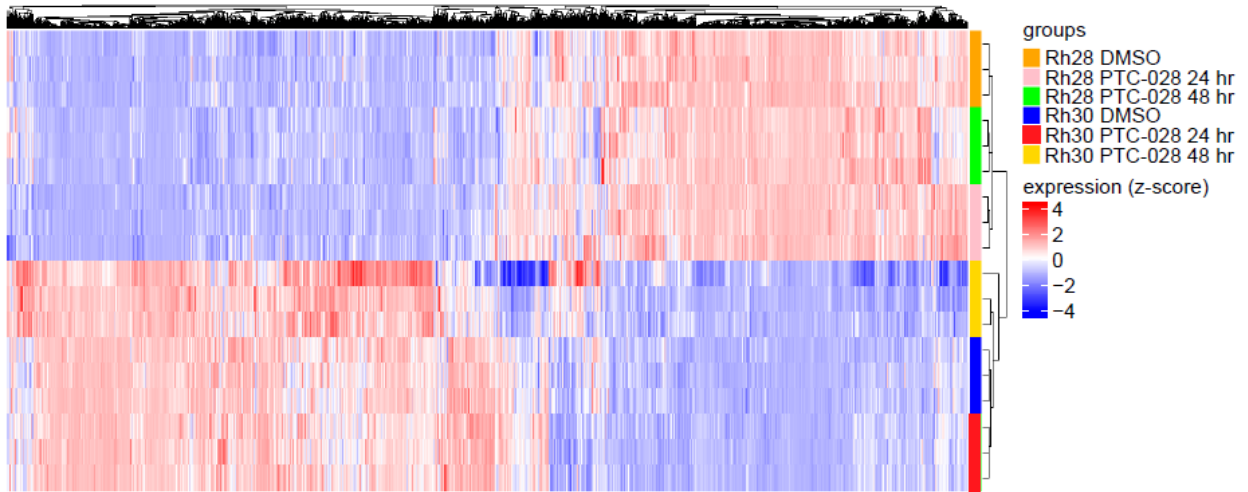
results in gene activation. We observed that muscle differentiation and pathways in cancer (DNA instability and p53 activity) are upregulated upon PTC-028 treatment (Fig. 3.2). This result suggests that BMI1 plays a role in DNA damage repair and may repress p53 signaling. This also indicates that the FP-RMS cells are likely becoming more differentiated and less proliferative upon treatment with PTC-028. While the primary role of PRC1 is repressive, secondary genetic effects may occur through the activation of transcriptional repressors and miRNAs. Thus, we next examined downregulated genes and observed that genes related to DNA replication were downregulated in Rh28, and RNA splicing was downregulated in Rh30 (Fig. 3.2). This result suggests that PTC-028 treatment leads to a loss of cell proliferation, a finding that is corroborated by our previous work. We combined DEGs from Rh28 and Rh30 to find similarities in PTC-028 response in the FP-RMS cell lines and found that muscle contraction and focal adhesion processes were upregulated. The process of myogenic differentiation may increase the number of focal adhesions and slower-moving cells, such as in myotube formation.<sup>226-228</sup> Next, only two downregulated DEGs were identified in Rh28 and Rh30: *MVD* (Mevalonate Diphosphate Decarboxylase) and *LOC102724250* (Fig. 3.2). MVD catalyzes the decarboxylation of mevalonate-5-diphosphate to produce isopentenyl diphosphate, which is necessary for the synthesis of isoprenoids<sup>229</sup>, such as cholesterol which is particularly important in dividing cancer cells.<sup>230</sup> Increased levels of cholesterol biosynthesis are associated with many cancers, particularly in glioblastoma multiforme.<sup>231</sup> We have discovered that BMI1 regulates pathways related to differentiation and metabolism in FP-RMS cells, a finding which has not been previously reported.

In our previous work, we discovered that BMI1 suppresses Hippo signaling.<sup>210</sup> Our previous study showed that BMI1 inhibition (PTC-028 treatment) increased LATS1/2 phosphorylation. The exact mechanism for this observation is unclear because BMI1 has no known kinase activity. In our current study, we identified putative kinases of LATS1/2 that BMI1 may epigenetically regulate. Data from OncoPPi<sup>222</sup> and our RNA-seq analysis suggest that the receptor tyrosine kinase EPHA2 (Ephrin type-A receptor 2) regulates increased phosphorylation of LATS1/2 in Rh28 cells and that receptor tyrosine kinase PDGFRA (Platelet-derived growth factor receptor alpha) carries out this activity in Rh30 cells (both kinases are also wild-type in these cell lines.<sup>232</sup> Protein-protein interactions identified through high throughput TR-FRET experiments support the interaction of EPHA2 and PDGFRA with LATS2.<sup>222</sup> It will be essential to confirm the activity of these kinases in FP-RMS by genetically knocking down EPHA2 or PDGFRA and observing the loss of LATS1/2 phosphorylation and gain of resistance against PTC-028. Additionally, chromatin profiling should be done to map BMI1 and associated chromatin features at the EPHA2 and PDGFRA genes. Since LATS1/2 phosphorylation prevents YAP/TAZ from entering the nucleus/binding TEAD to form YAP/TAZ/TEAD complexes and transcriptionally activate TMGs, we expected BMI1 inhibition to reduce the expression of highly-expressed TMGs. Our previous study observed downregulation of a few (3) canonical TEAD targets via western blot. In our current RNA-seq study, we identified 262 differentially regulated TMGs. While many TMGs showed downregulation as expected, others became upregulated, and we observed cell-line specific differences for most of the genes (155 of 262 total TMGs) (Fig. 3.3). For instance, canonical TEAD targets AXL, CTGF, and CYR61 showed lower mRNA and protein levels in PTC-028-treated Rh30 but higher levels in Rh28 (Supplementary Figure S3.2). Our results suggest that distinct

subsets of TEAD targets are highly transcribed in different FP-RMS cell lines. Inconsistent responses to BMI1 inhibition suggest a complex regulatory system where BMI1 might support activation (through Hippo) or repression (through PRC1) of TMGs in a locus-specific manner.

In conclusion, we discovered distinct gene expression profiles for two FP-RMS-derived cultured cell lines, that BMI1 inhibition induces anti-cancer gene expression states and cellular pathways. Hippo-regulated genes are affected by inhibition of BMI1 in a locus-specific and cell-line-specific manner.

A



B

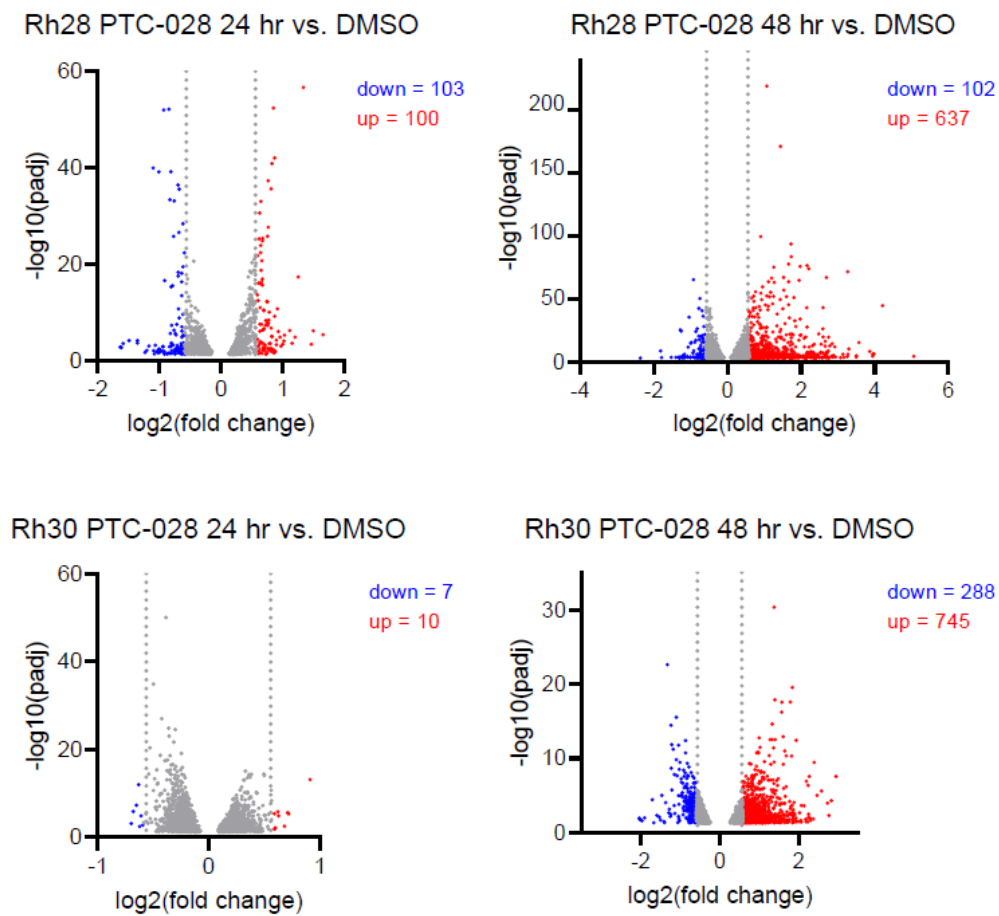


**Figure 3.1 BMI1 inhibition influences global gene expression in FP-RMS**

(A) Hierarchical cluster map of DMSO and PTC-028 treated Rh28 and Rh30 triplicate samples. Samples cluster according to cell line and condition as expected. Expression refers to the Z-score. (B) Volcano plots of Rh28 and Rh30 PTC-028 24/48 hrs vs. Rh28 DMSO,  $-\log_{10}(\text{padj})$  on y-axis and  $\log_2(\text{fold change})$  on x-axis.

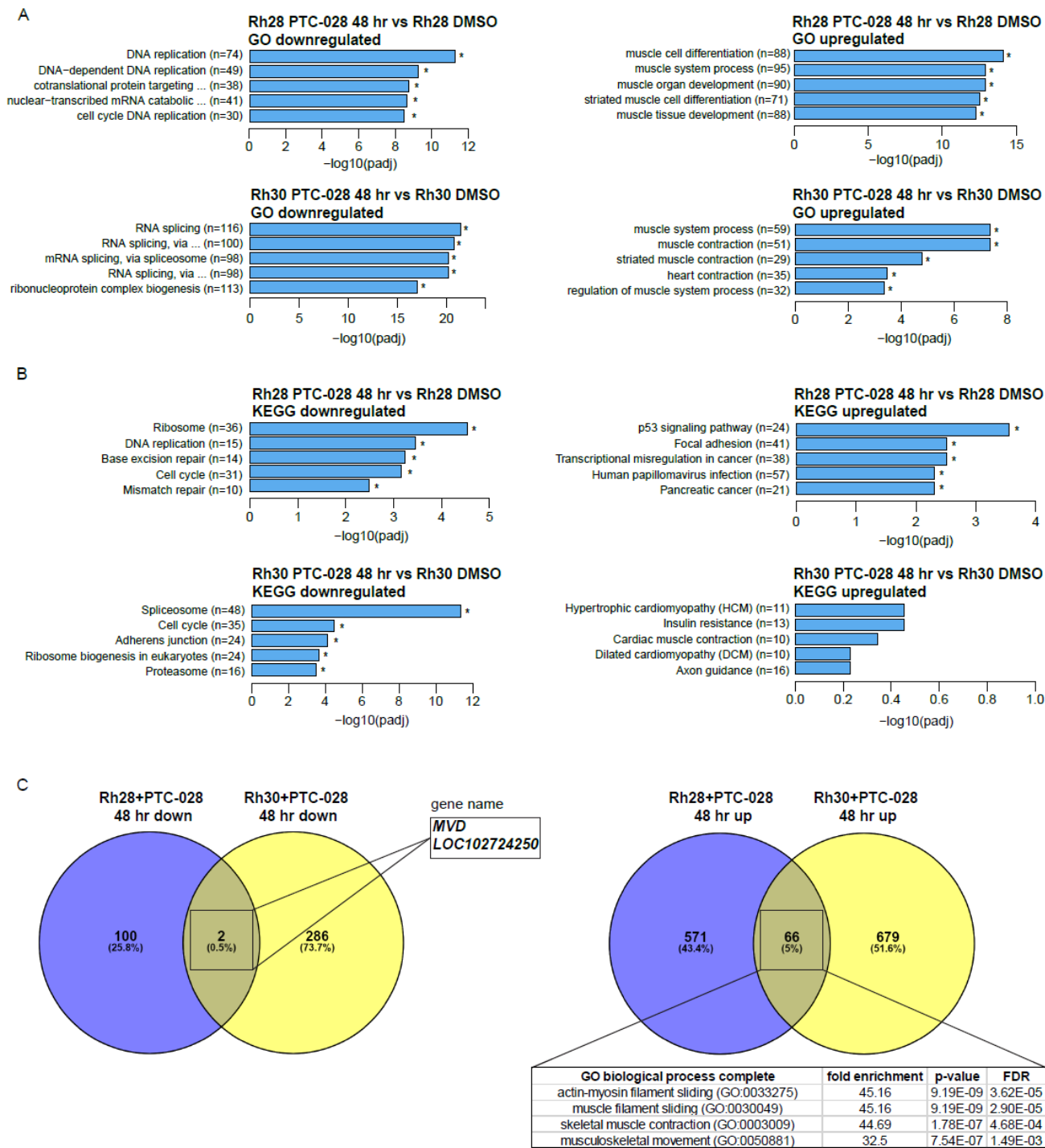


**Figure 3.2 Gene ontology analyses reveal pathways and biological activities affected by BMI1 inhibition**

(A) Bar charts of gene ontology (GO) biological processes affected in PTC-028 treated Rh28 and Rh30 cells. x-axes are  $-\log_{10}(\text{padj})$ . (B) Bar charts of KEGG pathway enriched in PTC-028 treated Rh28 and Rh30 cells. x-axes are  $-\log_{10}(\text{padj})$ . (C) Venn diagrams of significant differentially expressed genes (DEGs) with fold changes of greater than 1.5 in Rh28 PTC-028 48 hrs vs. DMSO and Rh30 PTC-028 48 hrs vs. DMSO.

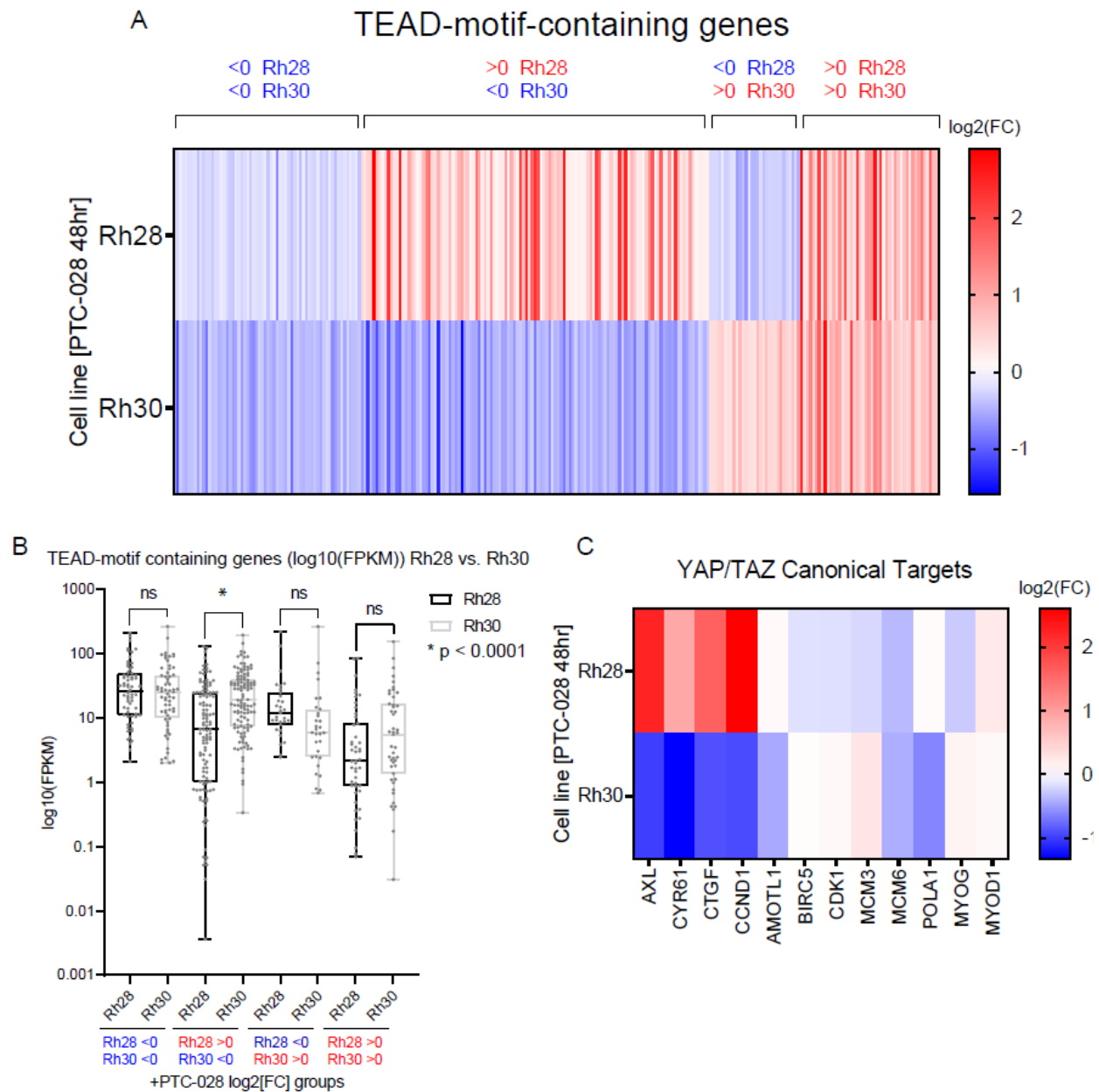


**Figure 3.3 Gene expression in Rh30 is more sensitive to BMI1 and Hippo pathway inhibition**

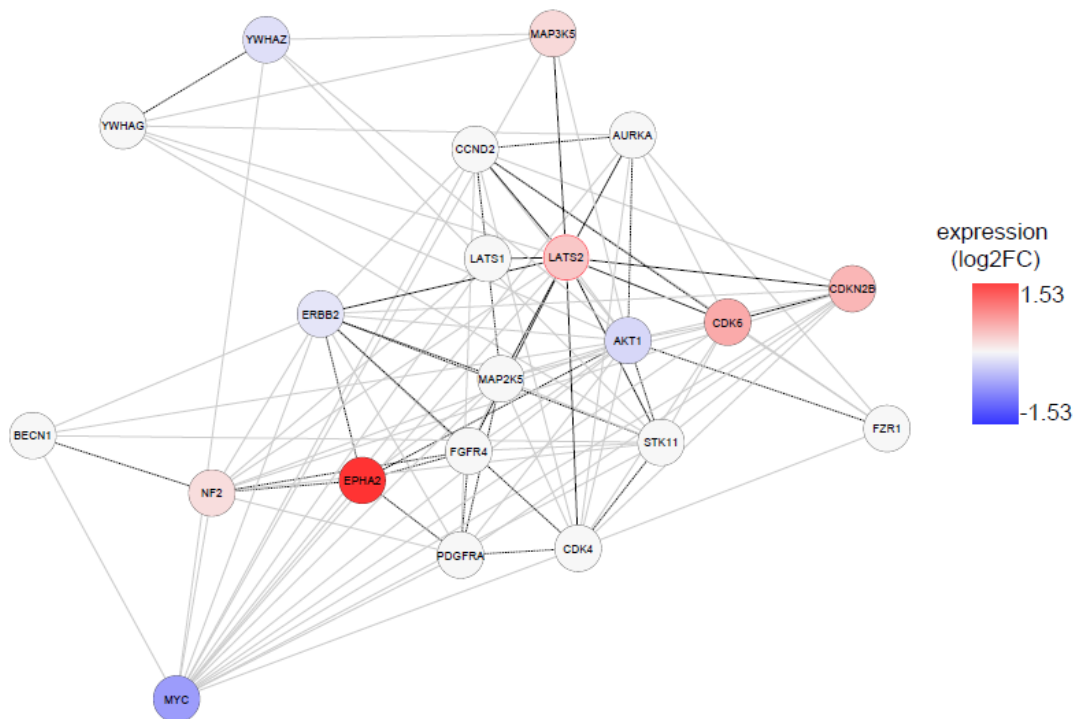
(A) Heat map of PTC-028 treated Rh28 and Rh30 cells. All genes are TEAD-motif-containing genes. They are grouped into sections: <0 in Rh30 and Rh28, <0 in Rh30 >0 in Rh28, >0 in Rh30 <0 Rh28, >0 Rh30 >0 Rh28. Expression is log<sub>2</sub>(fold change). (B)



Box and whisker plot of TEAD-motif-containing genes in untreated Rh28 vs. untreated Rh30 in  $\log_{10}(\text{FPKM})$ . Stratified by groups in (A). (C) Heatmap of YAP/TAZ/TEAD canonical targets in PTC-028 treated Rh28 and Rh30. Expression is  $\log_2(\text{fold change})$ . YAP/TAZ canonical targets include AXL, CYR61, and CTGF.

A

Rh28+PTC-028 LATS2 protein interaction network



B

Rh30+PTC-028 LATS2 protein interaction network

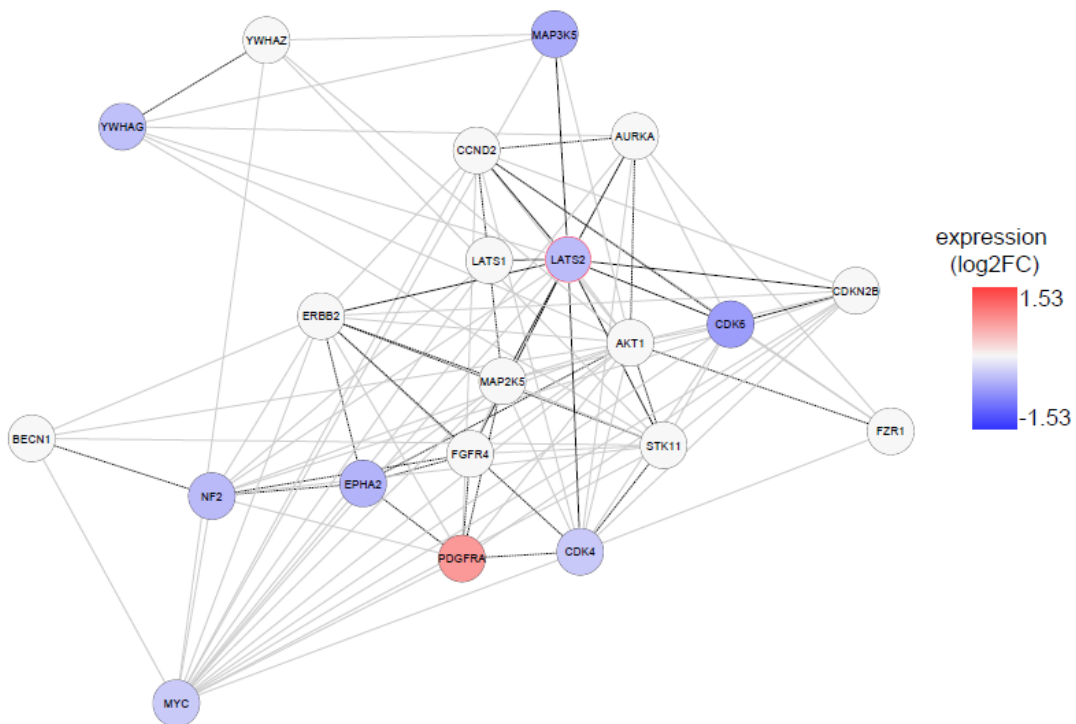


**Figure 3.4 BMI1 inhibition differentially affects expression of LATS1/2 kinases in Rh28 and Rh30**

(A) Network of proteins that interact with LATS2 based on OncoPPI data<sup>222</sup> (black lines for direct interactions, dotted lines for indirect interactions), with added edges from the STRING database<sup>223</sup> (gray lines). RNA-seq ( $\log_2(\text{fold change})$ ) Rh28+PTC-028 gene expression data is overlaid. (B) Network of proteins that interact with LATS2 based on OncoPPI data (black lines for direct interactions, dotted lines for indirect interactions), with added edges from the STRING database (gray lines). RNA-seq ( $\log_2(\text{fold change})$ ) Rh30+PTC-028 gene expression data is overlaid.

### Supplementary Table 3.1 Top differentially expressed genes (DEGs) in PTC-028 treated Rh28 and Rh30 cell lines

List of the top 10 DEGs in Rh28 PTC-028 48 hr vs. Rh28 DMSO (downregulated and upregulated) and Rh30 PTC-028 48 hr vs. Rh30 DMSO (downregulated and upregulated). DEGs are sorted by log<sub>2</sub>(fold change).

Rh28 PTC-028 48 hr vs Rh28 DMSO Downregulated DEGs				Rh28 PTC-028 48 hr vs Rh28 DMSO Upregulated DEGs			
Gene Name	log <sub>2</sub> FoldChange	p-value	adjusted p-value	Gene Name	log <sub>2</sub> FoldChange	p-value	adjusted p-value
<i>AC008013.3</i>	-2.357142908	0.00939	0.048321	<i>NRAP</i>	5.061972482	0.000306	0.002979
<i>SLC6A3</i>	-1.808506459	6.70E-09	1.90E-07	<i>KCNJ12</i>	4.216074147	4.74E-45	1.97E-42
<i>AC009054.2</i>	-1.781969048	0.003267	0.020922	<i>DKK1</i>	3.981093668	2.92E-06	4.94E-05
<i>OR9K1P</i>	-1.523868299	0.001877	0.013477	<i>RBFOX1</i>	3.952900369	2.29E-06	3.99E-05
<i>AC141557.2</i>	-1.389780951	0.002698	0.017982	<i>PHLDA2</i>	3.943885282	0.000187	0.001946
<i>HFM1</i>	-1.326109723	0.002082	0.014625	<i>HKDC1</i>	3.865835491	1.43E-08	3.84E-07
<i>AC098969.1</i>	-1.296318722	0.001865	0.013412	<i>XIRP1</i>	3.574560907	8.10E-16	5.59E-14
<i>AC093797.1</i>	-1.29619215	0.004746	0.027896	<i>AL359195.2</i>	3.502876641	0.001614	0.011892
<i>AC242376.2</i>	-1.283772722	0.004743	0.027892	<i>CDH5</i>	3.502435058	8.34E-05	0.000964
<i>BASP1-AS1</i>	-1.280536545	0.006906	0.037867	<i>APOC1</i>	3.298739642	1.39E-10	5.13E-09

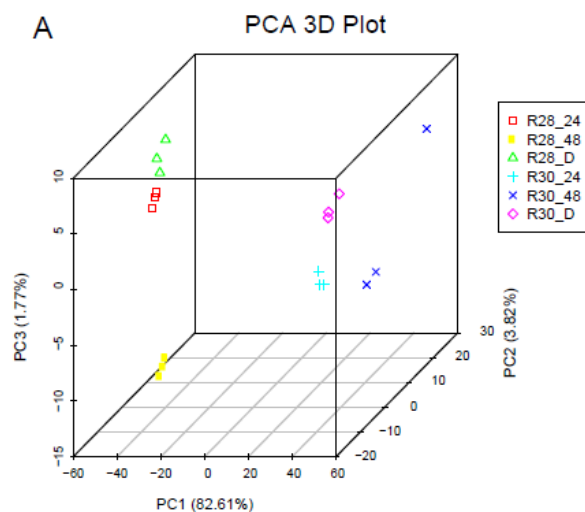
  

Rh30 PTC-028 48 hr vs Rh30 DMSO Downregulated DEGs				Rh30 PTC-028 48 hr vs Rh30 DMSO Upregulated DEGs			
Gene Name	log <sub>2</sub> FoldChange	p-value	adjusted p-value	Gene Name	log <sub>2</sub> FoldChange	p-value	adjusted p-value
<i>AC092881.1</i>	-2.032686106	0.001003	0.011779	<i>FRG2B</i>	2.944340252	1.14E-10	2.88E-08
<i>AC044802.1</i>	-2.02248179	0.001675	0.016911	<i>CALY</i>	2.829136371	7.92E-07	5.27E-05
<i>CALB2</i>	-1.96801154	0.003156	0.026241	<i>NOXA1</i>	2.763665363	0.000317	0.005194
<i>STARD13-AS</i>	-1.898552378	0.000902	0.010895	<i>COX6A2</i>	2.727803552	2.05E-06	0.000105
<i>EDN2</i>	-1.700970122	5.57E-07	3.91E-05	<i>PDK4</i>	2.574678736	2.24E-08	2.63E-06
<i>SNORD12B</i>	-1.669253278	0.007467	0.047371	<i>MARCHF2</i>	2.464567809	1.08E-07	1.01E-05
<i>EGR1</i>	-1.587916428	0.000302	0.005002	<i>A2M</i>	2.389397289	7.59E-13	3.71E-10
<i>LRRC32</i>	-1.525886351	0.000647	0.008565	<i>BCRP4</i>	2.375037137	0.001354	0.014521
<i>GPA33</i>	-1.494674432	0.002204	0.020466	<i>SIGLEC11</i>	2.298531747	0.002509	0.022492
<i>LINC01963</i>	-1.465875535	1.02E-07	9.67E-06	<i>ABCG1</i>	2.286642532	0.000931	0.011165

**Supplementary Table 3.2 TEAD-motif IDs**

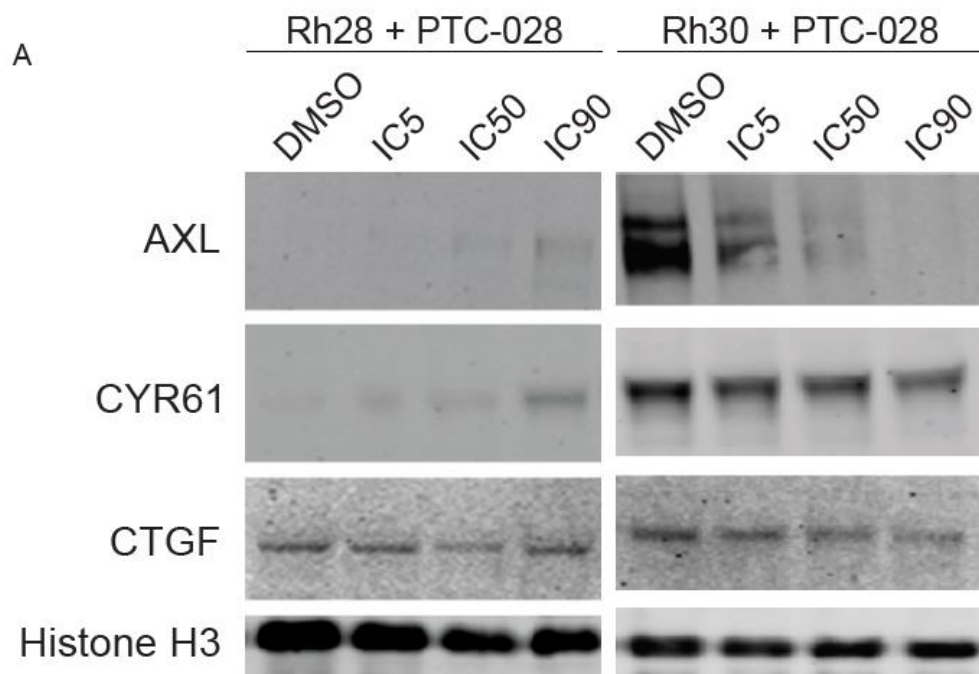
List of TEAD1, TEAD3, and TEAD4 motif IDs from the transcription factor binding site database (TFBS).<sup>221</sup>

<b>Gene</b>	<b>TFBS ID code</b>
TEAD1	TEAD1_MA0090.1, TEAD1_TEA_full_monomeric_10_1, TEAD1_TEA_full_dimeric_17_1
TEAD3	TEAD3_TEA_DBD_monomeric_8_1, TEAD3_TEA_DBD_dimeric_17_1
TEAD4	TEAD4_TEA_DBD_monomeric_10_1



**Supplementary Figure S 3.1 Principal component analyses plot of RNA-seq samples**

(A) 3D principal component analyses (PCA) of DMSO and PTC-o28 treated (24 hrs and 48 hrs) Rh28 and Rh30 samples. Samples cluster according to group except for one outlier (R30\_48).



**Supplementary Figure S 3.2 Western blot of YAP/TAZ targets in Rh28 and Rh30**

(A) Western blots of AXL, CYR61, and CTGF in DMSO and PTC-028 treated (72 hrs) Rh28 and Rh30 cells. Histone H3 as a loading control.

## **4. Discussion and future directions**



#### 4.1 Summary of findings in Chapters 2 and 3

FP-RMS is a rare, aggressive pediatric malignancy with no targeted therapies available. To date, efforts to target the PAX-FOXO1 fusion protein directly have not been clinically fruitful. Treatment options are limited to resection, multiagent chemotherapy, and radiation, which can have significant late effects on pediatric patients. Relapse and recurrence of FP-RMS is frequent in many patients as well; thus, novel therapies must be explored.

In Chapter 2, we hypothesized that the epigenome could be a potential target in FP-RMS. We began by searching for epigenetic targets that were overexpressed in RMS and other sarcomas. We defined BMI1 as highly expressed in RMS patient samples, PDX models, and cell lines to establish its potential as a target. We found that BMI1 was highly expressed, as is common in adult histotypes but more poorly defined in pediatric cancers.<sup>106,108,110,122,139,148,149</sup> To demonstrate the effectiveness of BMI1 inhibition, we knocked down BMI1 using shRNA and siRNA and showed that BMI1 inhibition resulted in a loss of viability in FP-RMS. Next, we utilized two independent pharmacological small molecule inhibitors PTC-209 and PTC-028 across a panel of FP-RMS cell lines and calculated the IC<sub>50</sub>s. These IC<sub>50</sub>s were in line with the effectiveness of PTC-209 and PTC-028 in other cancer types.<sup>117,159</sup> To further understand how BMI1 inhibition was affecting FP-RMS cells, we examined the cell cycle and apoptosis and found that the cells had a dose-dependent increase in the number of cells in early and late apoptosis (Figure 2.4) upon PTC-028 treatment and a decrease in the number of cells in S phase (Figure 2.4). These results are consistent with the literature showing that BMI1 controls the G1/S transition through inhibiting levels of *CDKN2A* (Cyclin-Dependent Kinase inhibitor 2A,

encodes p16-INK4a/p14-ARF). We then moved *in vivo* and tested the effectiveness of PTC-028 in a subcutaneous xenograft model of Rh30, which is an aggressive model of FP-RMS. Tumor burden was significantly reduced in mice, and there was an increase in progression-free survival. PTC-028 treatment reduced overall levels of BMI1, similar to other models. Finally, we hypothesized that BMI1 influenced the Hippo pathway based on the importance of this pathway in FP-RMS and the previously published data that BMI1 interacts with YAP in Ewing sarcoma. Our work has strengthened and broadened this finding in sarcomas, with implications for other cancer types as well. Through a series of experiments, we discovered that BMI1 suppresses phosphorylation of LATS1/2, leading to repression of Hippo signaling and activation of YAP/TAZ/TEAD targets, a novel finding that had not previously been reported. We also found that knocking down LATS1/2 or overexpressing YAP resulted in a rescue of BMI1 inhibition by PTC-028, suggesting that the Hippo pathway may represent one key target of BMI1 in RMS. BMI1 does have a role in regulating the Hippo pathway. Several questions remain unanswered, notably 1) how exactly BMI1 influences the Hippo pathway and 2) how BMI1-regulated pathways shape the malignant phenotype in ARMS. To begin to answer these questions, we turned to RNA-sequencing.

Thus, in Chapter 3, we investigated how BMI1 inhibition impacts the transcriptome of FP-RMS cells through RNA-sequencing. Inhibition of BMI1 resulted in the activation and repression of hundreds of genes in FP-RMS cells. We identified what pathways were being upregulated in response to BMI1 inhibition and observed alterations in gene networks corresponding to “muscle differentiation,” “muscle contraction,” and “p53 signaling.” Loss of plasticity and proliferation by BMI1 inhibition, as it is a stem cell

marker, is not surprising and is consistent with the literature. Genes related to “DNA replication,” “Cell cycle,” and “RNA splicing” were downregulated, indicating that BMI1 promotes cell proliferation, one of the seminal hallmarks of cancer. In both cell lines, Rh28 and Rh30, genes related to “Ribosome” and “Ribosome biogenesis” were downregulated as well, suggesting that translation may be inhibited by PTC-028 treatment. Our previous hypothesis and work demonstrated that BMI1 suppresses LATS1/2 phosphorylation, and so we examined the expression levels of genes containing TEAD-motifs. We expected the expression of TEAD targets to decrease since, upon BMI1 inhibition, Hippo was reactivated, and YAP/TAZ/TEAD are not able to form a complex and transcribe TEAD target genes. We found that Rh28 had higher expressions of TEAD targets upon PTC-028 treatment, while Rh30 had lower expressions as we hypothesized. To understand why, we looked at baseline expression levels of TEAD targets in both cell lines and saw that Rh28 generally had lower baseline expression of TEAD targets. This indicates that Rh28 may not be as reliant on the pro-growth and survival genes downstream of Hippo suppression compared to Rh30. Future work could model this across more RMS cell lines and patient-derived xenograft (PDX) models, seeking to understand the complex oncogenic signaling that is occurring. Then, to answer the question as to how BMI1 could be influencing LATS1/2 phosphorylation, we created a protein-protein interaction network to identify kinases of LATS1/2 and found that two different kinases (EPHA2 and PDGFRA) were upregulated in Rh28 and Rh30, suggesting that these two kinases could interplay with LATS1/2. However, further experiments would need to be carried out to begin to examine this hypothesis.

Our work has shown that BMI1 is a novel target in FP-RMS. Mainly, our research focused on exploring the effects of BMI1 inhibition by PTC-028 and examining the effects on cell proliferation, apoptosis, and the Hippo pathway, as well as nominating new pathways of interest through transcriptomics. However, it is well appreciated that cancer is characterized by multiple hallmarks. With this in mind, we will discuss the influence of BMI1 on some of these, including DNA damage repair, metabolism, and invasion/metastasis. Next, we will broaden our focus and consider the roles of other PRC1/2 protein members in RMS. Finally, building on the identification of BMI1 as an oncogenic vulnerability, we will outline how BMI1 may be combined with other therapies to improve the therapeutic arsenal within FP-RMS.

#### **4.2 DNA damage repair**

Genome instability and genetic mutations are hallmarks of cancer.<sup>9</sup> DNA damage can alter the genome and result in mutations that can confer advantages in subpopulations of cells, such as mutations in genes that monitor genomic integrity (*TP53*). This can potentiate the development of pre-cancerous and cancerous cells. Cancer cells also need to manage replication stress, as overexpression of oncogenes (*MYC*) and/or DNA damage results in re-replication and replication fork stalling.<sup>233</sup> There are multiple types of DNA damage, both from endogenous and exogenous sources. DNA damage can arise from oxidative damage from reactive oxygen species (ROS), base alkylation and base loss, DNA crosslinking, and bulky adduct formation. Ionizing radiation can also lead to base damage, single-strand breaks, and double-strand breaks. Indeed, PRC1 is known to play a role in repairing double-strand breaks and catalyzing the

monoubiquitination H2AK119, which is subsequently repaired through the homologous repair pathway. Accordingly, BMI1 is a necessary component for maintaining DNA damage repair in cells. High, sustained expression of BMI1 may provide an advantage for tumor cells by protecting them from replication stress.<sup>234,235</sup> Radiotherapy is sometimes used in FP-RMS treatment; however, the effectiveness can be limited due to radioresistance.<sup>24,236,237</sup> It would be of interest to see if BMI1 inhibition could synergize with radiotherapy.

In keeping with this hypothesis, in Chapter 3, we noted that upon BMI1 inhibition, pathways related to DNA replication were significantly downregulated in FP-RMS cells. In Chapter 2, our data supported that G1/S transition was also downregulated, which is consistent with the regulation of CDKN2A by BMI1. CDKN2A had increased expression at the protein level (Supplementary Figure S2.4A), however there was no significant change in mRNA level detected by our RNA-seq experiment. This could be due to temporal differences: the RNA for RNA-seq was collected at 48 hr of PTC-028 treatment, and the protein was collected at 72 hr of PTC-028 treatment. Another explanation could be various post-transcriptional mechanisms not captured by RNA-seq. There are DNA damage checkpoints throughout the cell cycle, including at the G1/S checkpoint. To confirm if DNA damage occurs in PTC-028 treated cells, future experiments could involve performing a comet assay, which can measure the amount of DNA fragments in a cell through single-cell gel electrophoresis. It would be interesting to evaluate DNA damage and determine whether BMI1 disruption affects DNA repair. BMI1 has mainly been reported to contribute to the repair of double-strand breaks, specifically homologous recombination. To test if double-strand breaks are occurring, we could treat FP-RMS cells

with PTC-028 and/or ionizing radiation and examine if  $\gamma$ H2AX (a marker of double-strand breaks<sup>142</sup>) foci form through immunofluorescence assays. We could also confirm if BMI1 co-localizes with the  $\gamma$ H2AX and if this is lost upon PTC-028 treatment. It will be of interest to see if BMI1 inhibition sensitizes cells *in vitro* and *in vivo* to DNA damage by ionizing radiation in RMS and other sarcomas.

### **4.3 Intersection of BMI1 with metabolic pathways**

Oxidative stress through reactive oxygen species (ROS) can also result in DNA damage and genome instability. Oxidation can damage the sugar-phosphate backbone of DNA and lead to DNA double-strand breaks. ROS can also oxidize nucleosides directly, resulting in a G-T or G-A transversion, ultimately leading to DSBs if not correctly repaired. BMI1 was found by Liu, *et al.* (2009) to suppress ROS through PRC1 repressing several genes involved in ROS generation and/or mitochondrial functions, such as ATOX5, CYP24A1, PMAIP1, and others.<sup>238</sup> Inhibiting BMI1 leads to upregulation of expression of these genes and a subsequent increase in ROS, leading to oxidative stress and cancer cell death.<sup>238</sup> Results from our RNA-seq data in Chapter 3 demonstrate that BMI1 does influence genes involved in metabolism. From our RNA-seq data, we found that BMI1 promotes cholesterol biosynthesis. This finding is corroborated by Dibenedetto, *et al.* (2017), who revealed that BMI1 overexpression in human myoblasts derived from Duchenne's muscular dystrophy patients increases levels of cholesterol biosynthesis.<sup>239</sup> Cholesterol integrates into lipid raft domains on cell membranes, which regulate signal transduction by raft proteins. Increased cholesterol levels and numbers of lipid rafts are associated with increased tumor growth and phosphorylation of

Akt.<sup>230,240,241</sup> Further research such as label-free liquid chromatography coupled to mass spectrometry-based metabolomics (LC-MS) in DMSO vs. PTC-028 treated FP-RMS cells could reveal more specific effects of BMI1 inhibition on the biosynthesis of isoprenoids/sterol synthesis. Combining this with ChIP-seq in normal and BMI1 inhibited cells could elucidate further details as to how BMI1/PRC1 influence the metabolic states of FP-RMS tumors.

#### **4.4 Invasion and metastasis**

BMI1 plays a crucial role in proliferation and survival and has also been implicated in regulating invasion and metastasis in the context of other malignancies. BMI1 was discovered by Ferretti, *et al.* (2016) to be a necessary component of melanoma metastasis *in vivo*. Deletion of BMI1 significantly decreased the number of lung metastases.<sup>107</sup> The epithelial-to-mesenchymal transition (EMT) is often considered a necessary process for invasion and metastasis. Epigenetic modifiers have been reported to interact with EMT transcription factors and promote the expression of genes involved in invasion.<sup>44,169,242</sup> While sarcomas, already being of mesenchymal origin, do not go through the “traditional” EMT that is most studied in carcinomas, they can progress through a similar EMT-like program. Sarcomas can have a mix of epithelial-like, metastable, or mesenchymal-like cells.<sup>243</sup> These metastable cells can transition to more epithelial-like or more mesenchymal-like depending on the environment and go through MET or EMT-like processes.<sup>243</sup> Various EMT-associated transcription factors, such as SNAIL, TWIST, and ZEB1/2, still contribute to EMT in sarcomas, including RMS.<sup>243-247</sup> Both PRC1 and PRC2 are essential regulators of EMT.<sup>44,242</sup> Our data from Chapter 2 and Chapter 3 primarily

focused on proliferation, apoptosis, and the Hippo pathway. YAP promotes EMT through its role in the Hippo pathway binding TEAD and promoting factors related to growth, proliferation, and migration.<sup>196,197,220,248-251</sup> Cell lines that have high YAP/TEAD activity typically have higher metastatic potential.<sup>251</sup> Much further investigation into BMI1 inhibition in the context of EMT and invasion/metastasis should be done in FP-RMS and other sarcomas. *In vitro* modeling of scratch-wound assays and Boyden chamber assays with BMI1 inhibitors could reveal if BMI1 regulates invasion in FP-RMS. Next, *in vivo* modeling of metastatic disease in FP-RMS could involve tail vein injections of cell lines such as Rh30 and then treatment with a BMI1 inhibitor.<sup>252</sup>

#### **4.5 Further modeling of PRC1 and BMI1 in FP-RMS**

Our studies have revealed that BMI1 inhibition decreases cell proliferation and increases apoptosis in FP-RMS cells. We have discussed future directions to examine other hallmarks of cancer. However, our studies involving Hippo signaling in Chapter 2 and RNA-seq study in Chapter 3 demonstrate that BMI1 inhibits Hippo activation through suppressing LATS1/2 phosphorylation. The primary question that remains is: how is BMI1 regulating the Hippo pathway? The canonical role of BMI1 is through its role in PRC1, contributing to H2AK119 monoubiquitination and gene repression. Further studies could involve ChIP-seq and exploring where PRC1/2 localizes with and without PTC-028 treatment by examining H2AK119Ub, H3K27me3, BMI1, and EZH2 localization across the genome. While a majority of studies have focused on BMI1 as an epigenetic regulator, it has additional functions. Pulldown studies of BMI1 in Ewing sarcoma<sup>179</sup> showed that BMI1 directly interacts with YAP. BMI1 has also been found to bind the



androgen receptor in the nucleus of prostate cancer cells.<sup>194</sup> In Chapter 3, we nominated EPHA2 and PDGFRA as potential kinases of LATS1/2, with our hypothesis being that BMI1 suppresses the expression of these kinases through PRC1. Once BMI1 is inhibited, EPHA2 and PDGFRA show increased expression and may phosphorylate LATS1/2, activating Hippo signaling and preventing YAP/TAZ from entering the nucleus, binding TEAD, and then transcribing TEAD targets (Figure 4.1).

However, BMI1 could be interacting physically with other proteins or even directly with LATS1/2 in the cytoplasm. BMI1 is primarily a nuclear protein, though it has been reported to interact with E4F1 in the cytoplasm of cells.<sup>253</sup> It is possible that BMI1 could bind LATS1/2 to block phosphorylation/activation of Hippo signaling. To determine if this hypothesis is accurate, we could immunoprecipitate BMI1 and perform western blots for LATS1/2. Additional experimentation such as tandem mass spectrometric analysis of BMI1 and LATS1/2 could reveal if they bind each other and other unknown proteins. A follow-up kinase assay of LATS1/2 with EPHA2 and/or PDGFRA and titration of BMI1 may also indicate if BMI1 prevents LATS1/2 phosphorylation through protein-protein interactions.

Our work primarily focused on BMI1; however, there are many other canonical PRC1 (PRC1.1-1.6) and variant PRC1 complexes that could be potential targets in FP-RMS as well (Figure 4.2). Other Polycomb complexes could compensate for the loss of PRC1.4 through BMI1 inhibition, and thus combining inhibition of PRC1 and PRC2 complexes may synergize to prevent compensation. A targeted CRISPR knockout screen of PRC1.1-6 and PRC2 components could demonstrate other necessary components that regulate

oncogenic signaling in FP-RMS and whether the effects of BMI1 inhibition we saw in our research are BMI1-specific or relate to PRC1. Combination therapies of BMI1 inhibition and EZH2 inhibition have been investigated in glioblastoma by Jin, *et al.* (2017) and were more effective than either single agent alone.<sup>118</sup> Since both glioblastoma and FP-RMS are heterogeneous solid tumors, this may apply to FP-RMS. Inhibition of other necessary PRC1 components, such as CBX proteins, have also been studied in numerous cancers.<sup>129,254-256</sup> CBX proteins contain chromodomains which are required to recognize H3K27me3 marks placed by PRC2.<sup>111</sup> Further studies of the inhibition of CBX proteins in FP-RMS could reveal more information about PRC1 regulation in this cancer.

#### **4.6 Combining BMI1 inhibition with other translatable targets**

We have established BMI1 as a potential target in FP-RMS with clinical promise. PTC-596, the newest version of BMI1 inhibitor, is currently in several active clinical trials, including other pediatric cancers (DIPG). However, the issue of single-agent resistance is a significant problem in cancer.<sup>152,206,257</sup> Tumor cells can overcome small molecule inhibitors over time through selection and molecular responses, such as upregulating drug efflux pumps.<sup>206,258</sup> Genome instability in heterogeneous cancers can also provide a growth/survival advantage to tumors, as tumor cells could acquire mutations of the target of the small molecule, which has been studied in EZH2 inhibition.<sup>257,259</sup> Bisselier and Wajapeyee (2018) developed EZH2-inhibitor-resistant DLBCL cell lines and discovered that EZH2 acquired secondary mutations and upregulated several survival pathways, such as PI3K and MEK signaling.<sup>259</sup> Their results suggest that continued treatment with

single-agent therapies, such as BMI1 inhibition alone, may not be sufficient for the complete elimination of highly heterogeneous malignancies like FP-RMS.

Our *in vivo* study in Chapter 2 used PTC-028 as a single agent therapy in a subcutaneous xenograft model and found that tumor burden was reduced. While these results are promising, future studies should combine BMI1 inhibition with standard of care chemotherapy like vincristine. However, another issue is chemoresistance in FP-RMS, in which subpopulations of cancer stem-like cells are resistant to chemotherapy and lead to relapse and recurrence.<sup>26,205</sup> Targeting cells that highly express BMI1 has been shown to largely eliminate residual stem-like cells in other cancer models<sup>110,155,156</sup>, though we have not yet investigated this FP-RMS. Future work could combine BMI1 inhibition with standard of care chemotherapy (such as vincristine) in chemoresistant models of FP-RMS. With *in vitro* studies, we could create chemotherapy-resistant FP-RMS cell lines and treat cells with BMI1 inhibitors to determine efficacy. Additionally, Slemmons, *et al.* (2021) pioneered a new FP-RMS cell culture method (based on previous work in FN-RMS<sup>260</sup>) in which cell lines form a spheroid called a rhabdosphere.<sup>261</sup> These rhabdospheres are reported to be more chemoresistant than 2D culture. Testing the effectiveness of BMI1 inhibition on rhabdospheres could support the hypothesis that BMI1 inhibitors target cancer stem-like cells and thus may be extremely valuable in preventing FP-RMS relapse or recurrence.

Another exciting avenue of future research could be the combination of BMI1 inhibition and immunotherapy. Previous work by Jia, Zhang, and Wang (2020) demonstrated that BMI1 inhibition by PTC-209 after anti-PD1 therapy resulted in a

decrease in cancer progression and prevention of tumor relapse in a 4-Nitroquinoline 1-oxide (4NQO) mouse model of HNSCC.<sup>155</sup> Anti-PD1 therapy with cisplatin briefly abrogated tumor burden, but recurrence was frequent. When combined with PTC-209, tumor recurrence and lymph node invasion drastically decreased. PTC-209 treatment led to an upregulation of type 1 interferon chemokines and increased CD8+ T-cell infiltration into tumors. Increased CD8+ T-cell infiltration could be extremely valuable in the context of FP-RMS. Typically, pediatric solid tumors have cold (non-inflammatory) tumors with low levels of T-cell infiltration compared to adult tumors.<sup>29,262</sup> Combining epigenetic drugs with immunotherapy may synergize to restructure the tumor microenvironment and mount an effective anti-cancer response, thus overcoming immunotherapy limitations for difficult to treat solid tumors. Combination therapies of epigenetic inhibitors and immunotherapies could be expanded to other sarcomas, particularly others with high BMI1 levels and low immune infiltration, such as osteosarcoma.<sup>189,263</sup>

#### **4.7 Final conclusions and thoughts**

In conclusion, this dissertation has established BMI1 as a potentially translatable target in FP-RMS. We have established novel connections of BMI1 to Hippo signaling and remarked on differential intertumor responses in FP-RMS that should be considered when exploring targeted cancer therapies to anticipate possible mechanisms of resistance. Further investigation should focus on the potential of combining BMI1 inhibition with other treatments to avoid resistance and consider the possibility of other PRC1/2 proteins as dependencies in RMS and other sarcomas.

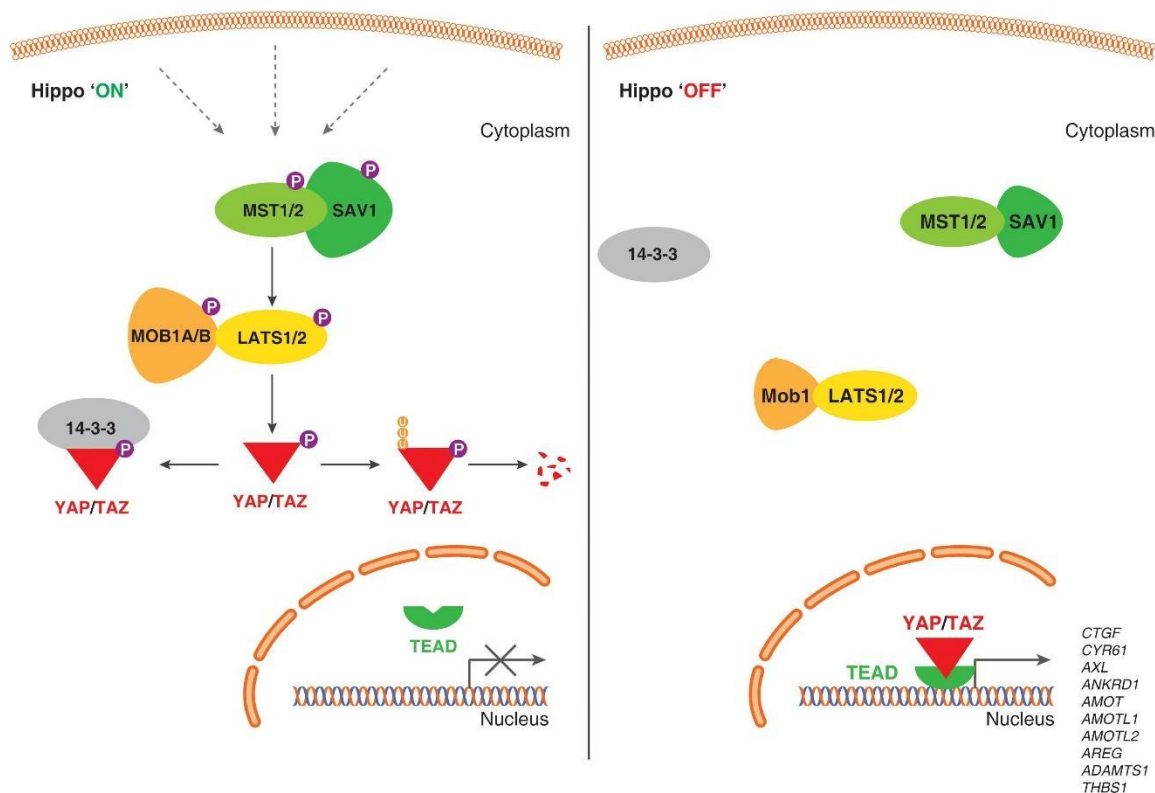


**Figure 4.1 Hippo pathway schematic.** Image adapted from Boopathy and Hong (2019).<sup>264</sup> Representation of the Hippo pathway. The left side shows Hippo 'ON' wherein outside signaling influences the phosphorylation of MST1/2, then MST1/2 phosphorylates LATS1/2, resulting in phosphorylation of YAP/TAZ and sequestration of YAP/TAZ by 14-3-3 proteins or ubiquitination and proteasome degradation. TEAD is not able to transcribe target genes in the nucleus without YAP/TAZ. The right side shows Hippo 'OFF'. MST1/2 and LATS1/2 remain unphosphorylated, and YAP/TAZ enter the nucleus, form a complex with TEADs, and promote transcription of pro-growth and proliferation target genes.

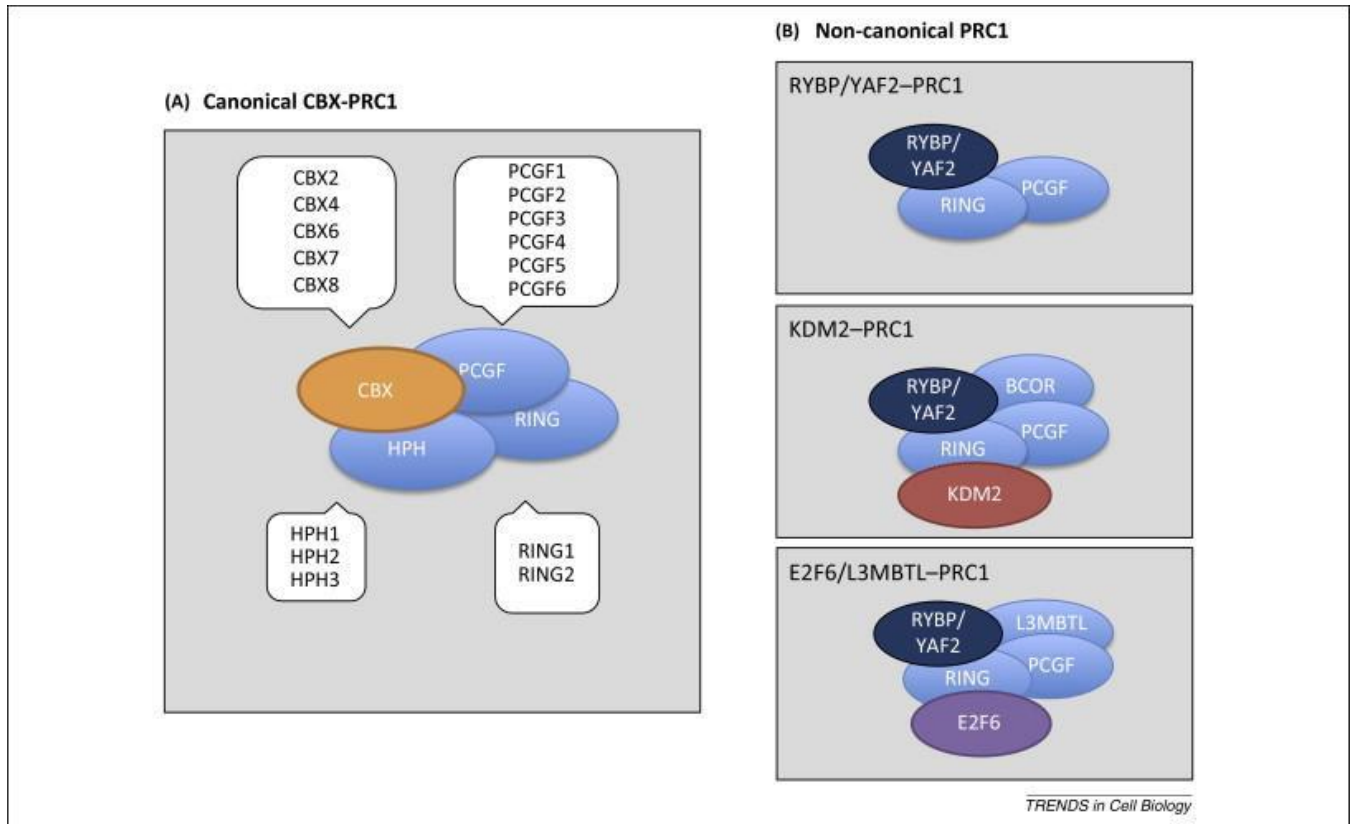


**Figure 4.2 Canonical and non-canonical PRC1 complexes.** Image adapted from Gil and O’Loughlen (2014).<sup>129</sup> (A) shows various components of canonical CBX-PRC1. (B) shows variant or non-canonical PRC1 complexes which contain RYBP/YAF, KDM2, or E2F6/L3MBTL.

## References

1. Biankin AV, Piantadosi S, Hollingsworth SJ. Patient-centric trials for therapeutic development in precision oncology. (1476-4687 (Electronic)).
2. Torre LA, Siegel RL, Ward EM, Jemal A. Global Cancer Incidence and Mortality Rates and Trends—An Update. *Cancer Epidemiology Biomarkers & Prevention*. 2016;25(1):16.
3. Weiss L. Early Concepts of Cancer. *Cancer and Metastasis Reviews*. 2000;19(3):205-217.
4. Edward JO, Patrick SR-Q, Maryna S, *et al*. Earliest hominin cancer: 1.7-million-year-old osteosarcoma from Swartkrans Cave, South Africa. *South African Journal of Science*. 2016;112(7/8).
5. Weinberg RA. Tumor suppressor genes. *Science*. 1991;254(5035):1138.
6. Cantley LC, Auger KR, Carpenter C, *et al*. Oncogenes and signal transduction. *Cell*. 1991;64(2):281-302.
7. Leslie A, Carey FA, Pratt NR, Steele RJ. The colorectal adenoma-carcinoma sequence. *Br J Surg*. 2002;89(7):845-860.
8. Hanahan D, Weinberg RA. The Hallmarks of Cancer. *Cell*. 2000;100(1):57-70.
9. Hanahan D, Weinberg RA. Hallmarks of cancer: the next generation. *Cell*. 2011;144(5):646-674.
10. Balkwill FR, Capasso M, Hagemann T. The tumor microenvironment at a glance. *J Cell Sci*. 2012;125(Pt 23):5591-5596.
11. Hanahan D, Coussens LM. Accessories to the crime: functions of cells recruited to the tumor microenvironment. *Cancer Cell*. 2012;21(3):309-322.
12. Ungefroren H, Sebens S, Seidl D, Lehnert H, Hass R. Interaction of tumor cells with the microenvironment. *Cell Commun Signal*. 2011;9:18-18.
13. Jung HY, Fattet L, Yang J. Molecular pathways: linking tumor microenvironment to epithelial-mesenchymal transition in metastasis. *Clin Cancer Res*. 2015;21(5):962-968.
14. Pastushenko I, Brisebarre A, Sifrim A, *et al*. Identification of the tumour transition states occurring during EMT. *Nature*. 2018;556(7702):463-468.
15. Lambert AW, Pattabiraman DR, Weinberg RA. Emerging Biological Principles of Metastasis. *Cell*. 2017;168(4):670-691.
16. Turajlic S, Swanton C. Metastasis as an evolutionary process. *Science*. 2016;352(6282):169-175.
17. Valastyan S, Weinberg RA. Tumor metastasis: molecular insights and evolving paradigms. *Cell*. 2011;147(2):275-292.
18. Erdogan B, Ao M, White LM, *et al*. Cancer-associated fibroblasts promote directional cancer cell migration by aligning fibronectin. *J Cell Biol*. 2017;216(11):3799-3816.
19. National Cancer Institute D, Surveillance Research Program. Surveillance, Epidemiology, and End Results (SEER) Program ([www.seer.cancer.gov](http://www.seer.cancer.gov)) SEER\*Stat Database: Incidence - SEER Research Data, 9 Registries, Nov 2019 Sub (1975-2017) - Linked To County Attributes - Time Dependent (1990-2017) Income/Rurality, 1969-2017 Counties. 2020.

20. Choi DK, Helenowski I, Hijiya N. Secondary malignancies in pediatric cancer survivors: Perspectives and review of the literature. *International Journal of Cancer*. 2014;135(8):1764-1773.
21. Mertens AC, Liu Q, Fau - Neglia JP, Neglia Jp Fau - Wasilewski K, *et al*. Cause-specific late mortality among 5-year survivors of childhood cancer: the Childhood Cancer Survivor Study. (1460-2105 (Electronic)).
22. Gröbner SN, Worst BC, Weischenfeldt J, *et al*. The landscape of genomic alterations across childhood cancers. *Nature*. 2018;555(7696):321-327.
23. Cormier JN, Pollock RE. Soft tissue sarcomas. *CA Cancer J Clin*. 2004;54(2):94-109.
24. Skapek SX, Ferrari A, Gupta AA, *et al*. Rhabdomyosarcoma. *Nat Rev Dis Primers*. 2019;5(1):1.
25. Amer KM, Thomson JE, Congiusta D, *et al*. Epidemiology, Incidence, and Survival of Rhabdomyosarcoma Subtypes: SEER and ICES Database Analysis. *Journal of Orthopaedic Research*. 2019;37(10):2226-2230.
26. Ognjanovic S, Linabery AM, Charbonneau B, Ross JA. Trends in childhood rhabdomyosarcoma incidence and survival in the United States, 1975-2005. *Cancer*. 2009;115(18):4218-4226.
27. Siegel RL, Miller KD, Jemal A. Cancer statistics, 2020. *CA: A Cancer Journal for Clinicians*. 2020;70(1):7-30.
28. Savina M, Le Cesne A, Blay J-Y, *et al*. Patterns of care and outcomes of patients with METAstatic soft tissue SARComa in a real-life setting: the METASARC observational study. *BMC Medicine*. 2017;15(1):78.
29. Chen C, Dorado Garcia H, Scheer M, Henssen AG. Current and Future Treatment Strategies for Rhabdomyosarcoma. *Frontiers in oncology*. 2019;9:1458-1458.
30. Siegel RL, Miller KD, Jemal A. Cancer statistics, 2019. *CA: A Cancer Journal for Clinicians*. 2019;69(1):7-34.
31. Egas-Bejar D, Huh WW. Rhabdomyosarcoma in adolescent and young adult patients: current perspectives. *Adolesc Health Med Ther*. 2014;5:115-125.
32. Barr FG. Gene fusions involving PAX and FOX family members in alveolar rhabdomyosarcoma. *Oncogene*. 2001;20(40):5736-5746.
33. Barr FG, Biegel JA, Sellinger B, Womer RB, Emanuel BS. Molecular and cytogenetic analysis of chromosomal arms 2q and 13q in alveolar rhabdomyosarcoma. *Genes, Chromosomes and Cancer*. 1991;3(2):153-161.
34. Shern JF, Chen L, Chmielecki J, *et al*. Comprehensive genomic analysis of rhabdomyosarcoma reveals a landscape of alterations affecting a common genetic axis in fusion-positive and fusion-negative tumors. *Cancer discovery*. 2014;4(2):216-231.
35. Stewart E, McEvoy J, Wang H, *et al*. Identification of Therapeutic Targets in Rhabdomyosarcoma through Integrated Genomic, Epigenomic, and Proteomic Analyses. (1878-3686 (Electronic)).
36. Renshaw J, Taylor Kr Fau - Bishop R, Bishop R Fau - Valenti M, *et al*. Dual blockade of the PI3K/AKT/mTOR (AZD8055) and RAS/MEK/ERK (AZD6244) pathways synergistically inhibits rhabdomyosarcoma cell growth in vitro and in vivo. (1078-0432 (Print)).
37. Megiorni F, Gravina GL, Camero S, *et al*. Pharmacological targeting of the ephrin receptor kinase signalling by GLPG1790 in vitro and in vivo reverts



- oncophenotype, induces myogenic differentiation and radiosensitizes embryonal rhabdomyosarcoma cells. *J Hematol Oncol.* 2017;10(1):161.
38. Wachtel M, Schafer BW. PAX3-FOXO1: Zooming in on an "undruggable" target. *Semin Cancer Biol.* 2018;50:115-123.
  39. Nguyen TH, Barr FG. Therapeutic Approaches Targeting PAX3-FOXO1 and Its Regulatory and Transcriptional Pathways in Rhabdomyosarcoma. *Molecules.* 2018;23(11):2798.
  40. Hettmer S, Li Z, Billin AN, *et al.* Rhabdomyosarcoma: current challenges and their implications for developing therapies. *Cold Spring Harb Perspect Med.* 2014;4(11):a025650-a025650.
  41. Pandey PR, Chatterjee B, Olanich ME, *et al.* PAX3-FOXO1 is essential for tumour initiation and maintenance but not recurrence in a human myoblast model of rhabdomyosarcoma. *J Pathol.* 2017;241(5):626-637.
  42. Allis CD, Jenuwein T. The molecular hallmarks of epigenetic control. *Nature Reviews Genetics.* 2016;17(8):487-500.
  43. Dawson Mark A, Kouzarides T. Cancer Epigenetics: From Mechanism to Therapy. *Cell.* 2012;150(1):12-27.
  44. Tam WL, Weinberg RA. The epigenetics of epithelial-mesenchymal plasticity in cancer. *Nature Medicine.* 2013;19(11):1438-1449.
  45. Khorasanizadeh S. The Nucleosome: From Genomic Organization to Genomic Regulation. *Cell.* 2004;116(2):259-272.
  46. Richmond TJ, Davey CA. The structure of DNA in the nucleosome core. *Nature.* 2003;423(6936):145-150.
  47. Murakami Y. Heterochromatin and Euchromatin. In: Dubitzky W, Wolkenhauer O, Cho K-H, Yokota H, eds. *Encyclopedia of Systems Biology.* New York, NY: Springer New York; 2013:881-884.
  48. Bannister AJ, Kouzarides T. Regulation of chromatin by histone modifications. *Cell Research.* 2011;21(3):381-395.
  49. Li B, Carey M, Workman JL. The Role of Chromatin during Transcription. *Cell.* 2007;128(4):707-719.
  50. Bowman GD, Poirier MG. Post-Translational Modifications of Histones That Influence Nucleosome Dynamics. *Chemical Reviews.* 2015;115(6):2274-2295.
  51. Gibney ER, Nolan CM. Epigenetics and gene expression. *Heredity.* 2010;105(1):4-13.
  52. Margueron R, Reinberg D. The Polycomb complex PRC2 and its mark in life. *Nature.* 2011;469(7330):343-349.
  53. Bracken AP, Helin K. Polycomb group proteins: navigators of lineage pathways led astray in cancer. *Nature Reviews Cancer.* 2009;9(11):773-784.
  54. Kim KH, Roberts CWM. Targeting EZH2 in cancer. *Nature Medicine.* 2016;22(2):128-134.
  55. Holliday R, Pugh JE. DNA modification mechanisms and gene activity during development. *Science.* 1975;187(4173):226-232.
  56. Smith ZD, Meissner A. DNA methylation: roles in mammalian development. *Nature Reviews Genetics.* 2013;14(3):204-220.
  57. Robertson KD. DNA methylation and human disease. *Nature Reviews Genetics.* 2005;6(8):597-610.

58. Deaton AM, Bird A. CpG islands and the regulation of transcription. *Genes Dev.* 2011;25(10):1010-1022.
59. Chan AO, Broaddus RR, Houlihan PS, Issa JP, Hamilton SR, Rashid A. CpG island methylation in aberrant crypt foci of the colorectum. *Am J Pathol.* 2002;160(5):1823-1830.
60. Ehrlich M. DNA hypomethylation in cancer cells. *Epigenomics.* 2009;1(2):239-259.
61. Cedar H, Bergman Y. Linking DNA methylation and histone modification: patterns and paradigms. *Nature Reviews Genetics.* 2009;10(5):295-304.
62. Schuettengruber B, Bourbon H-M, Di Croce L, Cavalli G. Genome Regulation by Polycomb and Trithorax: 70 Years and Counting. *Cell.* 2017;171(1):34-57.
63. Ingham pw. A clonal analysis of the requirement for the trithorax gene in the diversification of segments in *Drosophila*. *Development (Cambridge, England).* 1985;89(1):349-365.
64. Jacobs JJ, Kieboom K, Marino S, DePinho RA, van Lohuizen M. The oncogene and Polycomb-group gene *bmi-1* regulates cell proliferation and senescence through the *ink4a* locus. *Nature.* 1999;397(6715):164-168.
65. Park I-K, Morrison SJ, Clarke MF. *Bmi1*, stem cells, and senescence regulation. *The Journal of Clinical Investigation.* 2004;113(2):175-179.
66. Richly H, Aloia L, Di Croce L. Roles of the Polycomb group proteins in stem cells and cancer. *Cell Death & Disease.* 2011;2(9):e204-e204.
67. Haberland M, Montgomery RL, Olson EN. The many roles of histone deacetylases in development and physiology: implications for disease and therapy. *Nat Rev Genet.* 2009;10(1):32-42.
68. Goldberg AD, Allis CD, Bernstein E. Epigenetics: A Landscape Takes Shape. *Cell.* 2007;128(4):635-638.
69. Li Y, Seto E. HDACs and HDAC Inhibitors in Cancer Development and Therapy. *Cold Spring Harb Perspect Med.* 2016;6(10):a026831.
70. Fraga MF, Ballestar E, Villar-Garea A, *et al.* Loss of acetylation at Lys16 and trimethylation at Lys20 of histone H4 is a common hallmark of human cancer. *Nat Genet.* 2005;37(4):391-400.
71. Mann BS, Johnson JR, Cohen MH, Justice R, Pazdur R. FDA approval summary: vorinostat for treatment of advanced primary cutaneous T-cell lymphoma. *Oncologist.* 2007;12(10):1247-1252.
72. Sawas A, Radeski D, O'Connor OA. Belinostat in patients with refractory or relapsed peripheral T-cell lymphoma: a perspective review. *Ther Adv Hematol.* 2015;6(4):202-208.
73. Laubach JP, Moreau P, San-Miguel JF, Richardson PG. Panobinostat for the Treatment of Multiple Myeloma. *Clinical Cancer Research.* 2015;21(21):4767.
74. Mensah AA, Kwee I, Gaudio E, *et al.* Novel HDAC inhibitors exhibit pre-clinical efficacy in lymphoma models and point to the importance of CDKN1A expression levels in mediating their anti-tumor response. *Oncotarget.* 2015;6(7):5059-5071.
75. Khan DH, Davie JR. HDAC inhibitors prevent the induction of the immediate-early gene *FOSL1*, but do not alter the nucleosome response. *FEBS Lett.* 2013;587(10):1510-1517.
76. Zhang J, Zhong Q. Histone deacetylase inhibitors and cell death. *Cell Mol Life Sci.* 2014;71(20):3885-3901.

77. Dawson MA, Kouzarides T, Huntly BJ. Targeting epigenetic readers in cancer. *N Engl J Med*. 2012;367(7):647-657.
78. Filippakopoulos P, Qi J, Picaud S, *et al*. Selective inhibition of BET bromodomains. *Nature*. 2010;468(7327):1067-1073.
79. Alqahtani A, Choucair K, Ashraf M, *et al*. Bromodomain and extra-terminal motif inhibitors: a review of preclinical and clinical advances in cancer therapy. *Future Sci OA*. 2019;5(3):FSO372-FSO372.
80. Stathis A, Bertoni F. BET Proteins as Targets for Anticancer Treatment. *Cancer Discov*. 2018;8(1):24-36.
81. Trabucco SE, Gerstein RM, Evens AM, *et al*. Inhibition of bromodomain proteins for the treatment of human diffuse large B-cell lymphoma. *Clin Cancer Res*. 2015;21(1):113-122.
82. The BET Inhibitor Birabresib Is Safe in Patients with Solid Tumors. *Cancer Discovery*. 2018;8(7):792.
83. Lewin J, Soria JC, Stathis A, *et al*. Phase Ib Trial With Birabresib, a Small-Molecule Inhibitor of Bromodomain and Extraterminal Proteins, in Patients With Selected Advanced Solid Tumors. *J Clin Oncol*. 2018;36(30):3007-3014.
84. Tarantelli C, Bernasconi E, Gaudio E, *et al*. BET bromodomain inhibitor birabresib in mantle cell lymphoma: in vivo activity and identification of novel combinations to overcome adaptive resistance. *ESMO Open*. 2018;3(6):e000387-e000387.
85. Pasini D, Di Croce L. Emerging roles for Polycomb proteins in cancer. *Curr Opin Genet Dev*. 2016;36:50-58.
86. Miranda TB, Cortez CC, Yoo CB, *et al*. DZNep is a global histone methylation inhibitor that reactivates developmental genes not silenced by DNA methylation. *Mol Cancer Ther*. 2009;8(6):1579-1588.
87. Cheng LL, Itahana Y, Lei ZD, *et al*. TP53 Genomic Status Regulates Sensitivity of Gastric Cancer Cells to the Histone Methylation Inhibitor 3-Deazaneplanocin A (DZNep). *Clinical Cancer Research*. 2012;18(15):4201.
88. McCabe MT, Ott HM, Ganji G, *et al*. EZH2 inhibition as a therapeutic strategy for lymphoma with EZH2-activating mutations. *Nature*. 2012;492(7427):108-112.
89. Knutson SK, Wigle TJ, Warholc NM, *et al*. A selective inhibitor of EZH2 blocks H3K27 methylation and kills mutant lymphoma cells. *Nat Chem Biol*. 2012;8(11):890-896.
90. Morschhauser F, Tilly H, Chaidos A, *et al*. Tazemetostat for patients with relapsed or refractory follicular lymphoma: an open-label, single-arm, multicentre, phase 2 trial. *The Lancet Oncology*. 2020;21(11):1433-1442.
91. Gryder BE, Yohe ME, Chou HC, *et al*. PAX3-FOXO1 Establishes Myogenic Super Enhancers and Confers BET Bromodomain Vulnerability. *Cancer Discov*. 2017;7(8):884-899.
92. Bohm M, Wachtel M, Marques JG, *et al*. Helicase CHD4 is an epigenetic coregulator of PAX3-FOXO1 in alveolar rhabdomyosarcoma. *J Clin Invest*. 2016;126(11):4237-4249.
93. Enssle JC, Boedicker C, Wanior M, Vogler M, Knapp S, Fulda S. Co-targeting of BET proteins and HDACs as a novel approach to trigger apoptosis in rhabdomyosarcoma cells. *Cancer Lett*. 2018;428:160-172.

94. Hedrick E, Crose L, Linardic CM, Safe S. Histone Deacetylase Inhibitors Inhibit Rhabdomyosarcoma by Reactive Oxygen Species-Dependent Targeting of Specificity Protein Transcription Factors. *Mol Cancer Ther.* 2015;14(9):2143-2153.
95. Bharathy N, Berlow NE, Wang E, *et al.* Preclinical rationale for entinostat in embryonal rhabdomyosarcoma. *Skelet Muscle.* 2019;9(1):12.
96. Gryder BE, Wu L, Woldemichael GM, *et al.* Chemical genomics reveals histone deacetylases are required for core regulatory transcription. *Nature Communications.* 2019;10(1):3004.
97. Bharathy N, Berlow NE, Wang E, *et al.* The HDAC3-SMARCA4-miR-27a axis promotes expression of the PAX3:FOXO1 fusion oncogene in rhabdomyosarcoma. *Sci Signal.* 2018;11(557).
98. Bukowinski A, Chang B, Reid JM, *et al.* A phase 1 study of entinostat in children and adolescents with recurrent or refractory solid tumors, including CNS tumors: Trial ADVL1513, Pediatric Early Phase-Clinical Trial Network (PEP-CTN). *Pediatr Blood Cancer.* 2021;68(4):e28892.
99. Camero S, Camicia L, Marampon F, *et al.* BET inhibition therapy counteracts cancer cell survival, clonogenic potential and radioresistance mechanisms in rhabdomyosarcoma cells. *Cancer Letters.* 2020;479:71-88.
100. Marchesi I, Fiorentino FP, Rizzolio F, Giordano A, Bagella L. The ablation of EZH2 uncovers its crucial role in rhabdomyosarcoma formation. *Cell Cycle.* 2012;11(20):3828-3836.
101. Ciarapica R, Carcarino E, Adesso L, *et al.* Pharmacological inhibition of EZH2 as a promising differentiation therapy in embryonal RMS. *BMC cancer.* 2014;14:139-139.
102. Ciarapica R, De Salvo M, Carcarino E, *et al.* The Polycomb group (PcG) protein EZH2 supports the survival of PAX3-FOXO1 alveolar rhabdomyosarcoma by repressing FBXO32 (Atrogin1/MAFbx). *Oncogene.* 2014;33(32):4173-4184.
103. Aranda S, Mas G, Di Croce L. Regulation of gene transcription by Polycomb proteins. *Science Advances.* 2015;1(11):e1500737.
104. Francis NJ, Kingston RE, Woodcock CL. Chromatin Compaction by a Polycomb Group Protein Complex. *Science.* 2004;306(5701):1574.
105. Leeb M, Pasini D, Novatchkova M, Jaritz M, Helin K, Wutz A. Polycomb complexes act redundantly to repress genomic repeats and genes. *Genes Dev.* 2010;24(3):265-276.
106. Sahasrabudde AA. BMI1: A Biomarker of Hematologic Malignancies. *Biomarkers in cancer.* 2016;8:65-75.
107. Ferretti R, Bhutkar A, McNamara MC, Lees JA. BMI1 induces an invasive signature in melanoma that promotes metastasis and chemoresistance. *Genes Dev.* 2016;30(1):18-33.
108. Bhattacharya R, Mustafi SB, Street M, Dey A, Dwivedi SK. Bmi-1: At the crossroads of physiological and pathological biology. *Genes Dis.* 2015;2(3):225-239.
109. Paranjape AN, Balaji SA, Mandal T, *et al.* Bmi1 regulates self-renewal and epithelial to mesenchymal transition in breast cancer cells through Nanog. *BMC Cancer.* 2014;14(1):785.

110. Siddique HR, Saleem M. Role of BMI1, a stem cell factor, in cancer recurrence and chemoresistance: preclinical and clinical evidences. *Stem cells (Dayton, Ohio)*. 2012;30(3):372-378.
111. Gao Z, Zhang J, Bonasio R, *et al.* PCGF homologs, CBX proteins, and RYBP define functionally distinct PRC1 family complexes. *Molecular cell*. 2012;45(3):344-356.
112. Tavares L, Dimitrova E, Oxley D, *et al.* RYBP-PRC1 complexes mediate H2A ubiquitylation at polycomb target sites independently of PRC2 and H3K27me3. *Cell*. 2012;148(4):664-678.
113. Blackledge NP, Rose NR, Klose RJ. Targeting Polycomb systems to regulate gene expression: modifications to a complex story. *Nature Reviews Molecular Cell Biology*. 2015;16(11):643-649.
114. Blackledge NP, Farcas AM, Kondo T, *et al.* Variant PRC1 complex-dependent H2A ubiquitylation drives PRC2 recruitment and polycomb domain formation. *Cell*. 2014;157(6):1445-1459.
115. Taherbhoy AM, Huang OW, Cochran AG. BMI1–RING1B is an autoinhibited RING E3 ubiquitin ligase. *Nature Communications*. 2015;6(1):7621.
116. Bakhshinyan D, Venugopal C, Adile AA, *et al.* BMI1 is a therapeutic target in recurrent medulloblastoma. *Oncogene*. 2019;38(10):1702-1716.
117. Buechel M, Dey A, Dwivedi SKD, *et al.* Inhibition of BMI1, a Therapeutic Approach in Endometrial Cancer. *Mol Cancer Ther*. 2018;17(10):2136-2143.
118. Jin X, Kim LJY, Wu Q, *et al.* Targeting glioma stem cells through combined BMI1 and EZH2 inhibition. *Nature Medicine*. 2017;23(11):1352-1361.
119. Mayr C, Wagner A, Loeffelberger M, *et al.* The BMI1 inhibitor PTC-209 is a potential compound to halt cellular growth in biliary tract cancer cells. *Oncotarget*. 2016;7(1):745-758.
120. Bednar F, Schofield HK, Collins MA, *et al.* Bmi1 is required for the initiation of pancreatic cancer through an Ink4a-independent mechanism. *Carcinogenesis*. 2015;36(7):730-738.
121. Yang M-H, Hsu DS-S, Wang H-W, *et al.* Bmi1 is essential in Twist1-induced epithelial–mesenchymal transition. *Nature Cell Biology*. 2010;12(10):982-992.
122. van Leenders GJLH, Dukers D, Hessels D, *et al.* Polycomb-Group Oncogenes EZH2, BMI1, and RING1 Are Overexpressed in Prostate Cancer With Adverse Pathologic and Clinical Features. *European Urology*. 2007;52(2):455-463.
123. Liu L, Andrews LG, Tollefsbol TO. Loss of the human polycomb group protein BMI1 promotes cancer-specific cell death. *Oncogene*. 2006;25(31):4370-4375.
124. Creppe C, Palau A, Malinverni R, Valero V, Buschbeck M. A Cbx8-Containing Polycomb Complex Facilitates the Transition to Gene Activation during ES Cell Differentiation. *PLoS Genet*. 2014;10(12):e1004851.
125. Gao Z, Lee P, Stafford JM, von Schimmelmänn M, Schaefer A, Reinberg D. An AUTS2-Polycomb complex activates gene expression in the CNS. *Nature*. 2014;516(7531):349-354.
126. Kondo T, Isono K, Kondo K, *et al.* Polycomb Potentiates Meis2 Activation in Midbrain by Mediating Interaction of the Promoter with a Tissue-Specific Enhancer. *Developmental Cell*. 2014;28(1):94-101.

127. Loubiere V, Papadopoulos GL, Szabo Q, Martinez AM, Cavalli G. Widespread activation of developmental gene expression characterized by PRC1-dependent chromatin looping. *Science Advances*. 2020;6(2):eaax4001.
128. van Lohuizen M, Verbeek S, Scheijen B, Wientjens E, van der Gulden H, Berns A. Identification of cooperating oncogenes in E mu-myc transgenic mice by provirus tagging. *Cell*. 1991;65(5):737-752.
129. Gil J, O'Loghlen A. PRC1 complex diversity: where is it taking us? *Trends Cell Biol*. 2014;24(11):632-641.
130. Endoh M, Endo TA, Endoh T, *et al*. Histone H2A mono-ubiquitination is a crucial step to mediate PRC1-dependent repression of developmental genes to maintain ES cell identity. *PLoS Genet*. 2012;8(7):e1002774-e1002774.
131. Luis NM, Morey L, Di Croce L, Benitah SA. Polycomb in stem cells: PRC1 branches out. *Cell Stem Cell*. 2012;11(1):16-21.
132. Alkema MJ, Wiegant J, Raap AK, Berns A, van Lohuizen M. Characterization and chromosomal localization of the human proto-oncogene BMI-1. *Hum Mol Genet*. 1993;2(10):1597-1603.
133. Ginjala V, Nacerddine K, Kulkarni A, *et al*. BMI1 Is Recruited to DNA Breaks and Contributes to DNA Damage-Induced H2A Ubiquitination and Repair. *Molecular and Cellular Biology*. 2011;31(10):1972.
134. Park IK, Qian D, Kiel M, *et al*. Bmi-1 is required for maintenance of adult self-renewing haematopoietic stem cells. *Nature*. 2003;423(6937):302-305.
135. van der Lugt NM, Domen J, Linders K, *et al*. Posterior transformation, neurological abnormalities, and severe hematopoietic defects in mice with a targeted deletion of the bmi-1 proto-oncogene. *Genes Dev*. 1994;8(7):757-769.
136. Serrano M. The tumor suppressor protein p16INK4a. *Exp Cell Res*. 1997;237(1):7-13.
137. O'Brien CA, Kreso A, Jamieson CH. Cancer stem cells and self-renewal. *Clin Cancer Res*. 2010;16(12):3113-3120.
138. Dagogo-Jack I, Shaw AT. Tumour heterogeneity and resistance to cancer therapies. *Nat Rev Clin Oncol*. 2018;15(2):81-94.
139. Kreso A, van Galen P, Pedley NM, *et al*. Self-renewal as a therapeutic target in human colorectal cancer. *Nat Med*. 2014;20(1):29-36.
140. Hauer MH, Gasser SM. Chromatin and nucleosome dynamics in DNA damage and repair. *Genes Dev*. 2017;31(22):2204-2221.
141. Giglia-Mari G, Zotter A, Vermeulen W. DNA damage response. *Cold Spring Harb Perspect Biol*. 2011;3(1):a000745-a000745.
142. Mah LJ, El-Osta A, Karagiannis TC.  $\gamma$ H2AX: a sensitive molecular marker of DNA damage and repair. *Leukemia*. 2010;24(4):679-686.
143. Clouaire T, Rocher V, Lashgari A, *et al*. Comprehensive Mapping of Histone Modifications at DNA Double-Strand Breaks Deciphers Repair Pathway Chromatin Signatures. *Mol Cell*. 2018;72(2):250-262.e256.
144. Buchwald G, van der Stoop P, Weichenrieder O, Perrakis A, van Lohuizen M, Sixma TK. Structure and E3-ligase activity of the Ring-Ring complex of polycomb proteins Bmi1 and Ring1b. *Embo j*. 2006;25(11):2465-2474.
145. Li Z, Cao R, Wang M, Myers MP, Zhang Y, Xu RM. Structure of a Bmi-1-Ring1B polycomb group ubiquitin ligase complex. *J Biol Chem*. 2006;281(29):20643-20649.

146. Ben-Saadon R, Zaaroor D, Ziv T, Ciechanover A. The polycomb protein Ring1B generates self atypical mixed ubiquitin chains required for its in vitro histone H2A ligase activity. *Mol Cell*. 2006;24(5):701-711.
147. Gracheva E, Chitale S, Wilhelm T, *et al*. ZRF1 mediates remodeling of E3 ligases at DNA lesion sites during nucleotide excision repair. *J Cell Biol*. 2016;213(2):185-200.
148. Kim JH, Yoon SY, Jeong S-H, *et al*. Overexpression of Bmi-1 oncoprotein correlates with axillary lymph node metastases in invasive ductal breast cancer. *The Breast*. 2004;13(5):383-388.
149. Guo B-H, Feng Y, Zhang R, *et al*. Bmi-1 promotes invasion and metastasis, and its elevated expression is correlated with an advanced stage of breast cancer. *Molecular Cancer*. 2011;10(1):10.
150. Ganaie AA, Beigh FH, Astone M, *et al*. <em>BMI1</em> Drives Metastasis of Prostate Cancer in Caucasian and African-American Men and Is A Potential Therapeutic Target: Hypothesis Tested in Race-specific Models. *Clinical Cancer Research*. 2018;24(24):6421.
151. Celia-Terrassa T, Kang Y. Distinctive properties of metastasis-initiating cells. *Genes Dev*. 2016;30(8):892-908.
152. Turdo A, Veschi V, Gaggianesi M, *et al*. Meeting the Challenge of Targeting Cancer Stem Cells. *Frontiers in Cell and Developmental Biology*. 2019;7(16).
153. Elshamy WM, Duhe RJ. Overview: cellular plasticity, cancer stem cells and metastasis. *Cancer Lett*. 2013;341(1):2-8.
154. Hoenerhoff MJ, Chu I, Barkan D, *et al*. BMI1 cooperates with H-RAS to induce an aggressive breast cancer phenotype with brain metastases. *Oncogene*. 2009;28(34):3022-3032.
155. Jia L, Zhang W, Wang C-Y. BMI1 Inhibition Eliminates Residual Cancer Stem Cells after PD1 Blockade and Activates Antitumor Immunity to Prevent Metastasis and Relapse. *Cell Stem Cell*. 2020;27(2):238-253.e236.
156. Chen D, Wu M, Li Y, *et al*. Targeting BMI1(+) Cancer Stem Cells Overcomes Chemoresistance and Inhibits Metastases in Squamous Cell Carcinoma. *Cell Stem Cell*. 2017;20(5):621-634.e626.
157. Wang Q, Li Z, Wu Y, *et al*. Pharmacological inhibition of Bmi1 by PTC-209 impaired tumor growth in head neck squamous cell carcinoma. *Cancer Cell Int*. 2017;17:107-107.
158. Bansal N, Bartucci M, Yusuff S, *et al*. BMI-1 Targeting Interferes with Patient-Derived Tumor-Initiating Cell Survival and Tumor Growth in Prostate Cancer. *Clin Cancer Res*. 2016;22(24):6176-6191.
159. Dey A, Xiong X, Crim A, *et al*. Evaluating the Mechanism and Therapeutic Potential of PTC-028, a Novel Inhibitor of BMI-1 Function in Ovarian Cancer. *Mol Cancer Ther*. 2018;17(1):39-49.
160. Yong KJ, Basseres DS, Welner RS, *et al*. Targeted BMI1 inhibition impairs tumor growth in lung adenocarcinomas with low CEBPalpha expression. *Sci Transl Med*. 2016;8(350):350ra104.
161. Bolomsky A, Muller J, Stangelberger K, *et al*. The anti-mitotic agents PTC-028 and PTC596 display potent activity in pre-clinical models of multiple myeloma but challenge the role of BMI-1 as an essential tumour gene. *British Journal of Haematology*. 2020;190(6):877-890.

162. Flamier A, Abdouh M, Hamam R, *et al.* Off-target effect of the BMI1 inhibitor PTC596 drives epithelial-mesenchymal transition in glioblastoma multiforme. *npj Precision Oncology*. 2020;4(1):1.
163. Eberle-Singh JA, Sagalovskiy I, Maurer HC, *et al.* Effective delivery of a microtubule polymerization inhibitor synergizes with standard regimens in models of pancreatic ductal adenocarcinoma. *Clinical Cancer Research*. 2019;clinres.3281.2018.
164. Maeda A, Nishida Y, Weetall M, *et al.* Targeting of BMI-1 expression by the novel small molecule PTC596 in mantle cell lymphoma. *Oncotarget*. 2018;9(47):28547-28560.
165. Nishida Y, Maeda A, Kim MJ, *et al.* The novel BMI-1 inhibitor PTC596 downregulates MCL-1 and induces p53-independent mitochondrial apoptosis in acute myeloid leukemia progenitor cells. *Blood Cancer J*. 2017;7(2):e527-e527.
166. Infante JR, Bedard PL, Shapiro G, *et al.* Phase 1 results of PTC596, a novel small molecule targeting cancer stem cells (CSCs) by reducing levels of BMI1 protein. *Journal of Clinical Oncology*. 2017;35(15\_suppl):2574-2574.
167. Shapiro GI, O'Mara E, Laskin OL, *et al.* Pharmacokinetics and Safety of PTC596, a Novel Tubulin-Binding Agent, in Subjects With Advanced Solid Tumors. *Clin Pharmacol Drug Dev*. 2021.
168. PTC Therapeutics I. PTC Therapeutics Announces Key Regulatory Designations for PTC596 to Advance Treatment of Two Rare Oncology Indications. 2020. <https://ir.ptcbio.com/news-releases/news-release-details/ptc-therapeutics-announces-key-regulatory-designations-ptc596>. Published November 18, 2020. Accessed November 18, 2020.
169. Skrypek N, Goossens S, De Smedt E, Vandamme N, Berx G. Epithelial-to-Mesenchymal Transition: Epigenetic Reprogramming Driving Cellular Plasticity. *Trends in Genetics*. 2017;33(12):943-959.
170. Probst AV, Dunleavy E, Almouzni G. Epigenetic inheritance during the cell cycle. *Nature Reviews Molecular Cell Biology*. 2009;10(3):192-206.
171. Hawkins DS, Spunt SL, Skapek SX, Committee COGSTS. Children's Oncology Group's 2013 blueprint for research: Soft tissue sarcomas. *Pediatr Blood Cancer*. 2013;60(6):1001-1008.
172. Borinstein SC, Steppan D, Hayashi M, *et al.* Consensus and controversies regarding the treatment of rhabdomyosarcoma. *Pediatr Blood Cancer*. 2018;65(2):e26809.
173. Gryder BE, Pomella S, Sayers C, *et al.* Histone hyperacetylation disrupts core gene regulatory architecture in rhabdomyosarcoma. *Nature Genetics*. 2019;51(12):1714-1722.
174. Di Croce L, Helin K. Transcriptional regulation by Polycomb group proteins. *Nature Structural & Molecular Biology*. 2013;20(10):1147-1155.
175. Whitcomb SJ, Basu A, Allis CD, Bernstein E. Polycomb Group proteins: an evolutionary perspective. *Trends in Genetics*. 2007;23(10):494-502.
176. Cho JH, Dimri M, Dimri GP. A positive feedback loop regulates the expression of polycomb group protein BMI1 via WNT signaling pathway. *J Biol Chem*. 2013;288(5):3406-3418.
177. Wang E, Bhattacharyya S, Szabolcs A, *et al.* Enhancing Chemotherapy Response with Bmi-1 Silencing in Ovarian Cancer. *PLOS ONE*. 2011;6(3):e17918.



178. Zhao Q, Qian Q, Cao D, Yang J, Gui T, Shen K. Role of BMI1 in epithelial ovarian cancer: investigated via the CRISPR/Cas9 system and RNA sequencing. *J Ovarian Res.* 2018;11(1):31.
179. Hsu JH, Lawlor ER. BMI-1 suppresses contact inhibition and stabilizes YAP in Ewing sarcoma. *Oncogene.* 2011;30(17):2077-2085.
180. Douglas D, Hsu JH-R, Hung L, *et al.* BMI-1 promotes ewing sarcoma tumorigenicity independent of CDKN2A repression. *Cancer research.* 2008;68(16):6507-6515.
181. Di Foggia V, Zhang X, Licastro D, *et al.* Bmi1 enhances skeletal muscle regeneration through MT1-mediated oxidative stress protection in a mouse model of dystrophinopathy. *J Exp Med.* 2014;211(13):2617-2633.
182. Xia SJ, Holder DD, Pawel BR, Zhang C, Barr FG. High expression of the PAX3-FKHR oncoprotein is required to promote tumorigenesis of human myoblasts. *Am J Pathol.* 2009;175(6):2600-2608.
183. Schnepf RW, Khurana P, Attiyeh EF, *et al.* A LIN28B-RAN-AURKA Signaling Network Promotes Neuroblastoma Tumorigenesis. *Cancer Cell.* 2015;28(5):599-609.
184. Rader J, Russell MR, Hart LS, *et al.* Dual CDK4/CDK6 inhibition induces cell-cycle arrest and senescence in neuroblastoma. *Clin Cancer Res.* 2013;19(22):6173-6182.
185. Tomayko MM, Reynolds CP. Determination of subcutaneous tumor size in athymic (nude) mice. *Cancer Chemother Pharmacol.* 1989;24(3):148-154.
186. Bosse KR, Raman P, Zhu Z, *et al.* Identification of GPC2 as an Oncoprotein and Candidate Immunotherapeutic Target in High-Risk Neuroblastoma. *Cancer Cell.* 2017;32(3):295-309.e212.
187. Kaplan EL, Meier P. Nonparametric Estimation from Incomplete Observations. *Journal of the American Statistical Association.* 1958;53(282):457-481.
188. Rhodes DR, Yu J, Shanker K, *et al.* ONCOMINE: a cancer microarray database and integrated data-mining platform. *Neoplasia.* 2004;6(1):1-6.
189. Wu Z, Min L, Chen D, *et al.* Overexpression of BMI-1 promotes cell growth and resistance to cisplatin treatment in osteosarcoma. *PLoS One.* 2011;6(2):e14648.
190. Xu L, Zheng Y, Liu J, *et al.* Integrative Bayesian Analysis Identifies Rhabdomyosarcoma Disease Genes. *Cell Rep.* 2018;24(1):238-251.
191. The Genotype-Tissue Expression (GTEx) project. *Nat Genet.* 2013;45(6):580-585.
192. Hinson ARP, Jones R, Crose LES, Belyea BC, Barr FG, Linardic CM. Human rhabdomyosarcoma cell lines for rhabdomyosarcoma research: utility and pitfalls. *Frontiers in oncology.* 2013;3:183-183.
193. Chen D, Cox J, Annam J, *et al.* LIN28B promotes neuroblastoma metastasis and regulates PDZ binding kinase. *Neoplasia.* 2020;22(6):231-241.
194. Zhu S, Zhao D, Yan L, *et al.* BMI1 regulates androgen receptor in prostate cancer independently of the polycomb repressive complex 1. *Nat Commun.* 2018;9(1):500.
195. Crose LE, Galindo KA, Kephart JG, *et al.* Alveolar rhabdomyosarcoma-associated PAX3-FOXO1 promotes tumorigenesis via Hippo pathway suppression. *J Clin Invest.* 2014;124(1):285-296.

196. Oristian KM, Crose LES, Kuprasertkul N, *et al.* Loss of MST/Hippo signaling in a genetically engineered mouse model of fusion-positive rhabdomyosarcoma accelerates tumorigenesis. *Cancer Research*. 2018;canres.3912.2018.
197. Ma S, Meng Z, Chen R, Guan K-L. The Hippo Pathway: Biology and Pathophysiology. *Annual Review of Biochemistry*. 2019;88(1):577-604.
198. Xu MZ, Chan SW, Liu AM, *et al.* AXL receptor kinase is a mediator of YAP-dependent oncogenic functions in hepatocellular carcinoma. *Oncogene*. 2011;30(10):1229-1240.
199. Ghiso E, Migliore C, Ciciriello V, *et al.* YAP-Dependent AXL Overexpression Mediates Resistance to EGFR Inhibitors in NSCLC. *Neoplasia (New York, NY)*. 2017;19(12):1012-1021.
200. Calses PC, Crawford JJ, Lill JR, Dey A. Hippo Pathway in Cancer: Aberrant Regulation and Therapeutic Opportunities. *Trends in Cancer*. 2019;5(5):297-307.
201. Chan EH, Nousiainen M, Chalamalasetty RB, Schafer A, Nigg EA, Sillje HH. The Ste20-like kinase Mst2 activates the human large tumor suppressor kinase Lats1. *Oncogene*. 2005;24(12):2076-2086.
202. Fullenkamp CA, Hall SL, Jaber OI, *et al.* TAZ and YAP are frequently activated oncoproteins in sarcomas. *Oncotarget*. 2016;7(21):30094-30108.
203. Arndt CAS, Bisogno G, Koscielniak E. Fifty years of rhabdomyosarcoma studies on both sides of the pond and lessons learned. *Cancer Treat Rev*. 2018;68:94-101.
204. Oberlin O, Rey A, Lyden E, *et al.* Prognostic factors in metastatic rhabdomyosarcomas: results of a pooled analysis from United States and European cooperative groups. *J Clin Oncol*. 2008;26(14):2384-2389.
205. Missiaglia E, Williamson D, Chisholm J, *et al.* PAX3/FOXO1 fusion gene status is the key prognostic molecular marker in rhabdomyosarcoma and significantly improves current risk stratification. *J Clin Oncol*. 2012;30(14):1670-1677.
206. Housman G, Byler S, Heerboth S, *et al.* Drug resistance in cancer: an overview. *Cancers (Basel)*. 2014;6(3):1769-1792.
207. Kaminskas E, Farrell A, Abraham S, *et al.* Approval Summary: Azacitidine for Treatment of Myelodysplastic Syndrome Subtypes. *Clinical Cancer Research*. 2005;11(10):3604.
208. Christman JK. 5-Azacytidine and 5-aza-2'-deoxycytidine as inhibitors of DNA methylation: mechanistic studies and their implications for cancer therapy. *Oncogene*. 2002;21(35):5483-5495.
209. Silverman LR, Holland JF, Weinberg RS, *et al.* Effects of treatment with 5-azacytidine on the in vivo and in vitro hematopoiesis in patients with myelodysplastic syndromes. *Leukemia*. 1993;7 Suppl 1:21-29.
210. Shields CE, Potlapalli S, Cuya-Smith SM, *et al.* Epigenetic regulator BMI1 promotes alveolar rhabdomyosarcoma proliferation and constitutes a novel therapeutic target. *Molecular Oncology*. 2021;n/a(n/a).
211. Mortazavi A, Williams BA, McCue K, Schaeffer L, Wold B. Mapping and quantifying mammalian transcriptomes by RNA-Seq. *Nature Methods*. 2008;5(7):621-628.
212. The Gene Ontology resource: enriching a GOLD mine. *Nucleic Acids Res*. 2021;49(D1):D325-d334.

213. Ashburner M, Ball CA, Blake JA, *et al.* Gene ontology: tool for the unification of biology. The Gene Ontology Consortium. *Nature genetics*. 2000;25(1):25-29.
214. Thomas PD, Campbell MJ, Kejariwal A, *et al.* PANTHER: a library of protein families and subfamilies indexed by function. *Genome Res*. 2003;13(9):2129-2141.
215. Hazelton BJ, Houghton JA, Parham DM, *et al.* Characterization of cell lines derived from xenografts of childhood rhabdomyosarcoma. *Cancer Res*. 1987;47(16):4501-4507.
216. Rodriguez-Perales S, Martínez-Ramírez A, de Andrés SA, *et al.* Molecular cytogenetic characterization of rhabdomyosarcoma cell lines. *Cancer Genet Cytogenet*. 2004;148(1):35-43.
217. Mo JS, Park HW, Guan KL. The Hippo signaling pathway in stem cell biology and cancer. *EMBO Rep*. 2014;15(6):642-656.
218. Harvey KF, Zhang X, Thomas DM. The Hippo pathway and human cancer. *Nature Reviews Cancer*. 2013;13(4):246-257.
219. Zanconato F, Cordenonsi M, Piccolo S. YAP/TAZ at the Roots of Cancer. *Cancer Cell*. 2016;29(6):783-803.
220. Meng Z, Moroishi T, Guan K-L. Mechanisms of Hippo pathway regulation. *Genes & development*. 2016;30(1):1-17.
221. Plaisier CL, O'Brien S, Bernard B, *et al.* Causal Mechanistic Regulatory Network for Glioblastoma Deciphered Using Systems Genetics Network Analysis. *Cell Systems*. 2016;3(2):172-186.
222. Li Z, Ivanov AA, Su R, *et al.* The OncoPPi network of cancer-focused protein-protein interactions to inform biological insights and therapeutic strategies. *Nature Communications*. 2017;8(1):14356.
223. Szklarczyk D, Gable AL, Lyon D, *et al.* STRING v11: protein-protein association networks with increased coverage, supporting functional discovery in genome-wide experimental datasets. *Nucleic Acids Res*. 2019;47(D1):D607-d613.
224. Furth N, Aylon Y. The LATS1 and LATS2 tumor suppressors: beyond the Hippo pathway. *Cell Death & Differentiation*. 2017;24(9):1488-1501.
225. Berner JM, Forus A, Elkahoulou A, Meltzer PS, Fodstad O, Myklebost O. Separate amplified regions encompassing CDK4 and MDM2 in human sarcomas. *Genes Chromosomes Cancer*. 1996;17(4):254-259.
226. Keller C, Guttridge DC. Mechanisms of impaired differentiation in rhabdomyosarcoma. *Febs j*. 2013;280(17):4323-4334.
227. Quach NL, Biressi S, Reichardt LF, Keller C, Rando TA. Focal adhesion kinase signaling regulates the expression of caveolin 3 and beta1 integrin, genes essential for normal myoblast fusion. *Mol Biol Cell*. 2009;20(14):3422-3435.
228. Taulli R, Bersani F, Foglizzo V, *et al.* The muscle-specific microRNA miR-206 blocks human rhabdomyosarcoma growth in xenotransplanted mice by promoting myogenic differentiation. *The Journal of clinical investigation*. 2009;119(8):2366-2378.
229. Chen C-L, Paul LN, Mermoud JC, Steussy CN, Stauffacher CV. Visualizing the enzyme mechanism of mevalonate diphosphate decarboxylase. *Nature Communications*. 2020;11(1):3969.
230. Huang B, Song B-l, Xu C. Cholesterol metabolism in cancer: mechanisms and therapeutic opportunities. *Nature Metabolism*. 2020;2(2):132-141.

231. Lewis CA, Brault C, Peck B, *et al.* SREBP maintains lipid biosynthesis and viability of cancer cells under lipid- and oxygen-deprived conditions and defines a gene signature associated with poor survival in glioblastoma multiforme. *Oncogene*. 2015;34(40):5128-5140.
232. Broad D. *DepMap 21Q2 Public*. 2021.
233. Gaillard H, García-Muse T, Aguilera A. Replication stress and cancer. *Nature Reviews Cancer*. 2015;15(5):276-289.
234. Gorgoulis VG, Vassiliou LV, Karakaidos P, *et al.* Activation of the DNA damage checkpoint and genomic instability in human precancerous lesions. *Nature*. 2005;434(7035):907-913.
235. Bartkova J, Horejsí Z, Koed K, *et al.* DNA damage response as a candidate anti-cancer barrier in early human tumorigenesis. *Nature*. 2005;434(7035):864-870.
236. Petragnano F, Pietrantonì I, Camero S, *et al.* Clinically relevant radioresistant rhabdomyosarcoma cell lines: functional, molecular and immune-related characterization. *Journal of Biomedical Science*. 2020;27(1):90.
237. O'Sullivan B, Davis AM, Turcotte R, *et al.* Preoperative versus postoperative radiotherapy in soft-tissue sarcoma of the limbs: a randomised trial. *Lancet*. 2002;359(9325):2235-2241.
238. Liu J, Cao L, Chen J, *et al.* Bmi1 regulates mitochondrial function and the DNA damage response pathway. *Nature*. 2009;459(7245):387-392.
239. Dibenedetto S, Niklison-Chirou M, Cabrera CP, *et al.* Enhanced Energetic State and Protection from Oxidative Stress in Human Myoblasts Overexpressing BMI1. *Stem Cell Reports*. 2017;9(2):528-542.
240. Patra SK. Dissecting lipid raft facilitated cell signaling pathways in cancer. *Biochimica et Biophysica Acta (BBA) - Reviews on Cancer*. 2008;1785(2):182-206.
241. Zhuang L, Kim J, Adam RM, Solomon KR, Freeman MR. Cholesterol targeting alters lipid raft composition and cell survival in prostate cancer cells and xenografts. *The Journal of Clinical Investigation*. 2005;115(4):959-968.
242. Roche J, Gemmill RM, Drabkin HA. Epigenetic Regulation of the Epithelial to Mesenchymal Transition in Lung Cancer. *Cancers*. 2017;9(7):72.
243. Sannino G, Marchetto A, Kirchner T, Grünewald TGP. Epithelial-to-Mesenchymal and Mesenchymal-to-Epithelial Transition in Mesenchymal Tumors: A Paradox in Sarcomas? *Cancer Res*. 2017;77(17):4556-4561.
244. Zhao Z, Rahman MA, Chen ZG, Shin DM. Multiple biological functions of Twist1 in various cancers. *Oncotarget*. 2017;8(12):20380-20393.
245. Skrzypek K, Kot M, Konieczny P, *et al.* SNAIL Promotes Metastatic Behavior of Rhabdomyosarcoma by Increasing EZRIN and AKT Expression and Regulating MicroRNA Networks. *Cancers*. 2020;12(7):1870.
246. Ignatius MS, Hayes MN, Lobbardi R, *et al.* The NOTCH1/SNAIL1/MEF2C Pathway Regulates Growth and Self-Renewal in Embryonal Rhabdomyosarcoma. *Cell Rep*. 2017;19(11):2304-2318.
247. Liu C, Zhang L, Cui W, *et al.* Epigenetically upregulated GEFT-derived invasion and metastasis of rhabdomyosarcoma via epithelial mesenchymal transition promoted by the Rac1/Cdc42-PAK signalling pathway. *EBioMedicine*. 2019;50:122-134.

248. Nguyen CDK, Yi C. YAP/TAZ Signaling and Resistance to Cancer Therapy. *Trends Cancer*. 2019;5(5):283-296.
249. Slemmons KK, Crose LES, Riedel S, Sushnitha M, Belyea B, Linardic CM. A Novel Notch-YAP Circuit Drives Stemness and Tumorigenesis in Embryonal Rhabdomyosarcoma. *Mol Cancer Res*. 2017.
250. Mo J-S, Park HW, Guan K-L. The Hippo signaling pathway in stem cell biology and cancer. *EMBO Rep*. 2014;15(6):642-656.
251. Lamar JM, Stern P, Liu H, Schindler JW, Jiang Z-G, Hynes RO. The Hippo pathway target, YAP, promotes metastasis through its TEAD-interaction domain. *Proceedings of the National Academy of Sciences*. 2012;109(37):E2441.
252. Seitz G, Warmann SW, Fuchs J, et al. Imaging of cell trafficking and metastases of paediatric rhabdomyosarcoma. *Cell Prolif*. 2008;41(2):365-374.
253. Chagraoui J, Niessen SL, Lessard J, et al. E4F1: a novel candidate factor for mediating BMI1 function in primitive hematopoietic cells. *Genes Dev*. 2006;20(15):2110-2120.
254. Stuckey JI, Dickson BM, Cheng N, et al. A cellular chemical probe targeting the chromodomains of Polycomb repressive complex 1. *Nature Chemical Biology*. 2016;12(3):180-187.
255. Klauke K, Radulović V, Broekhuis M, et al. Polycomb Cbx family members mediate the balance between haematopoietic stem cell self-renewal and differentiation. *Nature Cell Biology*. 2013;15(4):353-362.
256. Zhang X-W, Zhang L, Qin W, et al. Oncogenic role of the chromobox protein CBX7 in gastric cancer. *Journal of Experimental & Clinical Cancer Research*. 2010;29(1):114.
257. Groenendijk FH, Bernards R. Drug resistance to targeted therapies: Déjà vu all over again. *Molecular Oncology*. 2014;8(6):1067-1083.
258. Moitra K. Overcoming Multidrug Resistance in Cancer Stem Cells. *Biomed Res Int*. 2015;2015:635745-635745.
259. Bissierier M, Wajapeyee N. Mechanisms of resistance to EZH2 inhibitors in diffuse large B-cell lymphomas. *Blood*. 2018;131(19):2125-2137.
260. Walter D, Satheesha S, Albrecht P, et al. CD133 positive embryonal rhabdomyosarcoma stem-like cell population is enriched in rhabdospheres. *PLoS one*. 2011;6(5):e19506-e19506.
261. Slemmons KK, Deel MD, Lin Y-T, et al. A method to culture human alveolar rhabdomyosarcoma cell lines as rhabdospheres demonstrates an enrichment in stemness and Notch signaling. *Biol Open*. 2021;10(2):bio050211.
262. Wedekind MF, Denton NL, Chen C-Y, Cripe TP. Pediatric Cancer Immunotherapy: Opportunities and Challenges. *Pediatric Drugs*. 2018;20(5):395-408.
263. Wu C-C, Beird HC, Andrew Livingston J, et al. Immuno-genomic landscape of osteosarcoma. *Nature Communications*. 2020;11(1):1008.
264. Boopathy GTK, Hong W. Role of Hippo Pathway-YAP/TAZ Signaling in Angiogenesis. *Frontiers in Cell and Developmental Biology*. 2019;7(49).